2015-08-10

The Influence of the Insulin-Like Gene Family and Diet-Drug Interactions on Caenorhabditis elegans Physiology: A Dissertation

Ashlyn D. Ritter
University of Massachusetts Medical School

THE INFLUENCE OF THE INSULIN-LIKE GENE FAMILY AND DIET-DRUG INTERACTIONS ON CAENORHABDITIS ELEGANS PHYSIOLOGY

A Dissertation Presented

By

ASHLYN DIXON RITTER

Submitted to the Faculty of the
University of Massachusetts Graduate School of Biomedical Sciences, Worcester
in partial fulfillment of the requirements for the degree of

DOCTOR OF PHILOSOPHY

August 10, 2015

Interdisciplinary Graduate Program

THE INFLUENCE OF THE INSULIN-LIKE GENE FAMILY AND DIET-DRUG INTERACTIONS ON *C. ELEGANS* PHYSIOLOGY

A Dissertation Presented By

Ashlyn D. Ritter

The signatures of the Dissertation Committee signify completion and approval as to style and content of the Dissertation.

[redacted]

A.J. Marian Walhout, PhD, Thesis Advisor

[redacted]

Mark Alkema, PhD, Member of Committee

[redacted]

David Guertin, PhD, Member of Committee

[redacted]

Michelle Mondoux, PhD, Member of Committee

[redacted]

Amy Walker, PhD, Member of Committee

The signature of the Chair of the Committee signifies that the written dissertation meets the requirements of the Dissertation Committee.

[redacted]

Yong-Xu Wang, PhD, Chair of Committee

The signature of the Dean of the Graduate School of Biomedical Sciences signifies that the student has met all graduation requirements of the school.

[redacted]

Anthony Carruthers, PhD
Dean of the Graduate School of Biomedical Sciences

Interdisciplinary Graduate Program

August 10, 2015

COPYRIGHT INFORMATION

Components of this dissertation have been published as:

Ritter, AD; Shen, Y; Fuxman Bass, J; Jeyaraj, S; Deplancke, B; Mukhopadhyay, A; Xu J; Driscoll M; Tissenbaum HA; Walhout AJ (2013). Complex expression dynamics and robustness in *C. elegans* insulin networks. *Genome Res*. 23, 954–965. doi: 10.1101/gr.150466.112

Watson, E; Macneil, LT; **Ritter, AD**; Yilmaz, LS; Rosebrock, AP; Caudy, AA; Walhout, AJM (2014). Interspecies systems biology uncovers metabolites affecting C. elegans gene expression and life history traits. *Cell*. 156(4), 759–770. doi: 10.1016/j.cell.2014.01.047

I dedicate this to my husband, my family, friends and mentors, without whom it was almost impossible for me to complete my thesis work.

ACKNOWLEDGEMENTS

This journey has indescribably molded me and will forever be the most profound experience I have ever completed. The following is my best effort to describe how appreciative I am for those who helped me along the way:

To my mentor, Marian: Your drive for perfection and will to succeed is infectious and inspiring. Thank you for teaching me the art of asking a question and telling a story. I bet $2.50, no one will ever shape my critical mind as much as you. You have elevated me to a level of achievement for which I never thought possible. Thank you for giving me this experience and walking with me along the way.

To Heidi Tissenbaum: Thank you for introducing me to the worm. Your enthusiasm for research is unwavering and, as a result, you encourage and excite others around you. Thank you for your mentorship. You are a role model for women in science and I am grateful for our time together.

To my thesis committee, Yong-Xu Wang, Mark Alkema, David Guertin, Amy Walker and Michelle Mondoux: Thank you for agreeing to take this journey with me. I have benefited tremendously from your insightful suggestions and critiques. Thank you for your time and dedication.

To the past and present members of the Walhout and Tissenbaum labs: Thank you for the countless conversations and contributions over the years. I've grown wiser from our interactions and discussions and have thoroughly enjoyed our time together. Thank you for your friendship and sharing your cultures and traditions. As a result, I have been "culturally transformed" and this has had a

tremendous positive influence on my creativity and compassion for others. I will never forget you.

To UMass Medical School and GSBS administration: Thank you for giving me the opportunity to learn in one of the best research institutions in the country and among some of the most accomplished scientists. Thank you for your dedication to students and our future success. A special thanks goes to Sharon Briggs, Darla Cavanaugh and Tina Nesbeda for all your assistance. I would have drowned in paperwork many times without you.

To my husband, Chad: You deserve an honorary degree. Thank you for the endless encouragement and love. You remind me of the bigger picture when I get overwhelmed with details and inspire me to persevere. You're the best partner, teammate and friend. Thank you for dedicating your life to us.

To my son, Jack: Thank you for reminding me that, "Play is the highest form of research." Because of you, I will have something left to learn all the days of my life. Stay as playful and curious as you are today. You are brilliant, baby boy.

To my family: Thank you for your support and encouragement, even when you may not have understood. You were the first to believe in me, mold me and push me to be my best self. You sacrificed so I could take this journey, and I will never, ever stop being grateful. You are my Giving Tree.

Finally, thanks to the worm, *Caenorhabditis elegans*, for teaching me:

"Simplicity is the ultimate form of sophistication."

ABSTRACT

Aging can be defined as the accumulation of changes affecting the maintenance of homeostatic processes over time, leading to functional decline and increased risk for disease and death. In its simplicity, aging is the system-wide deterioration of an organism. Genetic studies have identified many potential molecular mechanisms of aging including DNA damage, telomere shortening, mitochondrial dysfunction, increased oxidative stress, uncontrolled inflammation, and hormone dysregulation (reviewed in [1]). However, in reality, aging is likely to be a combination of some (or potentially all) of these mechanisms.

Interestingly, aging and metabolism are tightly coordinated. Aging is a major contributor to metabolic decline and related diseases, including type 2 diabetes, metabolic syndrome, and cancer. One of the best characterized metabolic pathways implicated in aging is the insulin/IGF-1 signaling (IIS) pathway. Downstream signaling components of the IIS pathway receptor have been well studied and include an interconnected network of signaling events that regulate many physiological outputs. However, less is known about the role of upstream signaling components and how intracellular pathways and physiology are regulated accordingly. In Part I, I present my work towards understanding upstream IIS pathway components using a systems biology approach. The goal of this study is to gain insight into the redundancy and specificity of the insulin gene family responsible for initiating IIS pathway activity in *Caenorhabditis elegans*. The information gained will serve as a foundation for future studies

dissecting the molecular mechanisms of this pathway in efforts to uncouple the downstream signaling and physiological outputs.

The clear impact of metabolism on aging and disease stimulated questions regarding the potential of promoting health and longevity through diet and dietary mimetics. Recent findings indicate reduced food intake, meal timing and nutritional modulation of the gut microbiome can ameliorate signs of aging and age-associated diseases. Aging, therefore, is also the result of dynamic and complex interplay between genes of an organism and its environment. In Part II, I will discuss my efforts to gain insight into how diet influences aging. This preliminary study has demonstrated that diet can affect lifespan in the model organism, *C. elegans*. Additionally, we observe diet-specific effects on drug efficacy that, in turn, modulates *C. elegans* lifespan and reproduction. The implications of these experiments, while limited, illustrate a potentially greater role in diet- and drug-mediated effects on lifespan.

TABLE OF CONTENTS

LIST OF FIGURES

PART I, CHAPTER 1

PART I, CHAPTER 2

PART I, CHAPTER 3

PART II, CHAPTER 4

Part II, Chapter 5

LIST OF TABLES

PART I, CHAPTER 1

PART I, CHAPTER 2

PART II, Chapter 5

LIST OF ABBREVIATIONS

IRS = insulin receptor substrate

SH2 = src homology 2

INS = insulin-like gene

DAF = abnormal dauer formation

IGF = insulin-like growth factor

IIS = insulin/insulin-like growth factor-1 signaling

FOXO = fork head box class O

TOR = target of rapamycin kinase

DILP = *Drosophila* insulin-like peptide

RTK = receptor tyrosine kinase

FUdR = 5-fluoro-2-deoxyuridine

dUMP = 2’-deoxyuridine 5’-monophosphate

dUTP = 2’-deoxyuridine 5’-triphosphate

TS = thymidylate synthase

INTRODUCTION

Caenorhabditis elegans as a model system

Dissecting the mechanisms of aging is almost impossible in humans given the long lifespan, genetic variability and complexity of diet. Therefore scientists have longed turned to model organisms as a system to investigate aging. A number of excellent model systems have been developed for aging research including the budding yeast *Saccharomyces cerevisiae,* the fruitfly *Drosophila melanogaster,* the mouse *Mus musculus* and the roundworm *Caenorhabditis elegans. C. elegans* was established as an aging model animal system in the 1970s and has probably become the most widely used for aging studies [2], [3]. *C. elegans* offers multiple unique advantages as a model organism, such as physiological simplicity (959 cells), short life cycle (~3 days, egg to egg), reproducible lifespan (~2 weeks), and short reproductive span (~6 days). *C. elegans* can be easily and cheaply propagated in the laboratory by feeding bacteria on standard agar plates [4], [5]. In addition, large, isogenic populations of *C. elegans* can be grown and visualized in liquid culture, which allows for testing of many biochemical compounds on physiology.

C. elegans are very amenable to genetic manipulations. Mutations can be induced in the animal through the use of chemicals (ethyl methane sulfonate), light (UV), or transposon-based methods, for example. The self-fertilizing capabilities of hermaphrodites, short generation times, and the abundance of progeny (~300 per worm) allow for quick isolation of genotypes and phenotypes.

These features allow for single-gene manipulations that can be directly tested for phenotypic effect using simple, well-defined assays that measure lifespan, brood size, and developmental timing [6], [7]. For instance, single genes have been identified that can significantly increase lifespan by over 100% [8]–[10]. Powerful forward and reverse genetic tools have also been established for use in *C. elegans* allowing for large, comprehensive and systems-level studies [5], [11]. Changes in gene expression can also be measured using high-throughput sequencing technologies such as RNA sequencing. *C. elegans* can be grown monoxenically, which offers the possibility of testing individual bacterial species for their role on aging [12]. In addition, the *C. elegans* diet can also be genetically manipulated to study the effect of dietary components ([13], [14] reviewed in [15]).

Genetic and physiological manipulations to *C. elegans* are also easily tractable. *in vivo* examination of tissues, proteins and single genes is possible as *C. elegans* is transparent and simply requires the application of dyes or fluorescent reporters to visualize [16]–[20]. Animals can then be observed directly with the use of dissecting microscopes [19], [21]. Changes in tissue integrity and fat composition can also be quantitatively measured [22]–[24]. Additionally, many image analysis tools are available that automate measures for animal size, fat content, behavior and lifespan [25]–[29].

C. elegans was the first multicellular organism to have its genome sequenced and, as a result, its genome is highly annotated and likely best understood. Surprising to most, *C. elegans* homologs have been identified for 60-

80% of human genes. Based on predictive surveys, ~42% of human disease genes have an ortholog in *C. elegans;* some of which, when mutated or knocked down, mimic morphological and/or functional defects of disease symptoms [30], [31]. In addition, its complete cell lineage is mapped providing a great tool for research on how genes influence cell fate, for example. A nervous system wiring diagram has also been constructed for all 302 neurons in the hermaphrodite [19], [21].

C. elegans share many similarities in aging with higher eukaryotes. The survival curves of worms and humans, for instance, share the same shape, despite differences in their lifespans [6], [32], [33]. Hallmarks of aging also seem conserved between worms and humans. *C. elegans* undergo muscle atrophy, increased susceptibility to infection and cognitive decline with age [34], [35]. Additionally, the molecular mechanisms that regulate longevity in *C. elegans* are highly conserved with genes and pathways in humans (reviewed in [36]). As a result, studying longevity in *C. elegans* has profoundly impacted therapeutic applications and our understanding of human aging.

PREFACE TO PART I

SUMMARY

Several factors influence longevity of an organism including genetics, the environment and diet. In Part I, I introduce a genetic pathway, the highly conserved insulin/IGF-1 signaling (IIS) pathway, which greatly influences longevity across species (Chapter 1). Studies examining the IIS pathway in many model organisms have continued to illustrate its key role in regulating longevity. I discuss the components and conservation of the IIS pathway with an emphasis on two main components: the receptor and its ligands. Chapter 1 serves as an introduction to my thesis research towards understanding the interactions between *C. elegans* IIS pathway ligands and physiology (Chapter 2). From this study and others, examining the insulin gene family by expression and mutation has revealed complex orchestration of physiology by the insulin ligands. In the last Chapter, I share my thoughts on how the insulins are functioning and what future directions would be most informative for gaining greater insight into this gene family (Chapter 3).

Chapter 2 has been published as:

Ritter, AD; Shen, Y; Fuxman Bass, J; Jeyaraj, S; Deplancke, B; Mukhopadhyay, A; Xu J; Driscoll M; Tissenbaum HA; Walhout AJ (2013). Complex expression dynamics and robustness in *C. elegans* insulin networks. *Genome Res*. 23, 954–965. doi: 10.1101/gr.150466.112

For data presented in Chapter 2:

Arnab Mukhopadjay, Bart Deplancke, Marian Walhout and Heidi Tissenbaum first conceived the project. Arnab Mukhopadjay and Bart Deplancke cloned a subset of promoters. Yuan Shen and Sankarganesh Jeyaraj performed the cloning created transgenic lines. Some strains were provided by the CGC, which is funded by NIH Office of Research Infrastructure Programs (P40 OD010440). Jian Xu and Dr. Monica Driscoll provided insulin RNAi constructs.

I analyzed all expression patterns, did the phenotypic analyses, made the figures and wrote the published manuscript together with Marian Walhout and Heidi Tissenbaum. Juan Fuxman-Bass assisted me with TsOC analysis and statistics.

For research presented in Part I, I was supported by the NIH Ruth L. Kirschstein National Research Service Award (NRSA) Individual Predoctoral Fellowship (AG041605).

PART I

Complex expression dynamics and robustness in *C. elegans* insulin networks

PART I, CHAPTER 1

The insulin/IGF-1 signaling pathway

The IIS pathway is critical for monitoring the macroenvironment and orchestrating a complex network of molecular mechanisms that modulate the appropriate physiological response. The IIS pathway regulates fundamental processes including growth/development, metabolism, reproduction, stress response and longevity [37], [38]. Interestingly, these physiological outputs are closely linked. For example, loss-of-function mutations in insulin signaling in both vertebrates and invertebrates lead to increased lifespan along with increased fat storage and improved stress response [39]. In humans, deregulation of this pathway can lead to age-associated diseases, such as type 2 diabetes, cardiovascular disease and cancer.

The highly conserved IIS pathway is mediated by a complex and highly integrated network [40]. In mammals, upon insulin/IGF-1 binding, the receptor undergoes autophosphorylation and catalyzes phosphorylation of scaffolding adaptor proteins, such as the IRS family [41]. Activated IRS tyrosine phosphorylation sites act as docking sites for SH2 domains of cellular proteins. SH2-domain proteins initiate interactions with signaling molecules that activate a diverse series of intracellular pathways, including PI(3)K/Akt activation, MAPK kinase cascade, mTOR pathways and downstream protein-kinase C (PKC)/NF-kB pathway. The IIS pathway ultimately impinges on FOXO transcription factors that regulate their target genes [40], [42].

There are two key components to the IIS pathway: the insulin/IGF ligands and their receptors. Homologues of the insulin/IGF-1 receptor have been identified in *Drosophila* and *C. elegans*, as well as metazoan marine sponges [43]–[46]. However, while at least three insulin/IGF-1 receptors exist in vertebrates, only one receptor has been identified for *Drosophila* and *C. elegans,* the insulin/IGF-1 receptor (dInR) and DAF-2, respectively [38]. The insulin/IGF-1 receptor belongs to a family of receptor tyrosine kinases and, in vertebrates, the insulin, IGF-I and insulin receptor-related receptor (IRR) all function as receptors for insulin/IGF ligands. Homodimeric and heterodimeric hybrid receptors can form and bind both insulin and IGF-1 with different affinities, depending on the insulin isoform [41]. While the binding of insulin to its receptor is complex, most mammalian studies illustrate the coexistence of high and low affinity binding sites. Dissociation studies have shown the existence of negative cooperativity between binding sites indicated by the accelerated dissociation of pre-bound ligand in the presence of unlabeled ligand [47]–[50].

The human genome encodes ten insulin-like peptides, including insulin, IGFs and relaxins, which together form a protein family called the insulin superfamily [51]. *Drosophila melanogaster* has eight insulin-like peptides, or DILPs [52]–[54]. Remarkably, the *C. elegans* genome encodes 40 insulin-like genes [55]–[58]. The human insulin gene encodes a 110-amino acid precursor, preproinsulin, which is translated in the endoplasmic reticulum and consists of four domains that are highly conserved across phylogeny: the signal peptide, A-chain, B-chain and C-peptide. Proteolytic cleavage by a signal peptidase

removes the signal peptide from preproinsulin to yield proinsulin, and three highly conserved disulfide bonds form between the A- and B-chains with the aid of ER chaperone proteins. After proper folding, the proinsulin precursor undergoes further cleavage to remove the C-peptide. The matured 51-amino acid insulin protein and the free C-peptide are then packaged in the Golgi. Insulin is stored in secretory granules as a hexamer of insulin peptide arranged as three dimers [59], [60]. Upon changes in nutrient availability, specifically glucose, amino acids and fatty acids, insulin is released from the cell via exocytosis where it circulates in the vascular system until binding its receptor [61]. All members of the insulin superfamily contain at least the A- and B-chain, although the length can be variable, and at least two of the conserved disulfide bonds. Historically, insulin was characterized to control carbohydrate and lipid metabolism, IGFs were mainly involved in growth and development and relaxins were involved in reproduction. However, classical genetic and functional genomic studies have revealed highly interconnected signaling between pathways modulated by these ligands [40].

While we have seen remarkable progress in dissecting intracellular signaling pathways responsible for outputs of the IIS pathway, the molecular basis for specificity of intracellular activity is still not fully understood. In order to dissect these molecular mechanisms, researchers have turned to model organisms in efforts to gain better resolution.

The IIS pathway in *Caenorhabditis elegans*

The discovery of the IIS pathway in *C. elegans* emerged from studies on dauer regulation and longevity. In response to unfavorable environmental conditions (*i.e.* high temperature, crowding and low food), *C. elegans* larvae undergo dauer arrest (Fig. 1.1). The IIS receptor, *daf-2,* and FOXO transcription factor, *daf-16,* were first characterized from a forward genetic screen designed to isolate mutants exhibiting deregulation of dauer arrest [62], [63]. These mutants illustrated dauer-constitutive and dauer-defective phenotypes, respectively. Not long after the identification of *daf-2* and *daf-16* genes*, age-1*, the *C. elegans* ortholog of the phosphoinositide 3-kinase (PI3K) p110 catalytic subunit, was isolated from a screen for long-lived animals [9], [64], [65]. Genetic epistasis experiments later illustrated *daf-2, daf-16* and *age-1* to be part of the IIS pathway leading to subsequent identification of pathway components [38], [44], [66]–[68]. These studies also revealed mutations in *daf-2* resulted in a remarkable lifespan extension twice that of wild-type animals [8], [45]. To date, the IIS pathway remains the best characterized regulator of longevity across species.

Further interrogation of the IIS pathway revealed even more conservation in IIS-mediated physiology. For instance, *daf-2* mutants illustrate increased fat content compared to wild-type animals; a phenotype attributed to changes in fat metabolism driven, at least in part, by *fat-* genes and metabolic regulators that upregulate metabolic processes including fatty acid desaturation and lipolysis, acyl-CoA and alcohol dehydrogenases, and glyoxylate cycle [69]–[71]. In addition, *daf-2* mutants illustrate increased stress resistance to many stressors

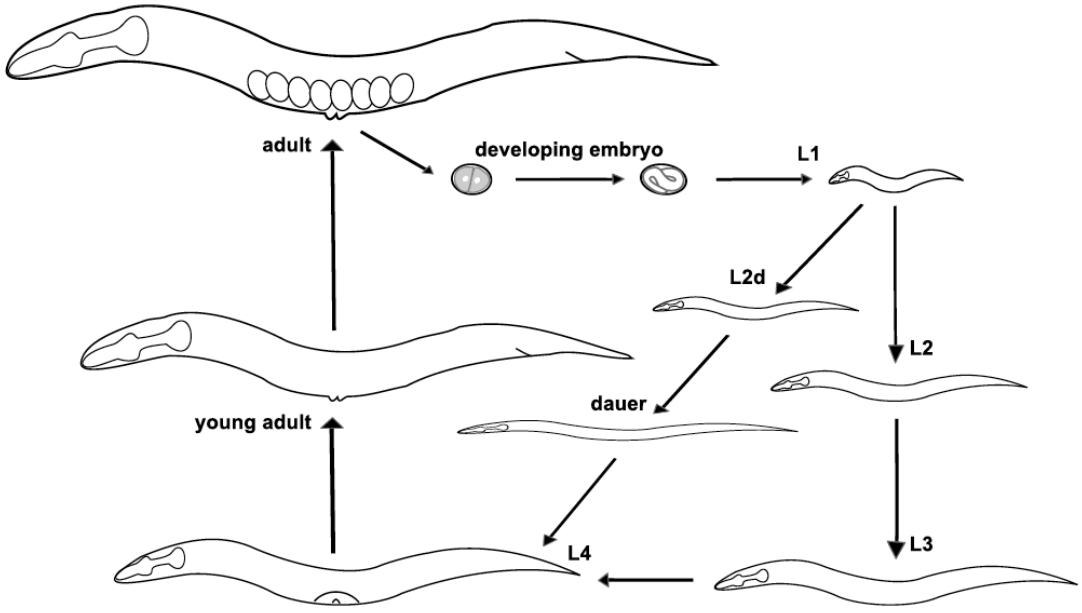

FIGURE 1.1: The life cycle of *C. elegans.* In a favorable growth environment, *C. elegans* develop from an egg through progressive larval stages (L1-L4) until reaching the adult stage. In an unfavorable growth environment, *C. elegans* enter a diapause stage (L2d-dauer) and remain as a dauer until the environment becomes favorable for growth. An unfavorable environment is defined by a high concentration of secreted pheromone, higher temperature and/or low food availability.

including heat and oxidative stress, to name a few [72]–[74]. Mutants of *daf-2* also illustrate extended reproductive span [74], [75]. While some studies illustrate *daf-2* mutants show delayed progression of age-associated neural decline, this is challenged by behavioral studies that illustrated impaired chemotaxis learning behaviors [76]–[79].

There are a few physiological differences among mammals and invertebrates. While in mammals, deregulation of the IIS pathway leads to metabolic and age-associated disease, in *C. elegans,* as well as *Drosophila,* deregulation leads to dauer and longevity phenotypes. However, despite these physiological differences, the intracellular signaling cascade remains highly conserved, and like mammals, *C. elegans* IIS pathway modulates metabolism, reproduction, stress and development (Fig. 1.2) [38]. As a result, the easily measurable phenotypes in *C. elegans*, namely dauer and lifespan, have been adopted as proxies for IIS pathway activity.

Both the gene and protein structures of insulin-like peptides in *C. elegans* and vertebrates are highly conserved and likely originated from a common ancestor [80], [81]. However, in mammals, it has been difficult to differentiate the activities of insulin, IGF and relaxins in their different contexts as signaling pathways downstream are highly similar and interconnected. Therefore, insulin-like peptide signaling in *C. elegans* may translate to mammals allowing for greater understanding of signaling specificity. Given the short life cycle and ease of culturing, *C. elegans* can be considered one of the best model organisms to utilize for determining how the IIS pathway contributes to physiology.

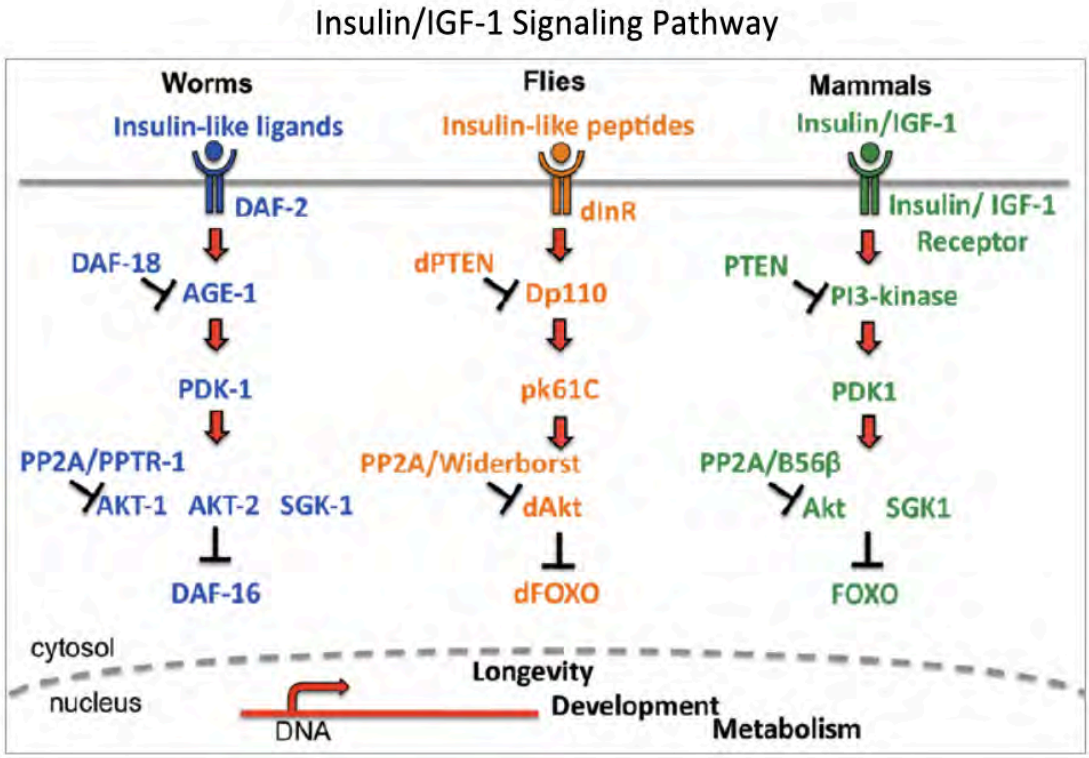

FIGURE 1.2: Insulin/IGF-1 signaling is conserved across species. Worms and flies have a single orthologue of the mammalian insulin/IGF-1 receptor tyrosine kinases, called DAF-2 and insulin receptor (InR), respectively. Downstream components such as PI3-kinase and FOXO are conserved in worms, flies and mammals. Under active IIS signaling, DAF-16/FoxO transcription factor is negatively regulated by phosphorylation and sequestered in the cytosol. This regulation is conserved across species (modified from [171]).

The expanded *C. elegans* insulin-like gene family

While the amino acid sequence of insulin is variable among species, the positions of the disulfide bonds are highly conserved across species [80]. Researchers utilized the conservation of amino acid sequence and protein structure to comprehensively identify forty insulin-like genes (*ins-1* through *ins-39* and *daf-28*; henceforth referred to as insulins) in *C. elegans* [56]–[58]. Interestingly, many of the insulins are organized in clusters of 3-7 along the chromosomes (Fig. 1.3). Insulins within a cluster tend to have closer sequence similarity than between members of a different cluster. However, with a range of 25-40% amino acid identity in the A- and B-peptide regions, the genes in the cluster are still highly divergent [56]. The clustering, tandem arrangement and closer sequence similarity suggests these genes arose from recent gene duplication events and that they may still be evolving. Further analyses comparing the insulin gene family of *C. elegans* with other ancestral *Caenorhabditis* species, for instance *C. briggsae*, will provide further insights into the evolution of this gene family.

The biochemical processing and physical binding of *C. elegans* insulins to its receptor remains largely unconfirmed. One biochemical study of INS-6 illustrated conserved insulin folds and binding to the human insulin receptor [82]. Secretion of DAF-28 has been demonstrated and regulated by a conserved gene, *asna-1*, an ATPase that functions to regulate growth [83]. This suggests some shared physiological mechanisms of insulin release with mammals exist [84]. Although not direct evidence, DAF-16 is nuclear localized in the presence of

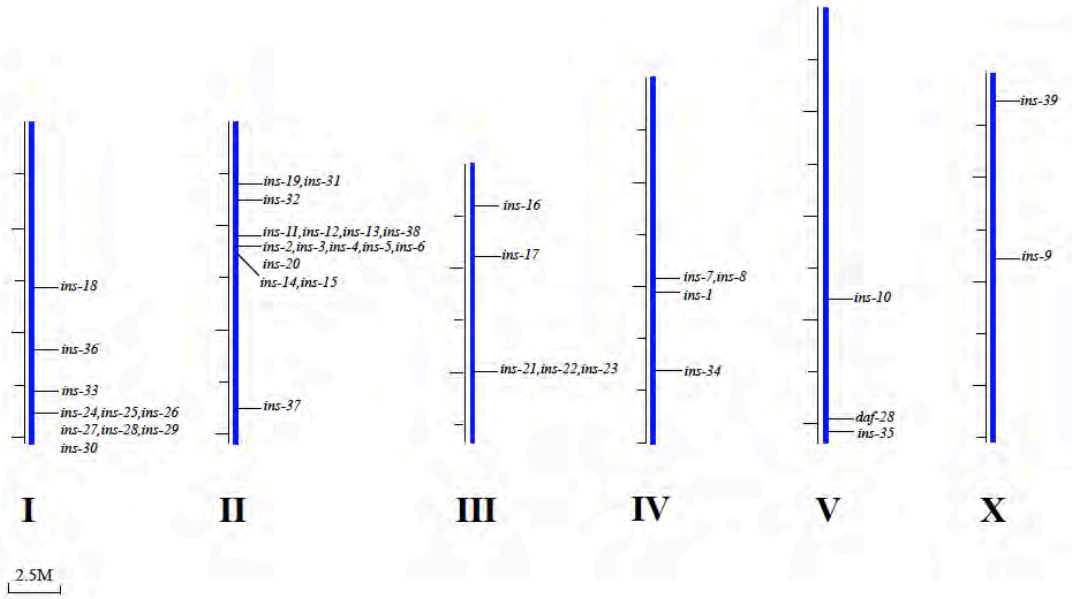

FIGURE 1.3: Organization of insulin-like genes on *C. elegans* chromosomes. Many insulin-like genes (*ins-)* can be found in clusters of two to seven along the chromosomes. The relative distances between the genes are indicated (scale bar, 2.5 million bp).

a *daf-28* mutation and the patterns of DAF-16 nuclear localization are similar to what is observed in *daf-2* loss-of-function animals [57]. Together, these data illustrate that the interactions between insulins and DAF-2 are plausible and biologically relevant, although not comprehensively illustrated for the entire gene family.

While the insulin receptor and downstream signaling pathways have been studied extensively through genetic approaches, little is known about the functionality of the *C. elegans* insulin gene family in regulating IIS pathway specificity. A vast majority of the insulins have no measured biological function, even upon loss or overexpression (Table 1.1). For some, genetic studies have shown insulins can regulate other insulins. Insulins can also function as receptor antagonists, agonists, or both, depending on a specific environmental condition examined [56], [71], [85]–[91]. A few insulins illustrate context-dependent phenotypes. For example, loss-of-function mutations in *ins-1* cause defects in salt chemotaxis learning [79]. *ins-7* loss-of-function mutants, along with increased lifespan, also have increased resistance to pathogenic infection [71], [92]. Loss-of-function mutations in *ins-3* leads to a reduced number of germ cells and decreased rate of dauer entry, although only in a sensitized *daf-28* mutant background that already promotes dauer formation [87].

How do we study gene families?

Expanded gene families are generated from gene duplication events, an important process for the evolution of functional and organismal diversity. After

Previously Published Phenotypes (compared to N2)

Insulin	Mutants	RNAi	Overexpression	Other
ins-1	defective in salt chemotaxis learning,[P] food-associated thermotactic behavioral plasticity,[D] and benzaldehyde-starvation plasticity[A]; more rapid aversive response off food[B], increased turning in AWC-dependent local search behavior & olfactory adaptation[S]		slightly enhanced dauer and extended lifespan[C]; partially abnormal thermotaxis movement[D]	deletion suppresses dauer entry in *daf-2(e1368)* mutants[R]
ins-7	extended lifespan[G], more resistant to pathogen[O]	extended lifespan of daf-2(+); *rrf-3(pk1426)*[F]; extended lifespan of N2[N]	in intestine: slightly shorter lifespan[G]	downregulated under daf-2(-) conditions[G]; ins-7 RNAi stimulates nuclear localization of DAF-16 & increased *Psod-3::GFP* expression; enhances *daf-2(e1370)* dauer arrest[F]
ins-17	decreased dauer formation[E]		enhanced dauer formation[E]	
ins-18	decreased dauer formation[Q]		enhanced dauer formation[C,Q], extended lifespan[Q]	
ins-33	reduced proliferative zone germline cells[J]	reduced number of proliferative zone germ cells[J]		
daf-28	induced dauer arrest[K,R], slightly extended lifespan[L,K]			suppressed dauer formation of TGFβ pathway mutants[L,M]
ins-9			high dose = some embryonic lethality and L1 arrest[C]	
ins-6				deletion of *ins-6* in *daf-2(e1368)* mutants strongly inhibited dauer exit[R]
ins-11	fat accumulation[N]	fat accumulation[N]		
ins-2				upregulated in *daf-2* mutants[D]
ins-21				slightly downregulated in *daf-2* mutants[D]
ins-3	reduced proliferative zone germline cells[J]	reduced number of proliferative zone germ cells[J]		
ins-4				suppresses dauer formation of TGFβ pathway mutants[L,M]

A: Lin et al, 2010
B: Harris et al, 2011
C: Pierce et al, 2001
D: Kodama et al, 2006
E: Matsunaga et al, 2012
F: Murphy et al, 2003
G: Murphy et al, 2007
H: McElwee et al, 2003
I: Hristova et al, 2005
J: Michaelson et al, 2010
K: Malone et al, 1994
L: Li et al, 2003
M: Kao et al, 2007
N: Kawano et al, 2006
O: Kawli et al, 2008
P: Tomioka et al, 2006
Q: Matsunaga et al, 2012
R: Cornils et al, 2011
S: Chalasani et al, 2010

TABLE 1.1: Previously published insulin phenotypes. Phenotypes reported in this table are compared to wild type (N2) and only include results from mutations, deletions, RNAi or overexpression in N2 backgrounds. References are indicated by superscript letters. For phenotypes in other mutant backgrounds (such as *daf-2*), see column titled “Other.”

duplication, the resulting identical paralogs diverge in both sequence and function. Neo-functionalization occurs when one paralog adopts a novel function that is not shared by the ancestral gene, while in sub-functionalization the ancestral function(s) are divided between the two paralogs [93], [94]. In addition to functional divergence, it can also be beneficial for paralogs to maintain (partial) redundancy, for instance to provide a buffer under adverse genetic or environmental conditions (Fig. 1.4) [95], [96]. Numerous gene families have been identified by whole genome sequencing and gene annotation. So far, only few families have been analyzed at a systems level, and the balance between divergence and redundancy is only beginning to be illuminated. For example, in *C. elegans*, basic helix-loop-helix transcription factors have extensively diverged in multiple functional parameters [97]. However, ETS transcription factors function redundantly in the mouse, by binding and regulating the same target genes [98].

C. elegans live in the soil and are exposed to many environmental conditions [5]. *C. elegans* use the IIS pathway to respond to environmental cues adjusting development and lifespan accordingly. For example, growth and reproduction in the worm are directly influenced by food availability and other environmental conditions such as temperature and crowding [63], [99]. With this knowledge, I hypothesized that there is a “division of labor” between the 40 insulins in *C. elegans*, as well as redundancy between some family members, which together enables a sophisticated and robust metabolic response during development, in physiology and to respond to environmental cues.

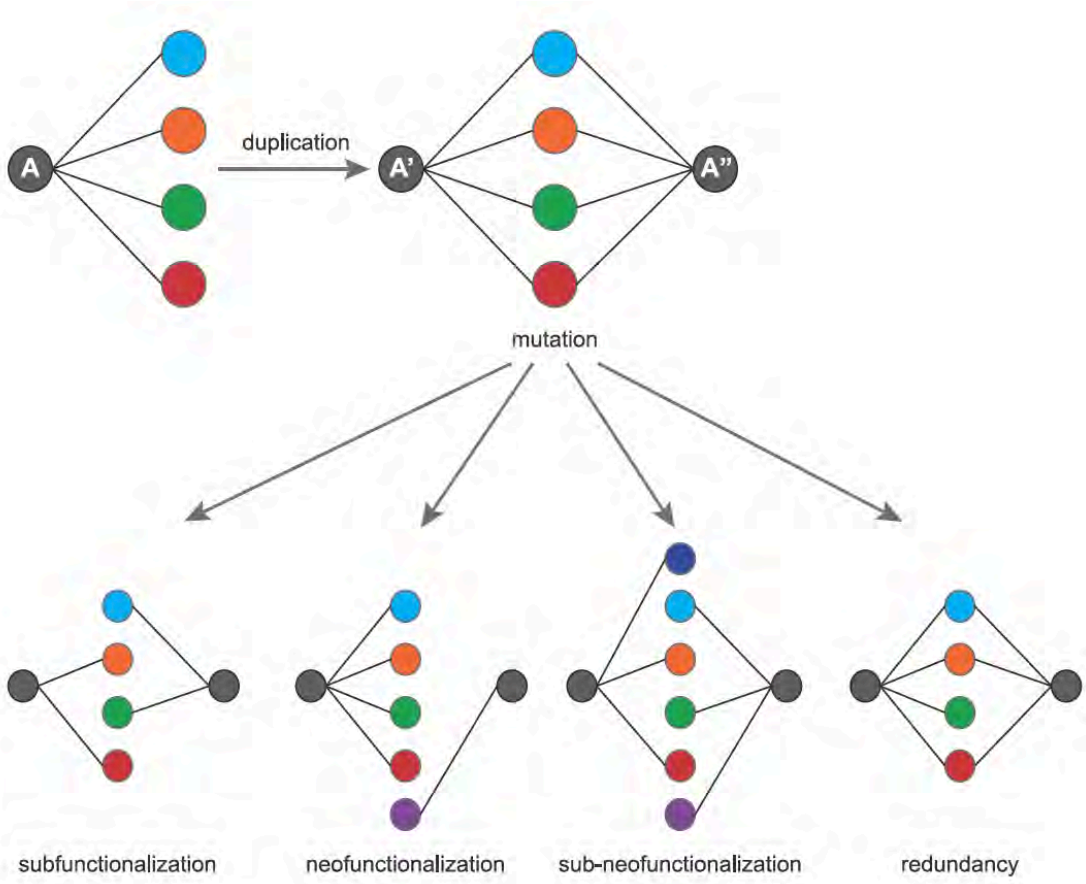

FIGURE 1.4: Gene duplication leads to functional diversification and/or redundancy. In this network, each gene duplicate (gray node) regulates (edge) a function (colored node). During gene duplication, replicate genes can undergo (from left to right) subfunctionalization, the ancestral function is partitioned between paralogs to create a “division of labor”; neofunctionalization, one paralog evolves a new, advantageous function different from its ancestral function; sub-neofunctionalization, after subfunctionalization paralogs can gain new function; or redundancy, functional overlap is conserved between paralogs. Gene duplication events lead to redundancy and specificity in the network that can promote “fine-tuning” of the response to environmental stimuli.

Different studies rely on different methods to examine redundant interactions between gene family members. Genetic redundancy can be inferred from computational or experimental approaches. Computationally, gene duplications can be examined by: 1) estimating increased dispensability, or centrality, of duplicates, whereby dispensability is defined by the probability a gene associates with an essential function; 2) quantitatively determining the fitness contribution of each duplicate; and/or 3) curating literature [100]–[104]. Experimentally, genetic redundancy is inferred with the use of classical epistasis analysis examining synthetic interactions. For instance, a comprehensive analysis of *C. elegans* Argonautes was conducted by knocking out combinations of all 27 genes. While all Argonautes bind to small RNAs, many perform specific roles at different steps in the same RNAi pathway or in different pathways all together. Conversely, a few, called secondary Argonautes, can be functionally interchangeable with other Argonautes. Interestingly, some elicit unique phenotypic consequences upon loss, such as chromosome segregation defects (*csr-1*) or reduced fertility (*prg-1*) [105].

The most intuitive way to test redundancy and specificity in the insulin gene family would be by taking a classical genetic approach. This would require generating strains bearing a mutation in each insulin gene or performing RNA interference (RNAi) knockdown of each insulin gene and then testing for IIS-related phenotypes including lifespan, metabolism, development and reproduction. In *Drosophila*, the use of this approach illustrated that the knockdown of individual insulin-like peptides (DILPS) confers no obvious

phenotypes. Severe phenotypes, such as lethality, are only observed upon loss of multiple DILPS. For instance, loss of *dilp2* increases *dilp3* and *5* transcripts and loss of all three leads to severe phenotypes under different conditions illustrating the functional redundancy and compensation between these genes [106], [107]. Testing multiple phenotypes and lifespan for 40 individual genes in *C. elegans*, however, is impractical. Importantly, if some insulins function redundantly, as I hypothesize, the loss of individual insulins might be masked or buffered by the function of another. If true, this would mean that double ([40x40]/2 = 800 possible combinations), or even triple insulin mutants are required to be tested for all the different phenotypes. Therefore, I utilized a different strategy whereby I will take a comprehensive “systems approach.”

Using a systems approach to dissect insulin function

Genes that act redundantly are often co-expressed, at least in part. Therefore, we decided to annotate spatiotemporal and conditional insulin expression as a starting point to indicate which insulins may function together. *C. elegans* are transparent and transgenic animals carrying promoter-driving green fluorescent protein (GFP) constructs can be used to annotate spatiotemporal gene expression in living animals [17], [97], [108], [109].

Relationships between genes and the cells or tissues in which they are expressed can be visualized into expression networks. In such networks, “nodes” represent insulin genes and individual cells/tissues and “edges” link the gene to the tissue where it is expressed illustrating the relationship [97], [109]. Visualizing

gene expression into network models is highly useful as it provides an instant glimpse into the complexity of gene expression. Expression networks can be formatted to display all the cells/tissues in which each insulin gene is expressed (gene-centric) or a direct view on which genes are expressed in particular cells/tissues (tissue-centric). Further, expression networks can be analyzed computationally to quantify co-expression of the genes of interest. For this, a tissue overlap coefficient (TsOC) is calculated that is defined as the number of tissues shared between two insulin genes divided by the smallest of the total number of tissues where either insulin gene is expressed [110], [111]. The TsOC for a pair of insulin genes defines the overlap of their tissue expression. For example, insulins that exhibit complete overlap in tissue expression are assigned a value of 1, whereas insulins with no overlapping expression have a score of 0. In order to generate high-resolution tissue expression networks, two important tools are required. First, a high-throughput method is needed that will unveil spatiotemporal gene expression for each gene of interest. This is accomplished by: 1) using Gateway cloning of gene promoter fragments upstream of an open reading frame encoding the green fluorescent protein (GFP), and 2) creating transgenic *C. elegans* that harbor each construct. Previous studies have shown that the use of only gene promoter fragments provides a high-confidence proxy for endogenous gene expression [108]. Second, a controlled vocabulary is needed to confidently assign gene expression to different tissues and cells [97], [109].

Because *C. elegans* has a simple anatomy, invariant cell lineage, and transparent body, it is relatively easy to generate such a controlled vocabulary. I defined 23 categories (hereafter referred to as “tissues”), including intestine, vulva, body muscle, etc. Some tissues are specific (e.g. distal tip cells), and others are broad (e.g. head neurons). To generate insulin expression networks, I will study where (spatio) and when (temporal) each insulin is expressed during development as well as how each insulin gene expression changes when the transgenic animals are exposed to a variety of relevant environmental conditions. Insulins that are co-expressed either in development or under different conditions are more likely to function redundantly. Conversely, insulins with unique patterns of expression may have functionally diverged and attained specific functionalities (for example, only affecting one phenotype of the IIS pathway). Taken together, this will allow a comprehensive investigation of the *C. elegans* insulin-like family by modeling the expression network to predicting the function of individual insulin genes (see Part I, Chapter 2).

PART I, CHAPTER 2

RESULTS

Lack of pair-wise redundancy between *C. elegans* insulins in dauer formation

We used dauer diapause, one of the main outputs of the IIS pathway, to explore the putative extent of redundancy and specificity in the insulin family. Loss-of-function mutations in the DAF-2 receptor result in a dauer-constitutive (Daf-c) phenotype [112]. We found that neither deletions in 12 insulins nor knockdown of any of the 40 insulins results in dauers (Fig. 2.1; Table 2.1). As some insulins have been reported to have antagonistic effects on the IIS pathway, we asked whether loss of individual insulins would prevent dauer formation. After dauer-inducing conditions, all mutants analyzed were capable of forming dauers, indicating that they are not dauer defective (Fig. 2.2). Together, these results indicate that no single insulin is the sole agonist or antagonist for coordinating dauer formation through the DAF-2 receptor. Next, we asked whether insulins may function in redundant pairs by knocking down each of the 40 insulins in the 10 insulin mutants. However, none of the combinations of insulin mutants and insulin RNAi resulted in the formation of dauers (Fig. 2.1). This suggests there is no simple pair-wise redundancy between insulins in regulating dauer formation, but rather that more complex patterns of redundancy may be involved.

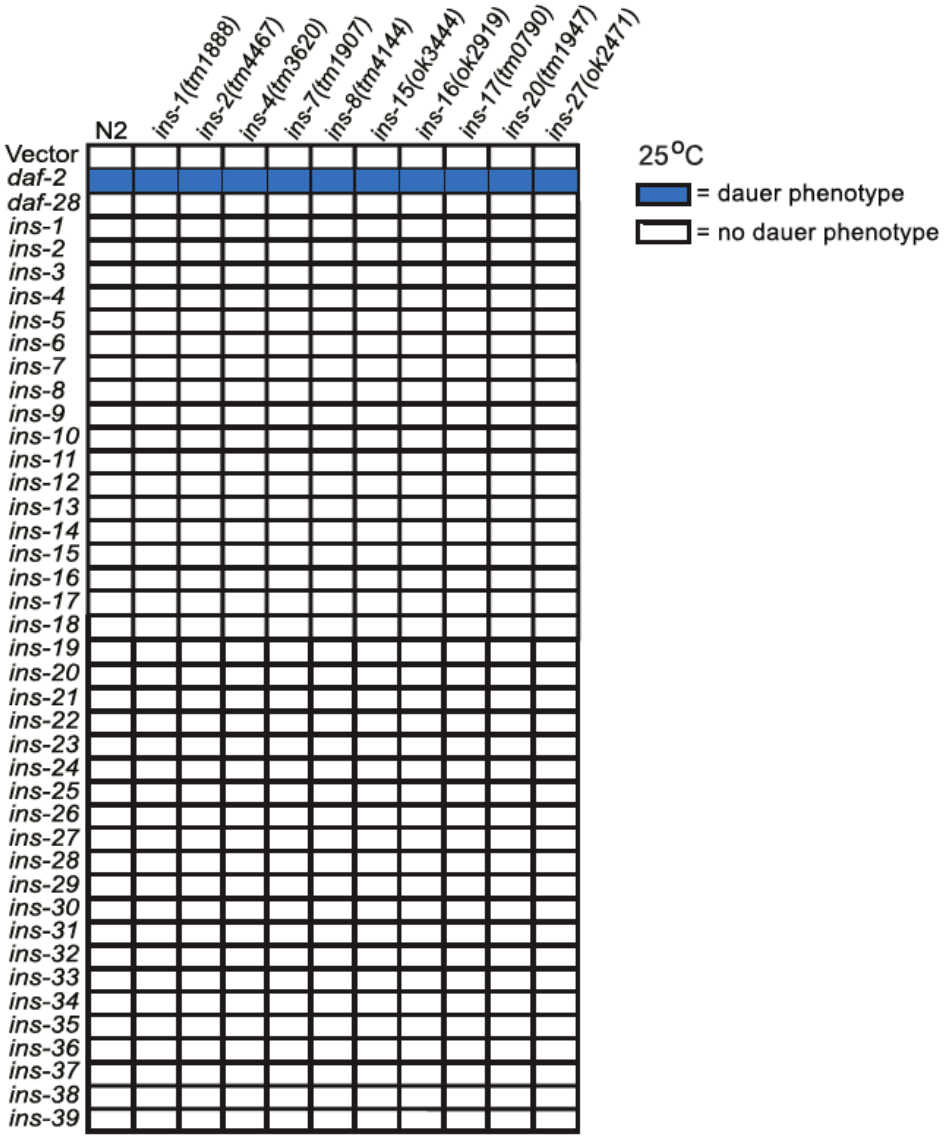

FIGURE 2.1: Examination of dauer formation upon insulin perturbation. Neither loss of individual insulins (columns), nor pairwise insulin perturbation by combined mutation and knockdown (rows) results in dauer formation.

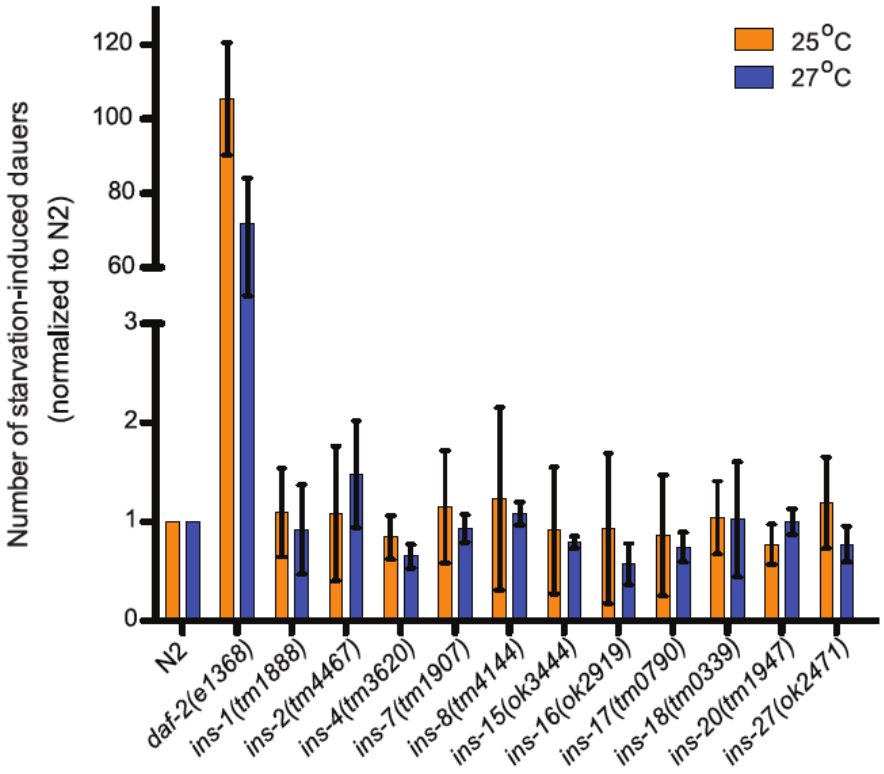

FIGURE 2.2: Individual insulin mutants form dauers in starvation-induced conditions similar to wild-type (N2), indicating that they are not dauer defective. Dauer formation is illustrated as the average of duplicate experiments; data is normalized to wild-type (N2) dauer formation. Additional data can be found in Table 2.1.

Daf-c analysis

Strain	RNAi	L4 larvae and adult	Dauer^{total}	N^{total}
N2	vector	384	0	384
	daf-2	700	8	708
*daf-2(e1368)**	vector	13	52	65
	daf-2	0	120	120
ins-1(tm1888)	vector	330	0	330
	daf-2	341	7	348
ins-2(tm4467)	vector	394	0	394
	daf-2	456	6	462
ins-4(tm3620)	vector	433	0	433
	daf-2	449	15	464
ins-7(tm1907)	vector	550	0	550
	daf-2	585	5	590
ins-8(tm4144)	vector	488	0	488
	daf-2	563	17	580
ins-15(ok3444)	vector	572	0	572
	daf-2	548	20	568
ins-16(ok2919)	vector	412	0	412
	daf-2	347	5	352
ins-17(tm0790)	vector	296	0	296
	daf-2	314	2	316
ins-18(tm0339)	vector	210	0	210
	daf-2	n.d.	n.d.	n.d.
ins-20(tm1947)	vector	215	0	215
	daf-2	223	1	224
ins-27(ok2471)	vector	314	0	314
	daf-2	379	7	386
ins-35(ok3297)	vector	n.d.	n.d.	n.d.
	daf-2	n.d.	n.d.	n.d.

Daf-d analysis

Strain	25°C			27°C		
	% Dauer^{avg}	N^{total}	Normalized to N2	% Dauer^{avg}	N^{total}	Normalized to N2
N2	0.73 ±0.4	773	1.00	1.3 ±0.3	1225	1.00
daf-2(e1368)	76 ±5	105	104	95 ±4	145	73.1
ins-1(tm1888)	0.79 ±0.1	764	1.08	1.2 ±0.8	621	1.08
ins-2(tm4467)	0.78 ±0.1	906	1.07	1.9 ±0.3	794	1.46
ins-4(tm3620)	0.61 ±0.5	624	0.836	0.86 ±0.3	677	0.638
ins-7(tm1907)	0.83 ±0.1	240	1.14	1.2 ±0.4	406	0.923
ins-8(tm4144)	0.90 ±0.2	572	1.23	1.4 ±0.4	554	1.08
ins-15(ok3444)	0.66 ±0.1	304	0.904	1.0 ±0.1	384	0.769
ins-16(ok2919)	0.67 ±0.2	434	0.918	0.75 ±0.4	395	0.577
ins-17(tm0790)	0.62 ±0.1	322	0.849	1.0 ±0.4	643	0.769
ins-18(tm0339)	0.76 ±0.7	510	1.04	1.4 ±0.5	306	1.08
ins-20(tm1947)	0.56 ±0.2	364	0.767	1.3 ±0.1	304	1.00
ins-27(ok2471)	0.87 ±0.1	698	1.19	1.0 ±0.03	397	0.769
ins-35(ok3297)	n.d.	n.d.	n.d.	n.d.	n.d.	n.d.

TABLE 2.1. Examination of dauer phenotypes of insulin mutants. Dauer phenotype data from Figure 6. Top – Daf-c assays. The total number of non-dauers and dauers from duplicate experiments. Data are normalized to wild type (N2) dauer formation. Bottom – Daf-d assays. Data represents the average from two replicates where starvation-induced dauers were counted after 1% SDS survival. Data are normalized to wild type (N2) dauer formation. *n.d.* = not determined.

Complex patterns of insulin expression

To determine spatiotemporal insulin expression patterns during development and under a variety of relevant physiological and environmental conditions, we cloned the promoters of each of the 40 *C. elegans* insulins upstream of an open reading frame encoding GFP, and generated transgenic animals as described [113]. Promoter activity is often a faithful proxy of endogenous gene expression gene; therefore, we refer to insulin promoter activity as “insulin expression” [97], [108], [109].

We annotated insulin expression using a controlled vocabulary to enable the direct comparison between different genes and between different tissues [97], [109]. In hermaphrodites, 36 of 40 insulin promoters conferred GFP expression in six major tissue types: nervous system, muscle, reproductive tissue, epithelia, the alimentary system and coelomocytes (Fig. 2.3). These were subcategorized into specific cells/tissues, totaling 19 different tissue/cell types (Fig. 2.4). We found that most tissues express multiple insulins (Fig. 2.4A), and, conversely, that most insulins are expressed in multiple tissues (Fig. 2.4B). Four insulin promoters did not drive GFP expression in hermaphrodites: *ins-19*, *ins-24*, *ins-31* and *ins-37*. However, *ins-19* and *ins-31* did exhibit GFP expression in males (Fig. 2.5) [114]. Altogether, we detected activity for 38 of 40 promoters (95%).

Spatiotemporal expression patterns have previously been reported for 17 insulins [56], [57], [70], [71], [86], [87]. Our data recapitulate the expression patterns for nine of these (Table 2.2): *ins-1, ins-3, ins-4, ins-7, ins-8, ins-9, ins-11, ins-18,* and *ins-33.* However, for all nine, we observed expression in additional

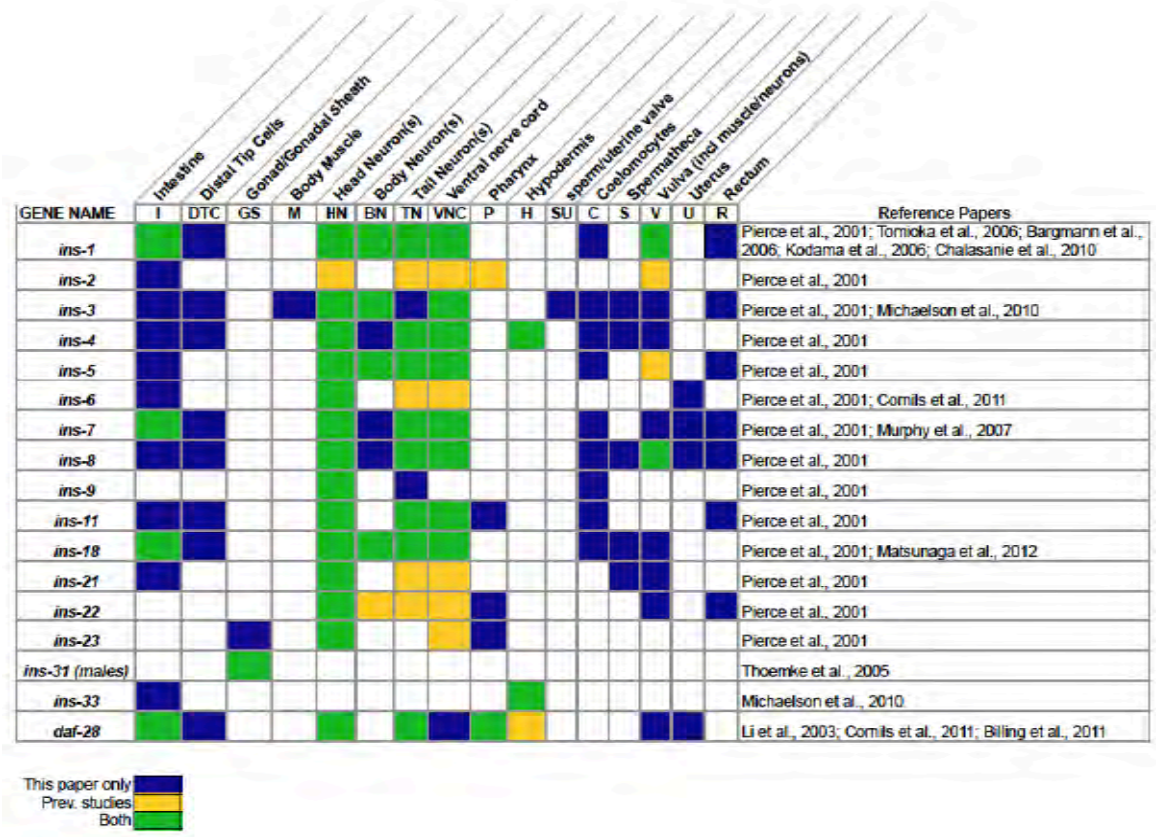

TABLE 2.2: Previously published insulin expression patterns. Expression in a tissue is indicated by blue if it is observed only in this study, orange if only in other recorded studies, or green if observed in both. A * indicates expression patterns observed that were not previously published (see Supplemental Fig. S2). Tissues are assigned as follows: I, intestine; DTC, distal tip cell; GS, gonadal sheath; M, muscle; HN, head neurons; BN, body neuron; TN, tail neuron; VNC, ventral nerve cord; P, pharynx; H, hypodermis; SU, spermatheca/uterine valve; C, coelomocytes; S, spermatheca; V, vulva/vulva muscle/vulva neurons; U, uterus; R, rectum.

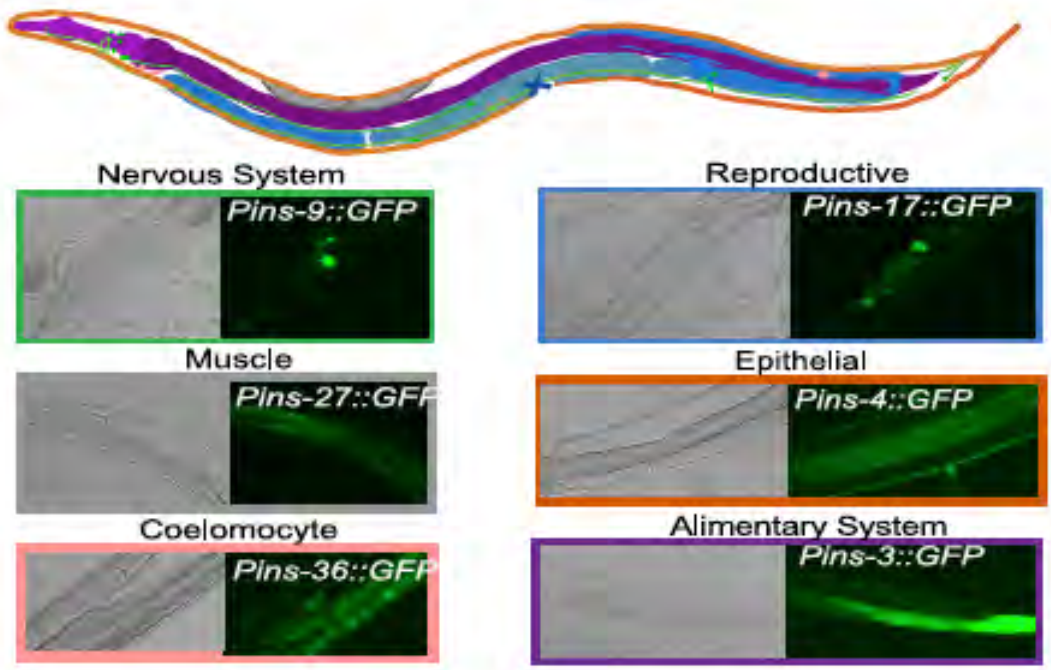

FIGURE 2.3: Cartoon of a *C. elegans* hermaphrodite with colors illustrating insulin expression in six major tissue types: nervous system (green), reproductive tissue (blue), muscle (gray), epithelial tissue (orange), coelomocytes (pink), and alimentary system (purple).

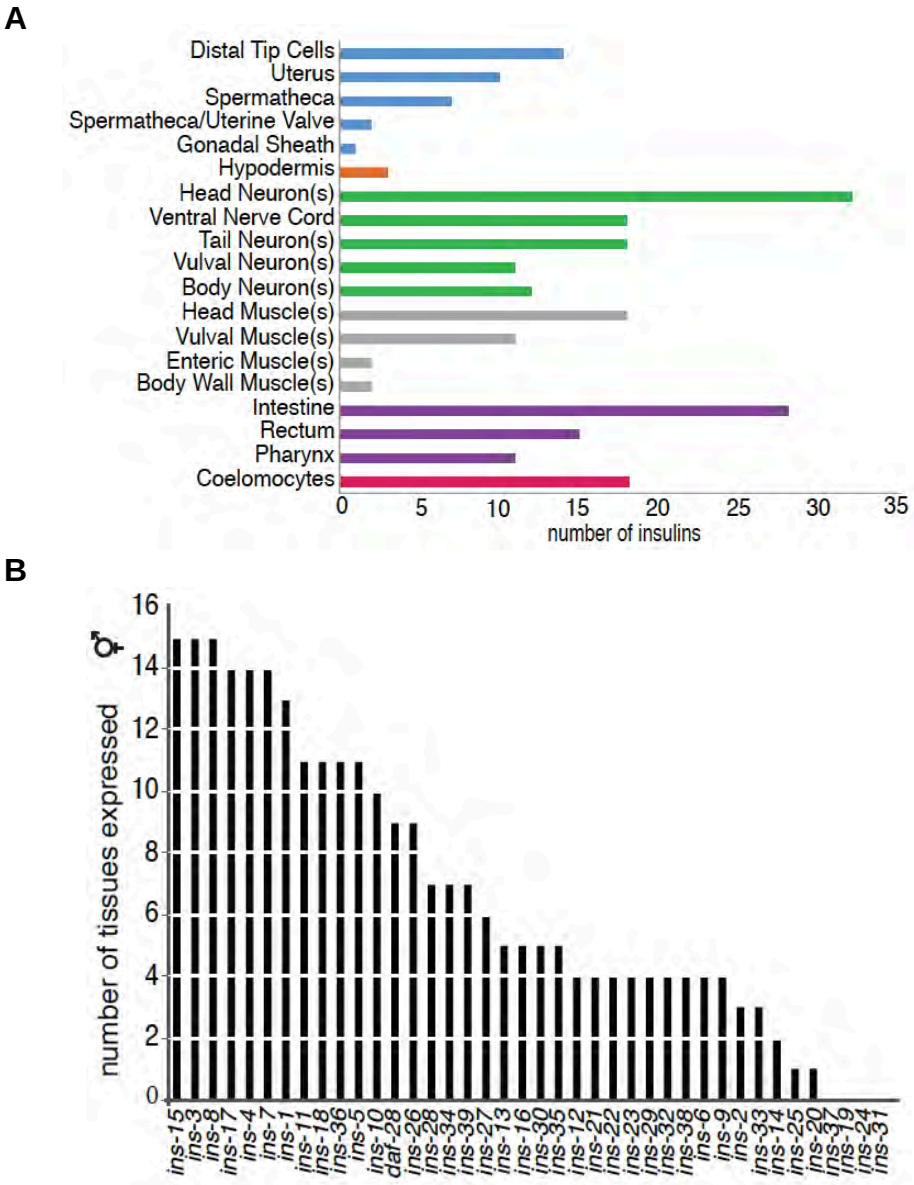

FIGURE 2.4: Spatial expression of the 36/40 insulins expressed in *C. elegans* young adult hermaphrodites. *(A)* Number of insulins expressed in each tissue/cell type. Colors correspond to the six major tissue types in Figure 7. *(B)* Number of tissues/cell types in which each insulin is expressed.

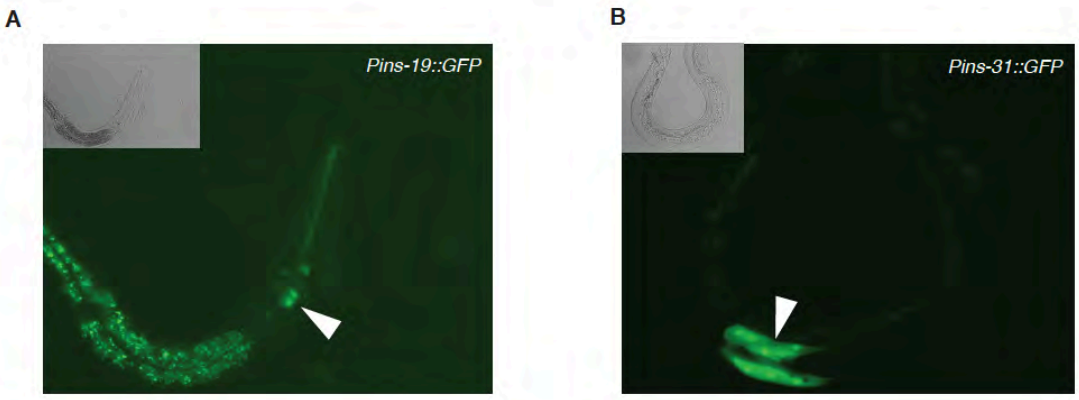

FIGURE 2.5: Insulin expression in males. *(A) Pins-19::GFP* transgenic strains show GFP expression in head neurons (arrowhead). *(B) Pins-31::GFP* transgenic strains show GFP expression in the gonad (arrowhead).

tissues. For seven insulins we found different expression patterns than reported previously. For example, we observed *ins-22* expression in head neurons, but not in the ventral nerve cord, body and tail neurons as reported previously [56]. Differences in insulin expression may result from the inclusion or exclusion of particular regulatory sequences in the promoter fragments used. Alternatively, expression pattern annotation may not have been examined with the same resolution in different studies and weak expression may have been missed. Indeed, for two strains, we observed additional expression patterns in previously published strains that were not reported (Fig. 2.6).

Next, we examined the expression patterns for the 36 insulins expressed in hermaphrodites. Almost all insulins are expressed in neurons, consistent with the reported importance of neuronal insulin signaling in different organisms [115]. Head neurons express the greatest number of insulins (n=32, Fig. 2.4A). We grouped head neuron expression into three classes: sensory (including amphid neurons), pharyngeal and ring motor/interneurons (Fig. 2.7A). As amphid sensory neurons are exposed to the environment, many can be visualized by DiI staining [116]. We stained all transgenic strains with DiI and annotated any overlap between DiI staining and GFP expression. DiI staining was also used to provide orientation for determining which insulins were expressed in each category of head neurons (Fig. 2.7B). In total, 25 insulins are expressed in sensory neurons, 14 of which are expressed in amphid neurons, 23 insulins in ring motor/interneurons and 13 in pharyngeal neurons. Twenty-two insulins are expressed in two or more general types of head neurons (Fig 2.7C).

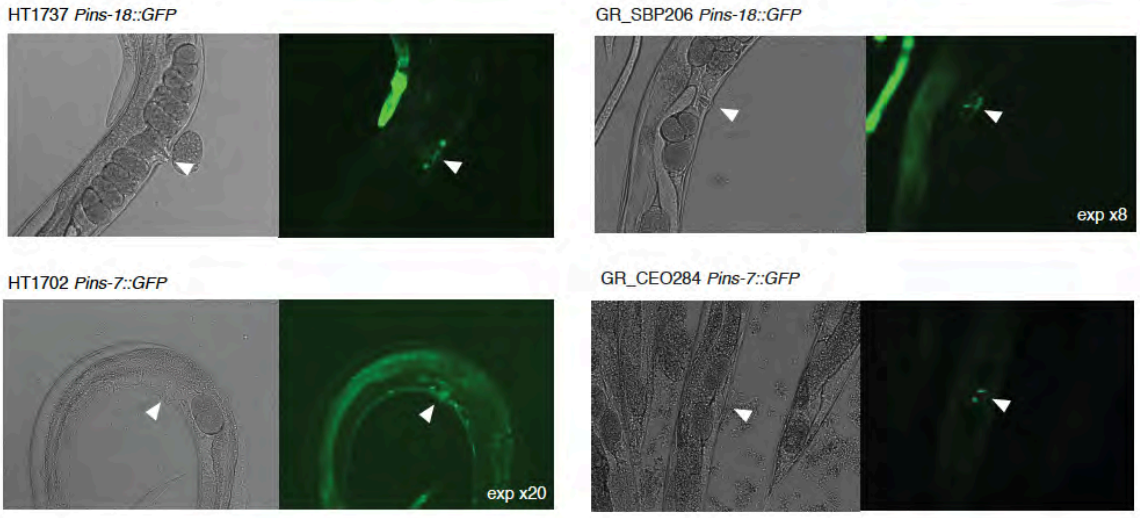

FIGURE 2.6: Previously published *Pins::GFP* transgenic strains illustrating GFP expression in the vulva (white arrowhead). This tissue expression was missed in previous publications.

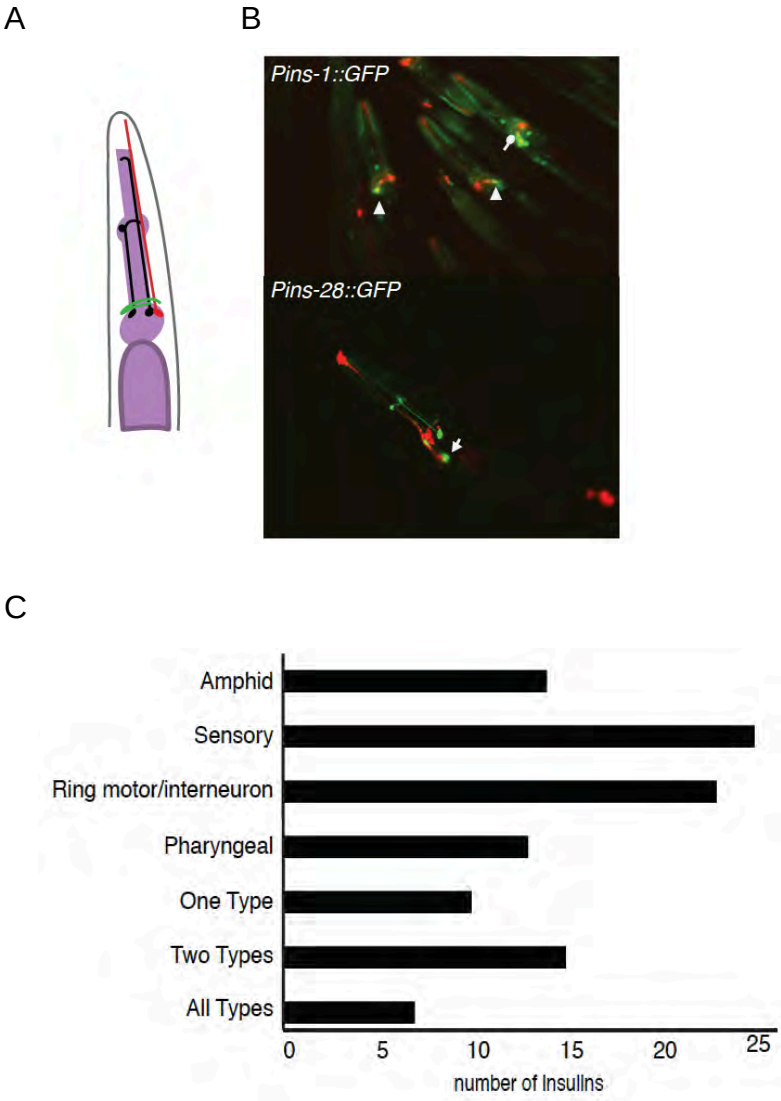

FIGURE 2.7: Insulin genes are expressed in head neurons. (*A)* Cartoon of three head neuron categories: sensory (red), pharyngeal (black), ring motor/interneurons (green). *(B)* Two examples: *Pins-1::GFP* exhibits GFP expression in many head neurons including amphid sensory neurons (arrow heads) and ring interneurons (circle arrow). *Pins-28::GFP* exhibits GFP expression in pharyngeal, but not amphid neurons (arrows). Amphid neurons were visualized by DiI staining (red). Yellow indicates that GFP expression (green) occurred in amphid neurons (red). *(C)* Summary of neuronal insulin expression in three types of head neurons: sensory, ring motor/interneuron, and pharyngeal. Insulins that exhibited overlapping GFP expression and DiI staining are defined as having amphid expression.

Dynamic changes in insulin expression during development

To determine insulin expression changes during development, we annotated GFP expression at each larval stage (L1-L4), in young adults and mature adults. A value of 1 or 0 was assigned to each tissue/cell type to indicate the presence or absence of GFP expression, respectively (Table 2.3). To capture tissue expression changes through development, we visualized the data into bipartite expression networks [97], [109]. These networks contain two types of nodes: genes and cells/tissues. Edges link the gene to the tissue in which it is expressed. We visualized insulin expression patterns into networks for each of the developmental stages by using Cytoscape [117] (Fig 2.8; Fig. 2.9A). Several tissues showed loss of insulin expression as the animals progress through development. For example, in 11 transgenic strains, GFP was expressed in the pharynx in early larval stages but only three insulin promoters remained active in the adult pharynx (Fig. 2.9B). Most tissues showed increased insulin expression during development, particularly when animals entered the L4 stage. For example, 14 insulins are expressed in the distal tip cell at the young adult stage but only one (*ins-13*) exhibited expression early, at the L2 stage (Fig. 2.9B). Some tissues/cells are formed later in development, which explains later expression; for instance the vulva, spermatheca, uterus and gonad have not fully developed until late-L4 and adult stages. Overall, insulins exhibit dynamic stage- and tissue-specific expression patterns during development (Fig. 2.10).

Gene	I	PI	DTC	GS	HM	BM	VM	EM	SN	RIM	PN	BN	VN	TN	VNC	P	H	SU	C	S	U	R
daf-28	0	1	1	0	0	0	1	0	1	1	0	0	0	1	1	1	0	0	0	0	1	0
ins-01	0	1	1	0	1	0	1	0	1	1	1	1	1	1	1	0	0	0	1	0	0	1
ins-02	1	1	0	0	1	0	0	0	0	0	0	0	0	0	0	0	0	0	0	0	0	0
ins-03	1	1	1	0	1	1	1	0	1	1	0	0	1	1	1	0	0	1	1	1	0	1
ins-04	0	1	1	0	1	0	1	0	1	1	1	1	1	1	1	0	1	0	1	1	0	0
ins-05	0	1	0	0	1	0	0	0	1	1	1	1	1	1	1	0	0	0	1	0	0	1
ins-06	0	1	0	0	0	0	0	0	1	1	0	0	0	0	0	0	0	0	0	0	1	0
ins-07	0	1	1	0	1	0	1	0	1	1	1	1	1	1	1	0	0	0	1	0	1	1
ins-08	0	1	1	0	1	0	1	0	1	1	1	1	1	1	1	0	0	0	1	1	1	1
ins-09	0	0	0	0	0	0	0	0	1	1	0	0	0	1	0	0	0	0	1	0	0	0
ins-10	0	1	0	0	1	0	0	0	0	1	1	1	1	1	1	0	0	0	1	0	0	1
ins-11	0	1	1	0	1	0	0	0	1	1	1	0	0	1	1	1	0	0	1	0	0	1
ins-12	0	1	0	0	0	0	0	0	1	1	0	0	0	0	0	0	0	0	0	0	0	1
ins-13	0	1	1	0	0	0	0	0	0	1	0	0	0	0	0	0	0	0	0	0	0	1
ins-14	0	0	0	0	0	0	0	0	1	1	0	0	0	0	0	0	0	0	0	0	0	0
ins-15	0	1	1	0	1	0	1	0	0	1	1	1	1	1	1	0	0	1	1	1	1	1
ins-16	0	1	1	0	0	0	0	0	1	1	0	0	0	0	0	1	0	0	0	0	0	0
ins-17	0	1	1	0	1	0	1	0	0	1	1	1	1	1	1	0	0	0	1	1	1	1
ins-18	0	1	1	0	1	0	0	0	1	0	1	1	1	1	1	0	0	0	1	1	0	0
ins-19	0	0	0	0	0	0	0	0	0	0	0	0	0	0	0	0	0	0	0	0	0	0
ins-20	0	0	0	0	0	0	0	0	1	0	0	0	0	0	0	0	0	0	0	0	0	0
ins-21	0	1	0	0	0	0	1	0	1	0	0	0	0	0	0	0	0	0	0	1	0	0
ins-22	0	0	0	0	0	0	1	0	1	0	0	0	0	0	0	1	0	0	0	0	0	1
ins-23	0	0	0	1	0	0	0	1	1	0	0	0	0	0	0	1	0	0	0	0	0	0
ins-24	0	0	0	0	0	0	0	0	0	0	0	0	0	0	0	0	0	0	0	0	0	0
ins-25	0	0	0	0	0	0	0	0	0	1	0	0	0	1	0	0	0	0	0	0	0	0
ins-26	0	1	0	0	1	0	0	0	0	1	1	1	0	1	1	1	0	0	1	0	0	0
ins-27	0	0	1	0	1	1	1	1	0	0	0	0	0	0	0	0	1	0	0	0	0	0
ins-28	0	1	0	0	0	0	0	0	0	1	1	1	1	1	0	0	0	0	1	0	0	0
ins-29	0	1	0	0	0	0	0	0	1	0	0	0	0	0	0	1	0	0	1	0	0	0
ins-30	0	1	0	0	1	0	0	0	1	0	0	1	0	0	0	1	0	0	0	0	0	0
ins-31	0	0	0	0	0	0	0	0	0	0	0	0	0	0	0	0	0	0	0	0	0	0
ins-32	0	1	0	0	0	0	0	0	1	0	0	0	0	1	1	0	0	0	0	0	0	0
ins-33	0	1	0	0	1	0	0	0	0	0	0	0	0	0	0	0	1	0	0	0	0	0
ins-34	0	1	0	0	1	0	0	0	0	0	0	0	0	0	1	1	0	0	1	0	1	1
ins-35	0	1	0	0	0	0	0	0	1	1	0	0	0	0	1	0	0	0	0	0	0	1
ins-36	0	1	0	0	1	0	0	0	1	1	1	0	0	0	1	1	1	0	1	0	1	1
ins-37	0	1	0	0	0	0	0	0	0	0	0	0	0	0	0	0	0	0	0	0	0	0
ins-38	0	0	0	0	0	0	0	0	1	1	0	0	0	0	1	0	0	0	1	0	0	0
ins-39	1	1	1	0	0	0	0	0	1	0	0	0	0	1	0	1	0	0	0	0	1	0

TABLE 2.3: Insulin expression annotation. GFP expression was examined in each *Pins::GFP* line throughout the animal. Expression in a tissue is indicated by a “1”; whereas, no expression is indicated by a “0”. Tissues are assigned as follows: I, intestine, PI, partial intestine; DTC, distal tip cell; GS, gonadal sheath; HM, head muscle; BM, body muscle; VM, vulva muscle; EM, enteric muscle; SN, sensory head neuron; RIM, ring interneuron/motor head neuron; PN, pharyngeal head neuron; BN, body neuron; VN, vulva neuron; TN, tail neuron; VNC, ventral nerve cord; P, pharynx; SU, spermatheca/uterine valve; C, coelomocytes; S, spermatheca; U, uterus; R, rectum.

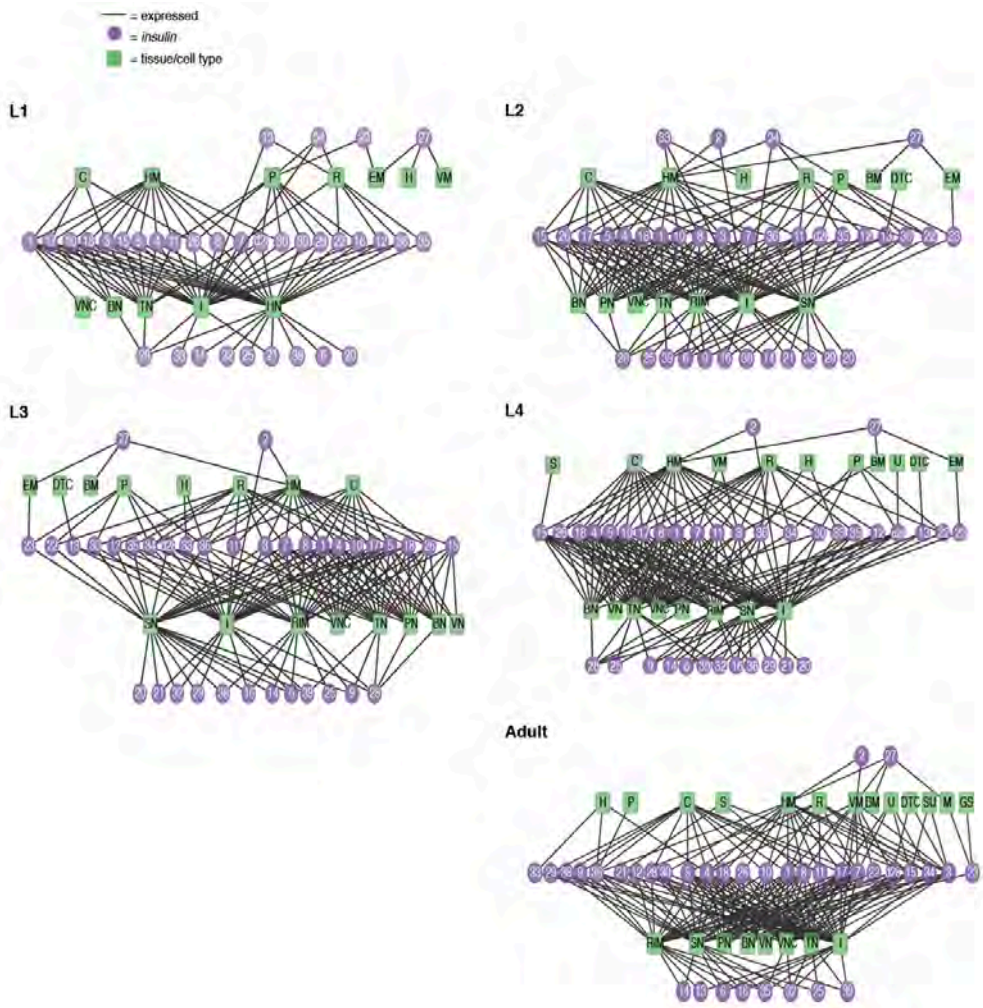

FIGURE 2.8 Insulin expression networks for each developmental stage. Bipartite networks of spatial expression of 36 insulins in the following stages of *C. elegans* hermaphrodites: L1, L2, L3, L4, Adult (~3-4 day old adult with eggs). See Fig. 12 for Young Adult stage. Circles represent insulins; squares represent cells/tissues as follows: S, spermatheca; C, ceolomocytes; R, rectum; HM, head muscle; VM, vulva muscle; DTC, distal tip cell; U, uterus; BM, body muscle; H, hypodermis; EM, enteric muscle; P, pharynx; BN, body neuron(s); VN, vulva neuron(s); TN, tail neuron(s); VNC, ventral nerve cord; HN, head neuron; PN, pharyngeal neuron(s); RIM, ring/intermotor neuron(s); SN, sensory neuron(s); I, intestine. An edge defines GFP expression of an insulin in that tissue. The network is organized as follows: (top to bottom) insulins with no neuronal expression; non-neuronal tissues (excluding the intestine); insulins with neuronal and non-neuronal tissue expression; neuronal tissues and the intestine, insulins with only neuronal and/or intestinal expression.

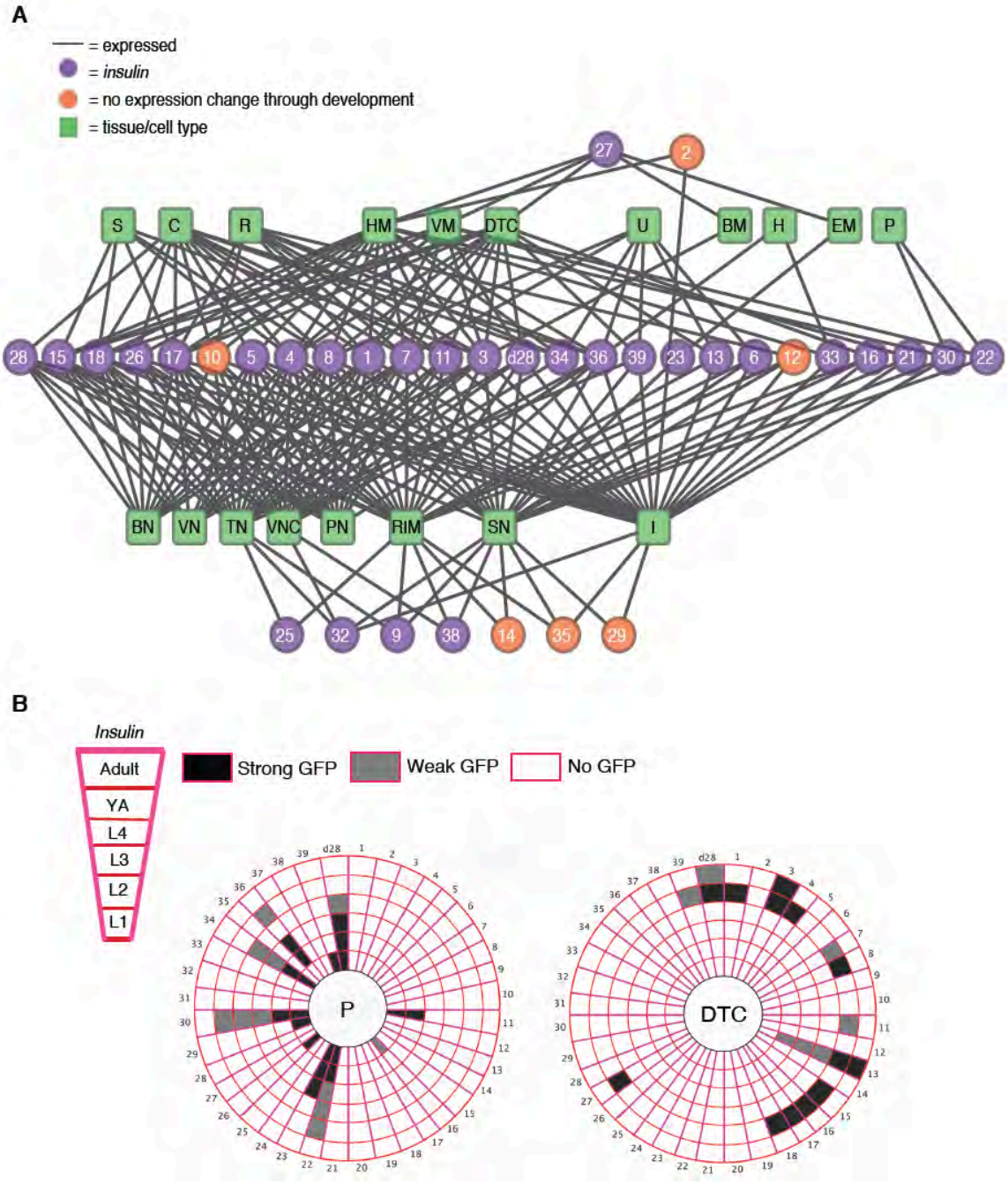
A
= expressed
= insulin
= no expression change through development
= tissue/cell type
27
2
S
C
R
HM
VM
DTC
U
BM
H
EM
P
28
15
18
26
17
10
5
4
8
1
7
11
3
d28
34
36
39
23
13
6
12
33
16
21
30
22
BN
VN
TN
VNC
PN
RIM
SN
I
25
32
9
38
14
35
29
B
Insulin
Adult
YA
L4
L3
L2
L1
Strong GFP
Weak GFP
No GFP
P
DTC

(continued from previous page)

FIGURE 2.9: Insulin expression networks illustrate dynamic tissue activity. *(A)* Bipartite network connecting 35 insulins to cell/tissues at the young adult stage. *Pins-20::GFP* animals did not exhibit GFP expression at the young adult stage and were excluded. Circles represent insulins; squares represent cells/tissues: S, spermatheca; C, ceolomocytes; R, rectum; HM, head muscle; VM, vulva muscle; DTC, distal tip cell; U, uterus; BM, body muscle; H, hypodermis; EM, enteric muscle; P, pharynx; BN, body neuron(s); VN, vulva neuron(s); TN, tail neuron(s); VNC, ventral nerve cord; PN, pharyngeal neuron(s); RIM, ring/intermotor neuron(s); SN, sensory neuron(s); I, intestine. Purple circles indicate insulins that change in spatial expression through development; orange circles are insulins that do not change. The network is organized as follows: (top to bottom) insulins with no neuronal expression; non-neuronal tissues (excluding the intestine); insulins with neuronal and non-neuronal tissue expression; neuronal tissues and the intestine, insulins with only neuronal and/or intestinal expression. *(B)* “Dartboards” depicting tissue-centered view of insulin expression. Each ring represents a developmental stage, starting from the center: larval stages L1, L2, L3 and L4, young adult and adult with eggs (~3-4 day old adult). Each slice represents an insulin with strong GFP (black), weak GFP (gray) or no GFP (white) expression. Left – dartboard profile of the pharynx (P); Right – dartboard profile of the distal tip cell (DTC)

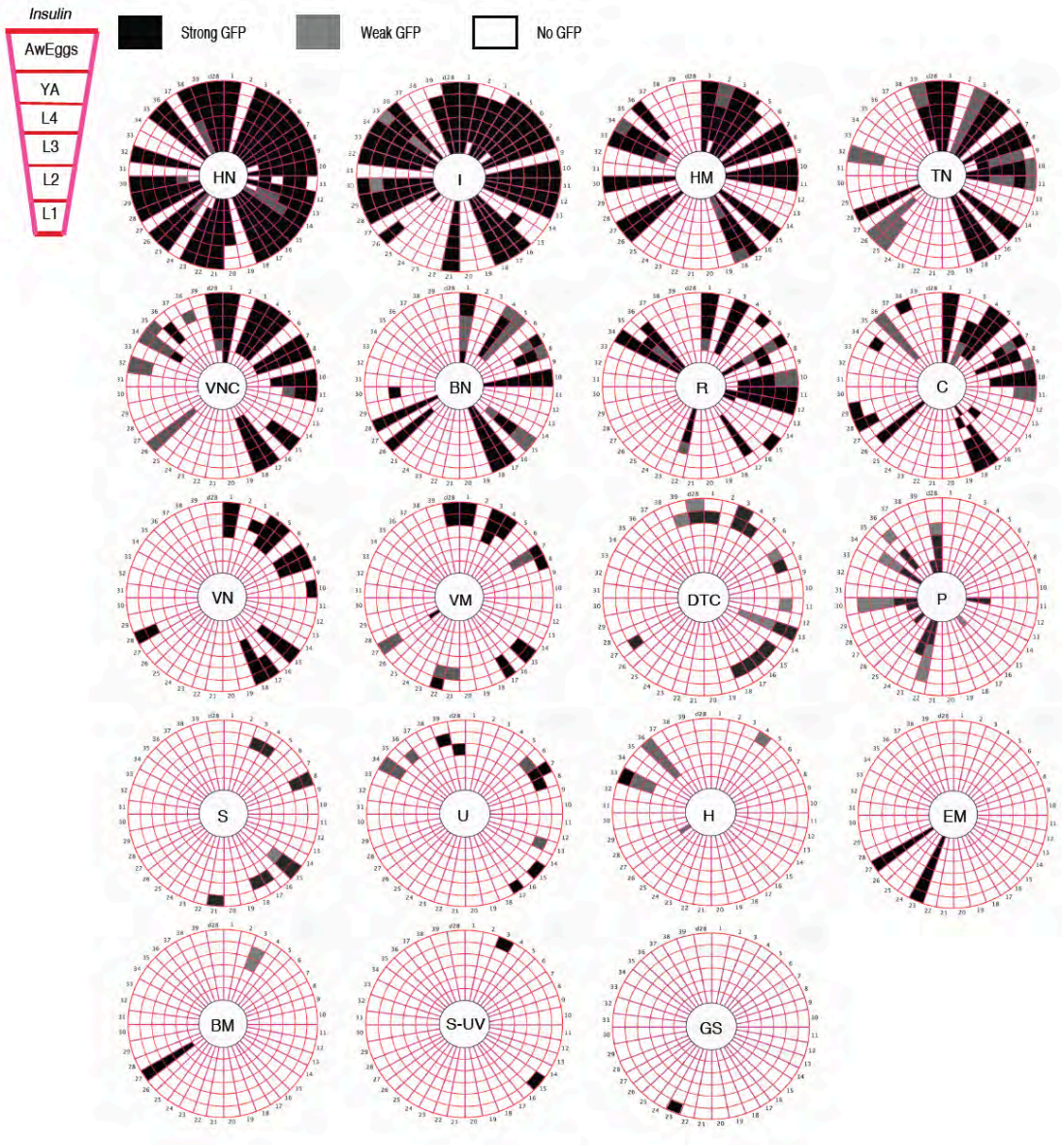

FIGURE 2.10: Tissue-centered dartboards illustrating insulin expression. Each ring represents a developmental stage, starting from the center: larval stages L1, L2, L3 and L4, Young Adult and Adult (~3-4 day old adult with eggs). Each slice represents an insulin with strong GFP (black), weak GFP (gray) or no GFP (white) expression. Tissues are assigned as follows: HN, head neurons; I, intestine; HM, head muscle; TN, tail neuron; VNC, ventral nerve cord; BN, body neuron; R, rectum; C, coelomocytes; VN, vulva neuron; VM, vulva muscle; DTC, distal tip cell; P, pharynx; S, spermatheca; U, uterus; H, hypodermis; EM, enteric muscle; BM, body muscle; SU, spermatheca/uterine valve; GS, gonadal sheath.

Conditional dynamics of insulin expression

The IIS pathway not only modulates *C. elegans* development, it is also utilized to respond to environmental conditions [112]. We investigated insulin expression in young adult transgenic strains exposed to relevant conditions including heat stress, dauer diapause, starvation, aging, oxidative stress, and glucose, and visually examined changes in GFP expression (Fig 2.11A; Fig 2.12).

Neither glucose nor oxidative stress affected insulin expression. However, we did observe changes in insulin expression with the other conditions. The greatest number of insulins changed expression in dauers (n=14) and with age (n=14); major phenotypic outputs of IIS pathway. Increased and decreased insulin expression was observed for all conditions, except heat stress. For example, ten insulins decreased in expression in dauer, whereas four increased. We also observed stage-specific responses in insulin expression. For instance, GFP expression increased dramatically after heat stress in L4 *Pins-4::GFP* hermaphrodites, but not in young adults (Fig. 2.12B). In total, four genes, *ins-3, ins-7, ins-11* and *ins-30,* exhibited changes in GFP expression in three conditions tested, four changed in two, 17 in one, and 14 did not change in any of the conditions tested.

We also observed specific conditional changes in spatial expression (Fig. 2.11; Fig. 2.13). *Pins-27::GFP*, for example, exhibits GFP expression in muscle in all stages of development, and muscle expression decreased as the animals age (Fig. 2.11B). This could reflect a loss of muscle integrity known to occur during the aging process [34] and perhaps the *Pins::27*::GFP transgenic

A

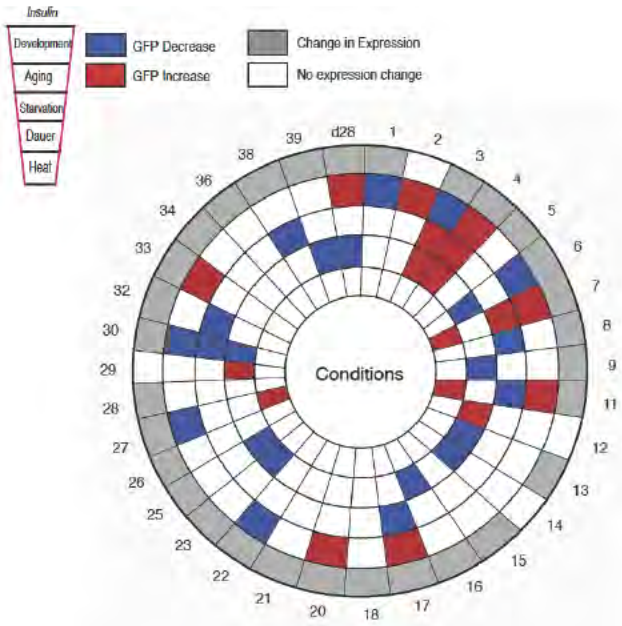

B

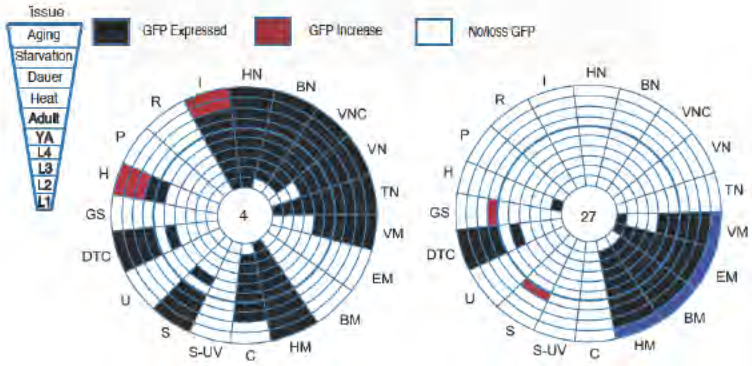

FIGURE 2.11: Conditional dynamics of insulin expression. *(A)* Dartboard depicting conditional changes in insulin expression. Each ring represents a condition; starting from the center, heat stress, dauer, starvation, aging and development. Each slice represents a different insulin. For each condition, activity is defined by at least one tissue exhibiting an increase (red) or decrease (blue) in GFP expression. Changes in expression pattern (gray) were recorded throughout development. *(B)* Dartboards depicting gene-centered view of insulin expression. Each ring represents a developmental stage or condition, starting from the center: L1, L2, L3 and L4, young adult and adult (~3-4 day old adult), heat stress, dauer, starvation, and aging. Each slice represents a tissue with GFP expression (black), no GFP (white) expression. Compare conditional changes to the young adult stage (5th ring). Red indicates a GFP increase; black, no change in GFP expression; white, no GFP observed. Left – dartboard of *ins-4* expression; Right – dartboard of *ins-27* expression.

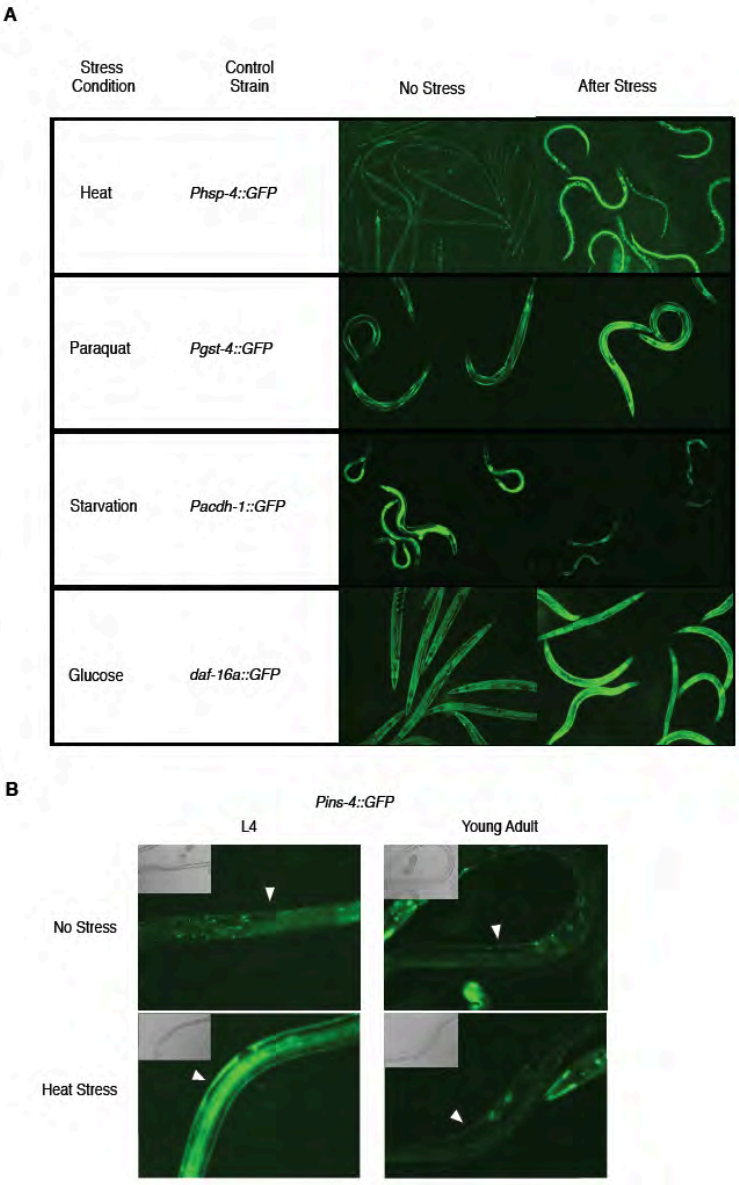

FIGURE 2.12: Environmental effects on insulin expression. *(A)* Controls for conditional expression changes. Environmental conditions (see Methods) were tested to ensure that each would illicit a biological response from the animal. A reporter transgenic strain harboring a gene previously illustrated to respond to the respective condition was used as follows: *Phsp-4::GFP* for heat stress, *Pgst-4::GFP* for paraquat, *Pacdh-1::GFP* for starvation, *daf-16a::GFP* for glucose. *(B) ins-4* stage-specific responses to heat stress. Under normal conditions (no stress), L4 and young adult stage *Pins-4::GFP* hermaphrodites do not express GFP in the hypodermis (top left and top right). After heat stress, GFP is expressed in the hypodermis of L4 (bottom left) but not young adult (bottom right) hermaphrodites (white arrowheads).

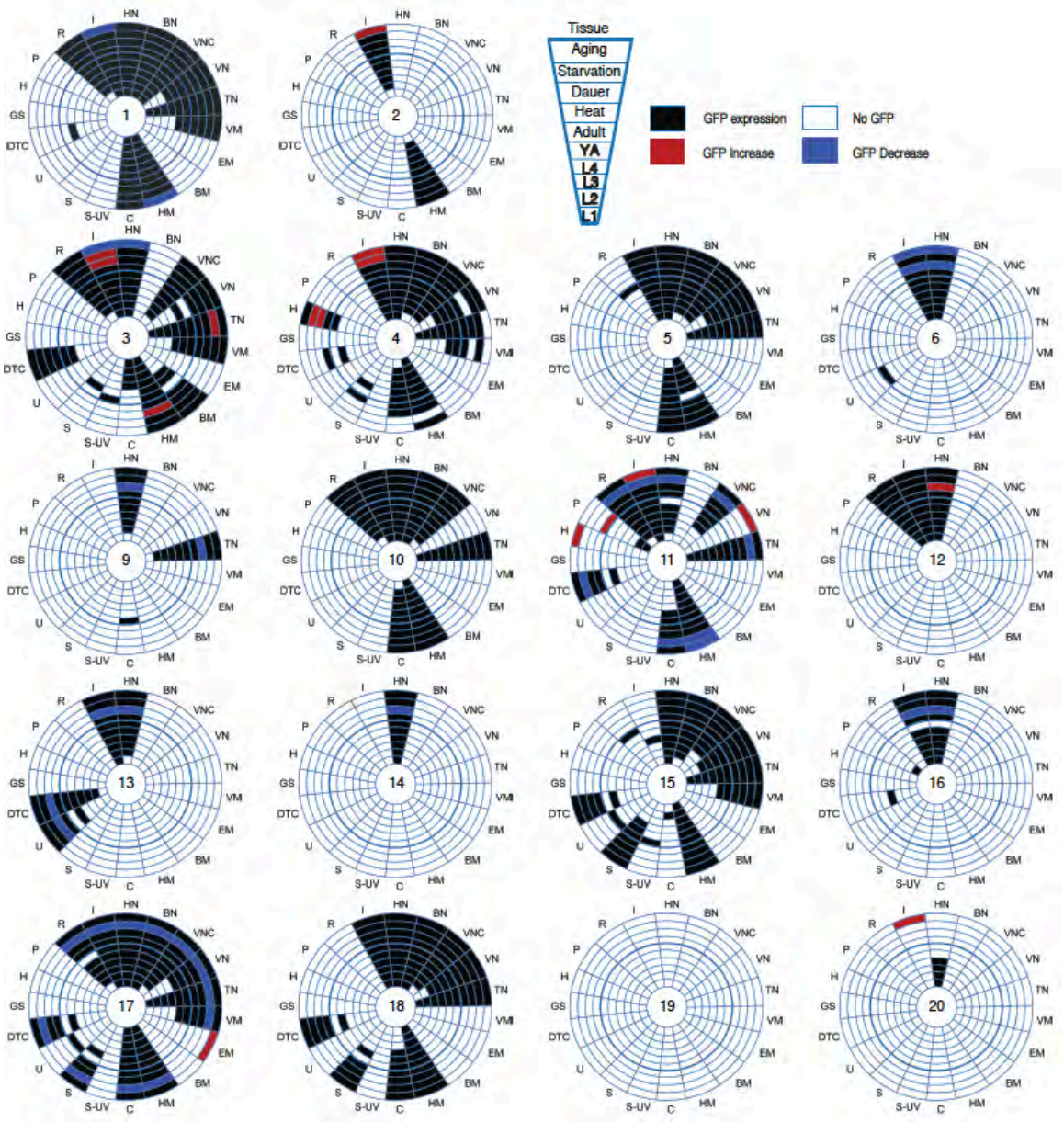
Tissue
Aging
Starvation
Dauer
Heat
Adult
YA
L4
L3
L2
L1
GFP expression
No GFP
GFP Increase
GFP Decrease
HN
BN
VNC
VN
TN
VM
EM
BM
HM
S-UV
C
S
U
DTC
GS
H
P
R
I
1
2
3
4
5
6
9
10
11
12
13
14
15
16
17
18
19
20

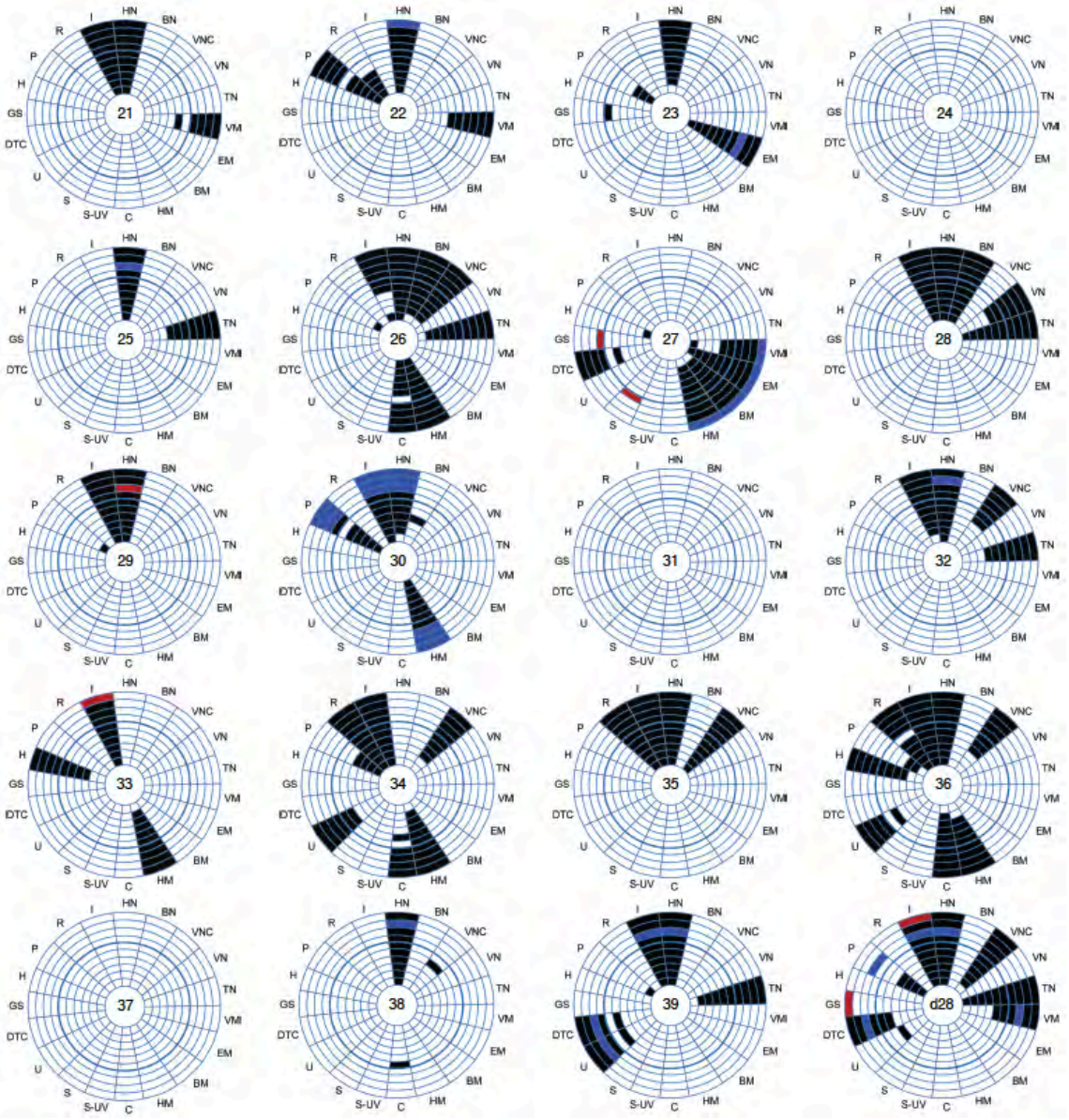
21
22
23
24
25
26
27
28
29
30
31
32
33
34
35
36
37
38
39
d28
HN
BN
VNC
VN
TN
VMI
EM
BM
HM
C
S-UV
S
U
DTC
GS
H
P
R
I

(continued from previous page)

FIGURE 2.13: Gene-centered dartboards illustrating insulin expression. Each ring represents a developmental stage or environmental condition, starting from the center: larval stages L1, L2, L3 and L4, Young Adult and Adult (~3-4 day old adult with eggs), heat stress, dauer, starvation and aging. Each slice represents a tissue with GFP expression (black), no GFP (white), GFP increase (red) or GFP decrease (blue). The number in the center indicates the insulin (*i.e.* 1 = *ins-1*; d28 = *daf-28*). Tissues are assigned as follows: HN, head neurons; I, intestine; HM, head muscle; TN, tail neuron; VNC, ventral nerve cord; BN, body neuron; R, rectum; C, coelomocytes; VN, vulva neuron; VM, vulva muscle; DTC, distal tip cell; P, pharynx; S, spermatheca; U, uterus; H, hypodermis; EM, enteric muscle; BM, body muscle; SU, spermatheca/uterine valve; GS, gonadal sheath.

strain may provide a convenient marker to observe the aging process in living animals**.** Another example is in *Pins-4::GFP* animals where GFP expression changes similarly in different conditions: it increases dramatically in the hypodermis of young adults after starvation and aging animals (Fig. 2.11B).

Comparing insulin expression patterns

We quantified the degree of expression overlap for pair-wise combinations of insulins at each stage of development using a Tissue Overlap Coefficient (TsOC) similarity index (Fig. 2.14A) [97], [109]. TsOC values were clustered to visually identify genes that share high overlap *versus* those with little to no overlap in expression. At the young adult stage, we observed two clusters of insulins that share high overlap (Fig. 2.14B). The lack of pair-wise gene expression clustering correlates with the lack of pair-wise phenotypic redundancy, indicating that there may be more complex patterns of redundancy. We next investigated to what degree expression overlap changes through development. Of 630 possible insulin pair-wise comparisons (of 36 insulins examined), 37 pairs, consisting of 22 genes, had a TsOC of zero throughout development, illustrating their mutually exclusive expression. There was no insulin that exhibited a unique expression pattern (*i.e.*, with a TsOC=0 with every other insulin). Further, although eleven insulin pairs consisting of 19 insulins exhibited complete overlap (TsOC=1) in a single larval stage, none exhibited complete overlap throughout development. Even though the degree of overlap between insulins changed from one larval stage to the next, most remained consistently higher or lower in their degree of expression overlap (Table 2.4).

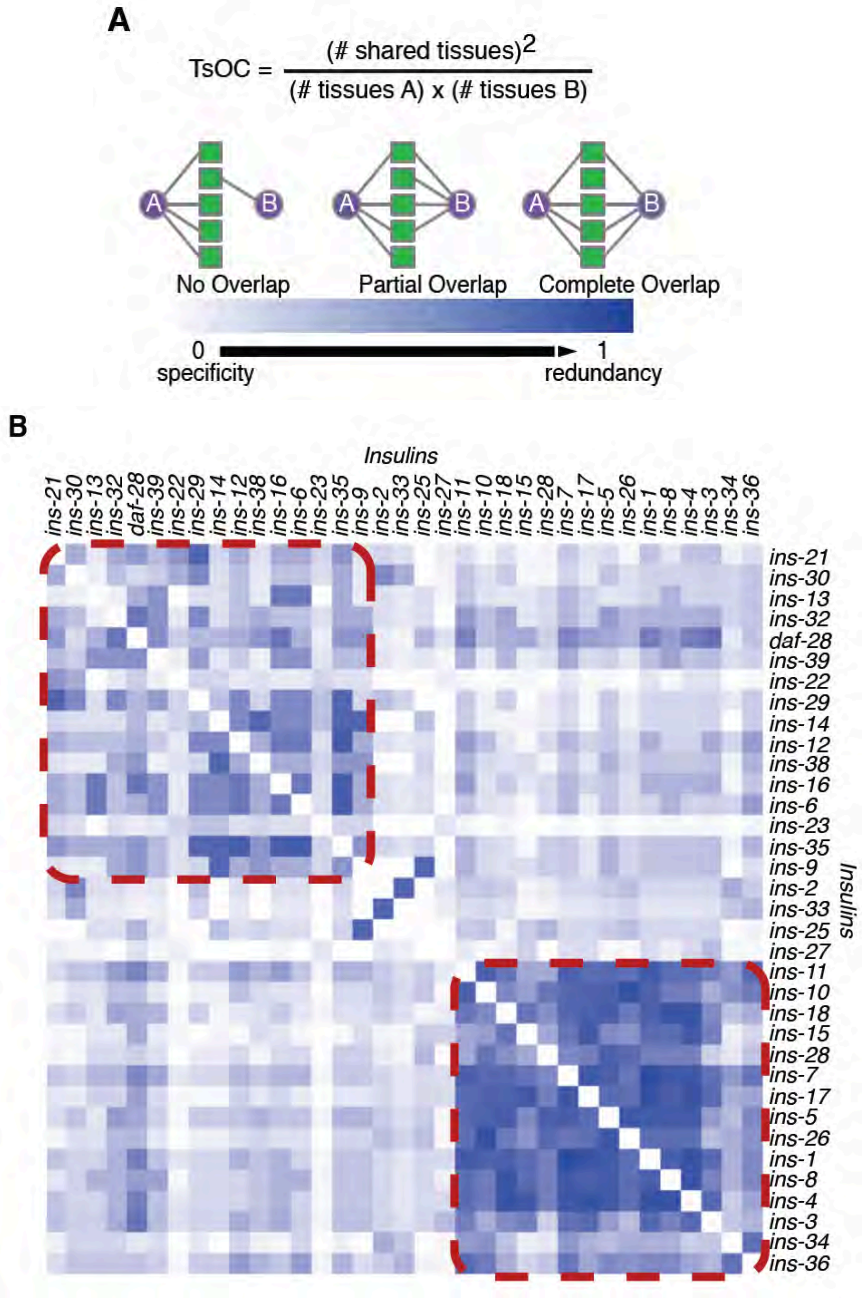

FIGURE 2.14: Comparing insulin gene expression illustrates specificity and overlap in expression. *(A)* Tissue overlap coefficients (TsOCs) define the expression overlap between all pairwise insulins (A and B). Insulins (circles) exhibit GFP expression (edges) in *C. elegans* tissues (squares). A TsOC of 1 indicates complete overlap while a TsOC of 0 indicates no overlap in expression. *(B)* Tissue overlap matrix using TsOC scores from the young adult stage. Red boxes highlight visually delineated clusters of highly overlapping insulins.

Gene Pair	L1 (no HN annot)	Gene Pair	L2	Gene Pair	L3	Gene Pair	L4	Gene Pair	YA	Gene Pair	AwEggs	Gene Pair	AVG of ALL
Top 50 pairs with highest TsOC scores													
4:5	1 000	4:5	1.000	29:32	1.000	4:5	1 000	1:7	0.929	38:9	1.000	4:5	0.891
38:6	1 000	29:32	1.000	21:32	1.000	32:39	1 000	10:26	0 889	16:6	1.000	14:38	0.889
32:6	1 000	21:32	1.000	21:29	1.000	21:29	1 000	4:8	0 852	1:7	0.923	1:17	0.847
32:38	1 000	21:29	1.000	16:6	1.000	16:6	1 000	17:4	0 852	17:7	0.846	4:8	0.841
29:39	1 000	16:6	1.000	14:38	1.000	14:38	1 000	1:4	0 852	1:4	0.840	10:17	0.840
25:6	1 000	14:38	1.000	12:35	1.000	12:35	1 000	1:17	0 852	1:5	0.833	12:35	0.830
25:38	1 000	12:35	1.000	10:17	1.000	10:17	1 000	18:8	0 846	1:10	0.833	1:4	0.829
25:32	1 000	1:5	0.900	4:5	0.900	1:8	1 000	18:4	0 846	10:5	0.810	16:6	0.816
20:6	1 000	1:4	0.900	1:4	0.900	5:8	0.909	26:5	0 800	4:7	0.776	1:5	0.799
20:38	1 000	1:17	0.900	1:17	0.900	4:8	0.909	7:8	0.791	5:7	0.769	21:29	0.796
20:32	1 000	5:8	0.889	1:10	0.900	1:5	0.909	4:7	0.791	10:7	0.769	18:4	0.792
20:25	1 000	4:8	0.889	4:8	0.889	1:4	0.909	17:7	0.791	4:8	0.758	1:7	0.789
16:39	1 000	26:5	0.889	1:5	0.810	18:5	0.900	5:8	0.769	17:4	0.758	18:5	0.788
16:29	1 000	26:4	0.889	5:8	0.800	18:4	0.900	4:5	0.769	1:8	0.758	5:8	0.783
14:6	1 000	17:26	0.889	18:5	0.800	7:8	0 826	15:4	0.769	1:17	0.758	1:10	0.776
14:38	1 000	1:8	0.800	1:8	0.800	1:7	0 826	15:17	0.769	35:6	0.750	17:4	0.761
14:32	1 000	1:7	0.800	1:7	0.800	18:8	0 818	1:5	0.769	18:4	0.750	1:8	0.750
14:25	1 000	1:3	0.800	1:3	0.800	17:8	0 818	1:11	0.769	16:35	0.750	4:7	0.744
14:20	1 000	1:26	0.800	17:4	0.790	10:8	0 818	35:6	0.750	12:6	0.750	7:8	0.741
12:36	1 000	17:5	0.790	10:4	0.790	1:18	0 818	16:35	0.750	12:16	0.750	10:5	0.719
10:18	1 000	17:4	0.790	26:4	0.778	1:17	0 818	12:35	0.750	1:18	0.750	5:7	0.719
1:17	0 857	18:5	0.778	17:26	0.778	1:10	0 818	18:5	0.736	10:17	0.736	1:18	0.716
17:3	0 833	18:4	0.778	10:26	0.778	17:26	0.778	17:8	0.716	18:5	0.711	35:6	0.708
17:18	0 833	10:17	0.778	7:8	0.766	10:26	0.778	1:8	0.716	10:18	0.711	17:26	0.705
10:17	0 833	7:8	0.766	3:8	0.766	11:36	0.766	5:7	0.714	28:5	0.700	17:7	0.696
5:7	0 800	3:8	0.766	3:7	0.766	35:6	0.750	11:7	0.714	10:28	0.700	14:6	0.694
4:7	0 800	3:7	0.766	35:6	0.750	16:35	0.750	10:5	0.711	10:26	0.700	10:26	0.691
3:5	0 800	26:8	0.766	16:35	0.750	12:6	0.750	10:11	0.711	7:8	0.699	38:9	0.689
3:4	0 800	11:7	0.766	12:6	0.750	12:16	0.750	28:5	0.700	18:7	0.692	18:8	0.686
18:5	0 800	35:6	0.750	12:16	0.750	5:7	0.736	17:18	0 699	4:5	0.675	10:4	0.682
18:4	0 800	16:35	0.750	17:5	0.711	4:7	0.736	1:18	0 699	10:4	0.675	17:5	0.681
18:28	0 800	15:26	0.750	10:5	0.711	3:7	0.736	10:17	0 692	17:8	0.669	17:8	0.677
10:5	0 800	12:6	0.750	26:5	0.700	11:8	0.727	1:10	0 692	14:9	0.667	26:5	0.676
10:4	0 800	12:16	0.750	1:26	0.700	11:7	0.727	29:35	0 667	14:6	0.667	10:7	0.670
10:28	0 800	10:28	0.714	4:7	0.681	1:11	0.727	25:9	0 667	14:38	0.667	26:4	0.669
d28:39	0.750	1:18	0.700	3:4	0.681	17:5	0.711	21:29	0 667	14:16	0.667	12:16	0.668
d28:29	0.750	1:10	0.700	18:4	0.681	17:4	0.711	2:33	0 667	13:6	0.667	14:9	0.667
d28:16	0.750	5:7	0.681	17:8	0.681	15:5	0.711	14:9	0 667	13:16	0.667	1:3	0.658
5:8	0.750	4:7	0.681	17:7	0.681	15:4	0.711	14:38	0 667	18:8	0.646	16:29	0.657
4:8	0.750	3:5	0.681	17:3	0.681	10:5	0.711	14:35	0 667	17:18	0.646	16:35	0.653
15:5	0.750	3:4	0.681	10:8	0.681	10:4	0.711	18:7	0 649	26:8	0.636	10:28	0.649
15:4	0.750	17:8	0.681	10:7	0.681	26:5	0.700	26:28	0 643	17:28	0.636	26:8	0.649
11:30	0.750	17:7	0.681	10:3	0.681	26:4	0.700	10:7	0 643	17:26	0.636	12:6	0.649
1:3	0.714	17:3	0.681	38:9	0.667	11:17	0 681	3:4	0 641	d28:3	0.600	3:7	0.647
1:18	0.714	38:9	0.667	38:6	0.667	10:11	0 681	17:3	0 641	10:11	0.600	17:18	0.643
1:10	0.714	38:6	0.667	32:6	0.667	38:9	0 667	1:3	0 641	36:4	0.593	18:7	0.639
35:36	0 667	32:6	0.667	32:39	0.667	38:6	0 667	11:5	0 640	28:4	0.583	29:32	0.639
22:35	0 667	32:39	0.667	29:6	0.667	29:6	0 667	11:36	0 640	26:4	0.583	21:32	0.639
21:8	0 667	29:6	0.667	29:39	0.667	29:39	0 667	17:5	0 623	1:28	0.583	10:18	0.637
21:39	0 667	29:39	0.667	21:6	0.667	29:32	0 667	15:8	0 623	1:26	0.583	1:26	0.632
21:36	0 667	21:6	0.667	21:39	0.667	25:9	0 667	11:8	0 623	5:8	0.582	38:6	0.630
Bottom 50 pairs with lowest TsOC scores													
23:32	0 000	10:32	0.071	15:16	0.056	27:34	0 067	15:2	0 050	15:21	0.030	21:26	0.092
23:3	0 000	10:29	0.071	14:17	0.056	27:30	0 067	14:15	0 050	15:16	0.030	17:29	0.091
23:28	0 000	10:21	0.071	13:15	0.056	16:34	0 067	13:27	0 050	28:34	0.029	28:33	0.091
23:25	0 000	10:14	0.071	10:38	0.056	13:34	0 067	11:23	0 050	27:36	0.028	30:38	0.091
22:33	0 000	28:33	0.067	10:32	0.056	13:30	0 067	d28:33	0 048	23:4	0.028	23:35	0.090
22:27	0 000	26:38	0.063	10:29	0.056	25:36	0 063	28:38	0 048	18:27	0.028	14:26	0.090
21:27	0 000	26:32	0.063	10:21	0.056	23:36	0 063	28:33	0 048	1:33	0.028	33:6	0.088
21:23	0 000	26:29	0.063	10:14	0.056	11:23	0 063	21:28	0 048	1:23	0.028	22:8	0.087
20:34	0 000	21:26	0.063	28:30	0.050	18:38	0 056	18:25	0 045	33:7	0.026	30:9	0.086
20:33	0 000	14:26	0.063	26:6	0.048	18:25	0 056	18:23	0 045	23:7	0.026	15:16	0.083
20:30	0 000	d28:33	0.056	26:39	0.048	18:23	0 056	14:18	0 045	10:27	0.025	21:25	0.083
20:27	0 000	17:38	0.056	26:33	0.048	17:38	0 056	23:3	0 042	15:27	0.023	12:23	0.083
20:23	0 000	17:32	0.056	26:27	0.048	17:29	0 056	21:26	0 042	d28:33	0.000	15:20	0.083
18:27	0 000	17:29	0.056	16:26	0.048	17:21	0 056	16:34	0 042	d28:2	0.000	14:18	0.082
18:23	0 000	17:21	0.056	13:26	0.048	15:38	0 056	27:39	0 040	34:9	0.000	23:36	0.081
17:27	0 000	15:6	0.056	27:8	0.042	15:29	0 056	23:8	0 038	34:39	0.000	10:14	0.081
17:23	0 000	15:39	0.056	27:7	0.042	15:21	0 056	23:4	0 038	34:38	0.000	15:35	0.081
16:27	0 000	15:33	0.056	27:3	0.042	14:18	0 056	17:29	0 038	33:9	0.000	15:39	0.080
15:34	0 000	15:27	0.056	23:8	0.042	14:17	0 056	14:17	0 038	33:39	0.000	22:4	0.077
15:33	0 000	15:16	0.056	23:7	0.042	14:15	0 056	1:23	0 038	33:38	0.000	d28:33	0.076
15:27	0 000	14:17	0.056	23:3	0.042	10:38	0 056	10:21	0 037	3:33	0.000	34:6	0.075
15:23	0 000	13:15	0.056	22:8	0.042	10:29	0 056	28:30	0 036	27:9	0.000	15:30	0.075
14:34	0 000	28:34	0.050	18:27	0.042	10:21	0 056	23:7	0 036	27:6	0.000	2:28	0.074
14:33	0 000	28:30	0.050	18:23	0.042	10:14	0 056	27:34	0 033	27:5	0.000	33:35	0.074
14:30	0 000	33:36	0.048	18:22	0.042	23:5	0 050	22:5	0 033	27:39	0.000	28:30	0.071
14:27	0 000	18:27	0.048	15:35	0.042	23:4	0 050	22:36	0 033	27:38	0.000	12:15	0.070
14:23	0 000	18:23	0.048	15:30	0.042	23:3	0 050	15:35	0 033	27:35	0.000	14:17	0.070
13:6	0 000	18:22	0.048	13:18	0.042	d28:33	0 048	15:33	0 033	27:33	0.000	13:15	0.067
13:38	0 000	13:18	0.048	12:15	0.042	26:6	0 048	15:22	0 033	27:32	0.000	11:23	0.067
13:32	0 000	10:27	0.048	28:34	0.040	26:39	0 048	15:21	0 033	27:29	0.000	27:33	0.067
13:27	0 000	10:22	0.048	27:4	0.037	26:33	0 048	11:22	0 033	27:28	0.000	20:28	0.063
13:25	0 000	27:8	0.042	27:36	0.037	26:32	0 048	18:22	0 030	25:34	0.000	11:20	0.063
13:23	0 000	27:7	0.042	23:4	0.037	26:27	0 048	22:8	0 026	25:33	0.000	13:18	0.062
13:20	0 000	27:3	0.042	22:4	0.037	16:26	0 048	17:22	0 026	25:30	0.000	d28:2	0.062
13:15	0 000	26:27	0.042	17:27	0.037	13:26	0 048	26:27	0 025	25:29	0.000	27:30	0.061
13:14	0 000	23:8	0.042	17:22	0.037	23:8	0 045	15:6	0 025	25:27	0.000	18:25	0.059
12:27	0 000	23:7	0.042	10:27	0.037	23:7	0 045	15:30	0 025	23:34	0.000	15:27	0.058
12:23	0 000	23:3	0.042	10:22	0.037	1:23	0 045	12:15	0 025	23:33	0.000	17:27	0.057
11:6	0 000	22:8	0.042	26:35	0.036	27:36	0 042	10:27	0 022	23:28	0.000	28:34	0.056
11:38	0 000	15:35	0.042	26:30	0.036	11:27	0 042	27:5	0 020	23:26	0.000	25:29	0.056
11:35	0 000	15:34	0.042	12:26	0.036	28:34	0 040	27:36	0 020	23:25	0.000	22:25	0.056
11:32	0 000	15:30	0.042	27:5	0.033	18:27	0 037	34:9	0 000	22:34	0.000	27:4	0.055
11:27	0 000	12:15	0.042	23:5	0.033	18:22	0 037	33:9	0 000	22:33	0.000	27:7	0.053
11:25	0 000	11:27	0.042	22:5	0.033	17:27	0 037	33:38	0 000	22:28	0.000	1:27	0.053
11:20	0 000	27:5	0.037	15:34	0.033	17:22	0 037	27:9	0 000	22:26	0.000	23:34	0.053
11:14	0 000	27:4	0.037	1:27	0.033	15:27	0 037	27:6	0 000	22:25	0.000	20:26	0.050
10:27	0 000	23:5	0.037	1:23	0.033	13:18	0 037	27:38	0 000	21:27	0.000	10:20	0.050
10:23	0 000	23:4	0.037	d28:27	0.000	10:27	0 037	27:35	0 000	21:25	0.000	27:34	0.050
1:27	0 000	22:5	0.037	34:9	0.000	10:22	0 037	27:32	0 000	2:9	0.000	15:33	0.049
1:23	0 000	22:4	0.037	34:38	0.000	26:35	0 036	27:29	0 000	2:6	0.000	11:27	0.048

All pairwise scores can be accessed at http://edgedb.umassmed.edu/IndexAction.do

(continued from previous page)

TABLE 2.4: Ranking of TsOC scores for each transgenic strain throughout development. “Gene pair” describes the pair-wise comparison between insulins. TsOC scores for all pair-wise combinations are ranked by life stage. Life stages are defined as: L1, L2, L3, L4, Young Adult and Adult (~3-4 day old adult with eggs). Each pairwise combination has been averaged across all 6 stages (AVG of ALL).

To capture the overall degree of overlap of the insulin expression patterns throughout the lifetime of the animal, we averaged the TsOCs between all stages. The top 5% TsOC values (TsOC ≥ 0.68) were distributed among 18 genes (Fig. 2.15A). Some insulins (*e.g., ins-4*), shared high overlap with many other genes in this group, while others, (*e.g., ins-26)*, shared high overlap with only two other genes.

Next, we quantified similarity in conditional expression. We first assigned the following values for each condition: -1 for a GFP decrease/loss, 0 for no changes, and +1 for a GFP increase/additional tissue expression. Then, using a Spearman rank test, we compared all pair-wise combinations to identify insulins that correlate in their response. A conditional overlap of 1, for example, indicates that two insulins responded the same under every condition tested. In contrast, a score of -1 indicates that two insulins responded oppositely. Of 325 pair-wise combinations (among 26 insulins that exhibit a conditional change), 23 insulin pairs, consisting of 18 genes, shared a score of -1, thus responding oppositely. Thirty-six pairs, consisting of 18 genes, shared a score of +1, thus responding the same under the conditions tested. Finally, no pair exhibited high correlation both during development and under different conditions (Fig. 2.15B, red box). This suggests that no insulins are completely coexpressed over all conditions and stages.

ins-8 expression increases upon loss of *ins-7*

Intuitively, one might expect that close homologs that share high expression overlap may exhibit redundancy. When we compared pairwise insulin

A

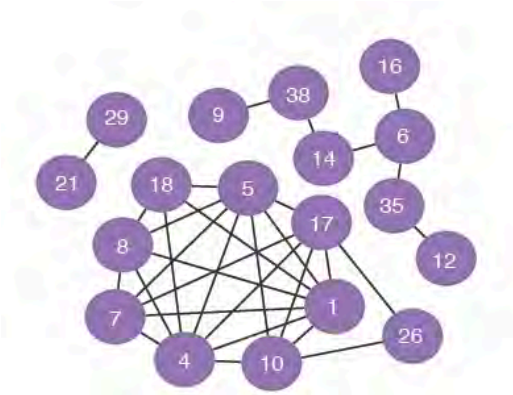

B

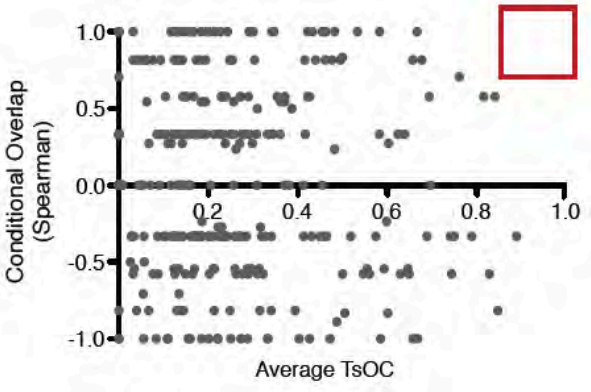

FIGURE 2.15: Comparing insulin gene expression TsOC scores. *(A)* Co-expression network of insulins (circles) that share the top 5% average TsOC scores through six larval/adult stages. An edge represents an average TsOC ≥ 0.68; maximum average TsOC = 0.89 (*ins-4* and *ins-5*). *(B)* No gene pairs (red box) share the same expression in both conditional (as measured by a Spearman rank test) and developmental tissue expression. TsOC is presented as an average of the six TsOC values for each developmental stage.

protein sequence identity to their average TsOC scores we did not observe a correlation between sequence and expression similarity (Fig. 2.16A).

One outlying pair of insulins, *ins-7* and *ins-8*, is both similar in sequence and in spatiotemporal expression (Fig 2.16). To test putative redundancy between these insulins, we first examined developmental timing and dauer formation in single *ins-7(tm1907)* or *ins-8(tm4144)* mutants and found no differences compared to wild type animals (Fig 2.1, Fig 2.2, Table 2.1). Close paralogs can compensate each other's loss by an increase in expression [95], [118]. We examined endogenous *ins-7* expression in an *ins-8* mutant and *vice versa* and found that while loss of *ins-8* did not result in a change in *ins-7* expression, loss of *ins-7* resulted in a ~15-fold increase in *ins-8* expression (Fig. 2.16C). In a recent study it was reported that endogenous *ins-7* is expressed at higher levels than *ins-8* throughout development [119]. *ins-7* and *ins-8* are less than 1kb apart in the genome; therefore, in the *ins-7(tm1907),* the *ins-8* gene resides in closer proximity to the (stronger) *ins-7* promoter (Fig. 1.3). To test whether this could explain the observed increase in expression, we examined *ins-8* expression upon *ins-7* RNAi in both wild type (N2) and RNAi hypersensitive *rrf-3(pk1426)* mutants [120]. Again, we observed an increase in *ins-8* expression upon perturbation of *ins-7*, albeit to a lesser extent (Fig. 2.16D. Therefore, the up-regulation of *ins-8* in the *ins-7* mutant background is not due to the close proximity of the two genes. This data also illustrates that RNAi targeting *ins-7* does not elicit a complete knockdown.

ins-7 expression increases upon dauer formation (Fig. 2.16B). However, *ins-7* mutants do not have any defects in dauer formation (Fig. 2.1; Fig. 2.2; Table 2.1). Since *ins-8* expression increases upon perturbation of *ins-7*, we asked if *ins-8* functions redundantly with *ins-7* in modulating dauer formation. The genomic proximity of the two genes precludes the generation of double mutants. However, neither RNAi of *ins-7* in an *ins-8* mutant, or *vice versa,* either in wild type or in *rrf-3(pk1426)* mutants conferred a dauer formation phenotype or any other phenotypes including lethality, L1 arrest, or developmental delay compared to vector control RNAi or wild type animals (data not shown).

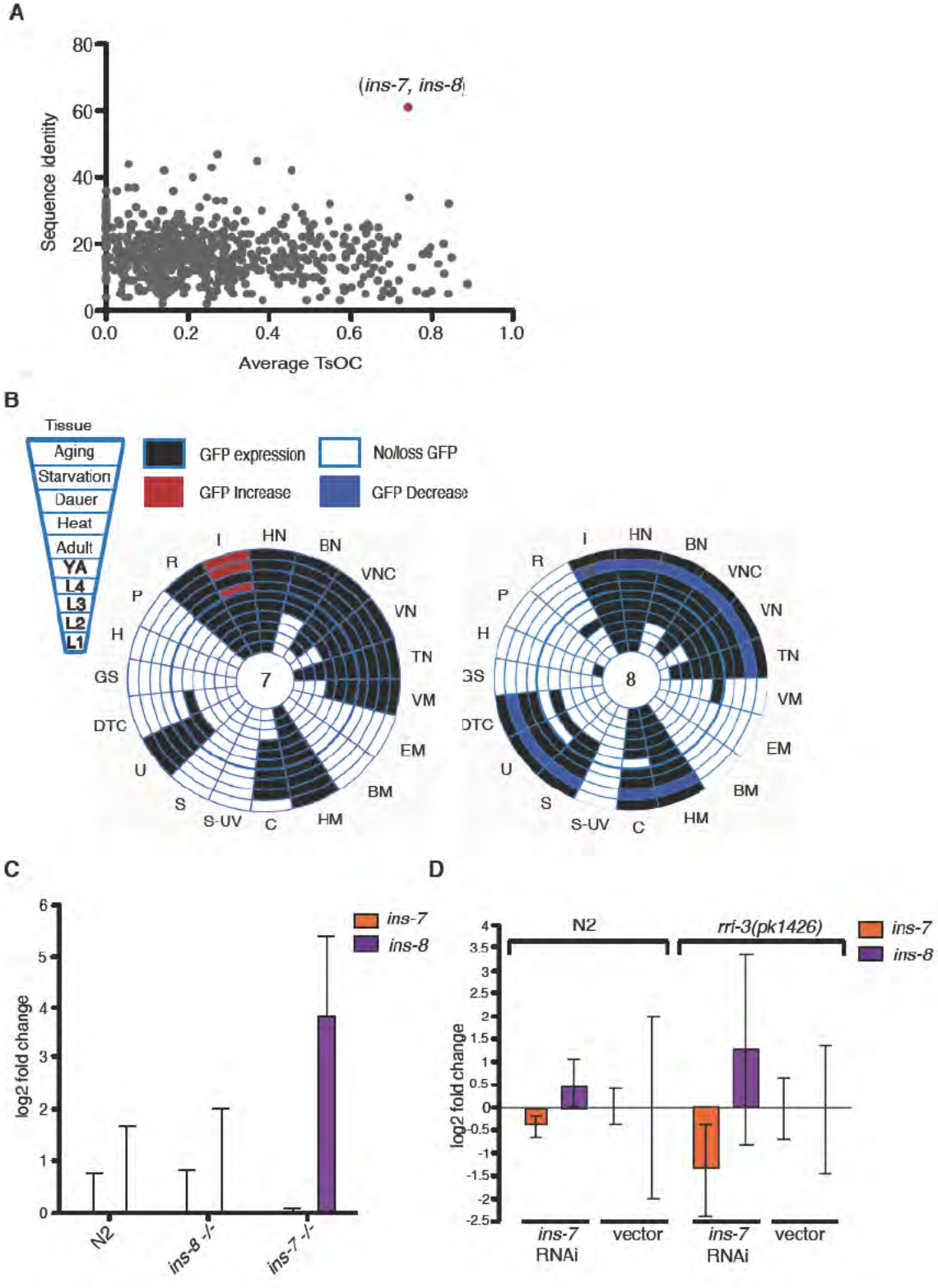
A
80
60
40
20
0
Sequence Identity
(ins-7, ins-8)
0.0
0.2
0.4
0.6
0.8
1.0
Average TsOC
B
Tissue
Aging
Starvation
Dauer
Heat
Adult
YA
L4
L3
L2
L1
GFP expression
No/loss GFP
GFP Increase
GFP Decrease
I
HN
BN
VNC
VN
TN
VM
EM
BM
HM
C
S-UV
S
U
DTC
GS
H
P
R
7
8
C
log2 fold change
ins-7
ins-8
N2
ins-8 -/-
ins-7 -/-
D
N2
rrf-3(pk1426)
ins-7
ins-8
log2 fold change
ins-7 RNAi
vector
ins-7 RNAi
vector

(continued from previous page)

FIGURE 2.16: Divergence, overlap and compensation in expression between *ins-7* and *ins-8*. *(A)* There is no clear positive correlation between the degree of overlap in expression through development (average TsOC) and sequence similarity of insulins. *ins-7* and *ins-8* (red dot) are the only pair that share both high sequence similarity and high TsOC. TsOC is presented as an average of the six TsOC values for each developmental stage. *(B) ins-7* and *ins-8* exhibit high overlap in expression under standard laboratory conditions (first 6 rings, from L1 to adult) but exhibit different conditional changes in expression (4 outermost rings). Red = GFP increase; blue = GFP decrease; black = no change in GFP expression, white = no GFP observed. *(C)* In the absence of *ins-7* (orange), *ins-8* (purple) expression is increased. *(D) ins-8* increases in both wild type (N2) ($p < 0.0001$) and *rrf-3(pk1426)* mutants ($p = 0.054$) upon RNAi knockdown of *ins-7*. mRNA abundance was measured by qRT-PCR for *(C)* and *(D)*. Triplicate repeats from biological duplicate samples were measured. One biological sample is illustrated here. The error bar indicates variation between triplicates.

PART I MATERIALS AND METHODS

Strain Maintenance

All strains were maintained at 15℃ using standard *C. elegans* techniques [4]. Males were generated by heat shocking L4 larvae at 30°C for 6 hours.

Generation of Pins::GFP transgenic animals

We used gene predictions available in WormBase WS150 (http://ws150.wormbase.org). In total, 22 of the 40 promoter constructs were obtained from the Promoterome collection [121]. The remaining promoters were PCR amplified and cloned as described [121]. Primer sequences are provided in Table 2.5. Transgenic animals were generated by microparticle bombardment as described [122]. For each Pins::GFP reporter construct, 2-6 independent lines were obtained. At least two lines were examined for GFP expression and the line that showed highest transmission was used further. Nineteen of 40 Pins::GFP strains harbored the GFP construct integrated in the genome. For all nonintegrated lines, 50-100 animals were analyzed to capture each component of the expression pattern. An increase in expression was recorded if the level of GFP dramatically increased and/or if expression in additional tissues was observed, while an expression decrease was defined by a dramatic reduction in GFP levels and/or a complete loss of expression in at least one cell/tissue type. All strains are available from the C. elegans Genetics Center, or upon request.

Genotyping

The genotype of each transgenic line was confirmed by PCR (Table 2.5), followed by DNA sequencing. One gravid animal was added to 5µL of solution containing 2µL 20mg/mL proteinase K and 100µL lysis buffer (30mM Tris pH8, 8mM EDTA, 100mM NaCl, 0.7% NP40, 0.7% Tween 20) and incubated at 60°C for 1hr followed by 95°C for 15 minutes. Each 50µL PCR reaction included 1µL dNTP, 5µL 10X Buffer, 0.4µL of each Fwd and Rev primers (at 25 µM), 0.2uL Taq polymerase, 1µL $MgCl_2$, 32.4µL water, 10µL template obtained from worm lysis. PCR conditions included 34 cycles of (95°C for 2 minutes 45 seconds, 56° for 1 minute, 72°C for 3 minutes) followed by 68°C for 7 minutes, 10°C for 30 minutes.

RNAi

Bacterial feeding of RNAi clones was performed as described [123]. Control (empty vector) and *unc-22* clones were used as negative and positive controls, respectively. Each clone was verified by PCR and sequence analysis.

Dauer analyses

For analysis of dauer constitutive phenotypes, wild type and mutant animals were grown on vector and *daf-2* RNAi for one generation at 25°C. Approximately 10 adults from the F1 progeny were added to new RNAi culture plates and allowed to lay eggs for 6-8 hours at 25°C. Plates containing eggs were incubated at 25°C and analyzed after 2-3 consecutive days by counting dauers and non-dauers.

Dauers were determined by survival of 1% SDS treatment for 15 minutes. To test for a dauer defective phenotype, two young adult animals were placed on OP50 plates and left at 25°C or 27°C to reproduce. Plates were checked daily to examine the bacterial lawn. 3-4 days after no food remained, the number of animals on the plate were scored and then 1.5mL of 1% SDS was added to each plate. After 15 minutes, the number live thrashing animals (*i.e.* dauers) were counted. Assays were performed in duplicate.

Pins::GFP expression pattern annotation

GFP expression was examined in 40-50 animals by fluorescence microscopy using a Zeiss Axioscope 2 plus as described previously [97], [122], [124]. Temporal expression patterns were classified into six stages: four larval stages (L1-L4), young adult (no eggs) and ~3-4 day adult with eggs. Developmental stages were defined by the length and number of cells in the gonad (wormatlas.org). Spatial expression patterns were classified into 19 categories that correspond to tissues, cell types, organs, and individual cells. Temporal and spatial expression was standardized into a binary code, where “1” represents expression detected and “0” indicates no expression detected.

Tissue overlap analysis

Tissue overlap coefficient (TsOC) analysis was performed as described [97], [124], [125], with minor modifications to annotate more specific tissues. Nodes were defined as insulins and the cell/tissue in which they are expressed. TsOC was analyzed for each pair of nodes by a geometric formula [126].

Conditional expression analysis

Each stress was determined sufficient by testing with genes known to respond to the respective condition (Fig. 2.12A). Oxidative stress: 1mL 200mM paraquat was added to 10mL OP50-seeded NGM plates. Young adults were added and incubated at 20°C for 6 hours. Verified using Pgst-4::GFP transgenics [127]. Glucose: 1mL 2% glucose was added to 10mL OP50-seeded NGM plates. Young adults were added and incubated at 20°C for 1-, 6-, 12- and 24-hours. Verified using daf-16a::GFP transgenics [128]. Heat stress: L4 larvae and young adults were placed on OP50-seeded NGM plates and incubated at 30°C for 6 hours. Plates were not stacked to assure heat was equally distributed among all plates. Verified by using Phsp-4::GFP transgenics [129]. Starvation: L4 and young adult animals were washed twice using 1X M9 buffer then placed on peptone-free plates without bacteria. Animals were incubated at 20°C for 24 hours. Verified by using Pacdh-1::GFP transgenics [130]. Dauer: We obtained dauers by allowing plates to starve. Strains were grown at 20°C until no food remained. Dauers were picked 3-4 days after plates were starved. Aging: one-day old adults were placed on OP50-seeded 5-fluorodeoxyuridine (FuDR) plates. GFP expression was recorded on days 5, 10, and 15. In all experiments, the presence of GFP expression was translated into a numbers where “1” represents a GFP increase, “0” represents no change in GFP, and “-1” represents GFP decrease. Correlations (i.e. conditional overlap) were determined using Spearman’s rank test.

Quantitative RT-PCR

For all qRT-PCR experiments, strains were maintained at 20°C and mixed late-L4/YA stage animals were used. Worms were collected and washed 2x with sterile 1x M9 buffer (3g KH_2PO_4, 6g Na_2HPO_4, 5g NaCl, 1mL 1M $MgSO_4$, H_2O to 1 liter; Sterilize by autoclaving). Supernatant was removed and 10x volume of TRIzol reagent (Invitrogen, USA) was added to the worm pellet. Pellet was frozen at -80°C until RNA extraction. Total RNA was purified by phenol:chloroform extraction and ethanol precipitation followed by column purification using a RNeasy Mini Kit (Qiagen, USA). The quality of RNA isolated was determined by checking the 28S and 18S RNA on an agarose gel and quantity measured by NanoDrop® ND-1000 Spectrophotometer. 1µg of total RNA was used to make cDNA using the SuperScript® III First Strand Synthesis Kit (Invitrogen, USA). The expression of *ins-7* and *ins-8* genes was checked by quantitative PCR using the SYBR® Green PCR Master Mix (Invitrogen, USA) and StepOnePlus™ Real-Time PCR System (Applied Biosystems, USA). Samples were analyzed three times in triplicate from two independent worm cDNA preps and two different cDNA sample dilutions. mRNA levels were normalized for *act-1* mRNA and expressed as log2 fold change compared to controls. Significance was determined by Student's t-test. Primers used for RT-PCR experiments can be found in (Table 2.5).

Gene	Sequencing Primers	Product Size
daf-28	Fwd: ggggacaactttgtatagaaaagttgtagccaaaactgtagtaat	2061
	Rev: ggggactgcttttttgtacaaacttgtcatgttgagatagttgttga	
ins-1	Fwd: ggggacaactttgtatagaaaagttggttttcatctttttactttt	2061
	Rev: ggggactgcttttttgtacaaacttgtcattgcgtactgtcgtagcgtgtgg	
ins-2	Fwd: ggggacaactttgtatagaaaagttgctgaaaaacatctgagata	2061
	Rev: ggggactgcttttttgtacaaacttgtcatggtagattttagaatgg	
ins-3	Fwd: ggggacaactttgtatagaaaagttgtgagtgatcaaagctgaaa	2061
	Rev: ggggactgcttttttgtacaaacttgtcattattcagaacaggaattgataaa	
ins-4	Fwd: ggggacaactttgtatagaaaagttgattaattcagtttgaagtt	2061
	Rev: ggggactgcttttttgtacaaacttgtcattctcttggagcttttg	
ins-5	Fwd: ggggacaactttgtatagaaaagttgaaaaacagtcgtccaacaa	1769
	Rev: ggggactgcttttttgtacaaacttgtcattttccttgaagattgaagagt	
ins-6	Fwd: ggggacaactttgtatagaaaagttgaattggatcccagaataag	1716
	Rev: ggggactgcttttttgtacaaacttgtcattataatgatatggataacggaa	
ins-7	Fwd: ggggacaactttgtatagaaaagttggaactaaactctccaaataaa	654
	Rev: ggggactgcttttttgtacaaacttgtcatctggaaaaagtaatattatataaa	
ins-8	Fwd: ggggacaactttgtatagaaaagttgtttcttctatcataaattaacaaaaatt	1374
	Rev: ggggactgcttttttgtacaaacttgtcatctggaaataattaatatcagaac	
ins-9	Fwd: ggggacaactttgtatagaaaagttgacgttttgtaccaatttgtctttttatacc	1238
	Rev: ggggactgcttttttgtacaaacttgtcatcgtttcactcctcgaatta	
ins-10	Fwd: ggggacaactttgtatagaaaagttggaacgcagaacaaaaatgattatttaaatat	2061
	Rev: ggggactgcttttttgtacaaacttgtcattgttagaagtgctggaaattgtga	
ins-11	Fwd: ggggacaactttgtatagaaaagttgagttatcgaggttatagtggt	2061
	Rev: ggggactgcttttttgtacaaacttgtcatatttaacgattcctaca	
ins-12	Fwd: ggggacaactttgtatagaaaagttgctgtttgcggagtcggat	2061
	Rev: ggggactgcttttttgtacaaacttgtcatttttgttttggctgtgattattgt	
ins-13	Fwd: ggggacaactttgtatagaaaagttgtgacttcaaaagtgattttgggat	236
	Rev: ggggactgcttttttgtacaaacttgtcatgataaatttgaagcgaaaagaatttgaaa	
ins-14	Fwd: ggggacaactttgtatagaaaagttgtttcaaatttctagtttcagagcttcgg	1854
	Rev: ggggactgcttttttgtacaaacttgtcatctcggtggtaaaatgaagcccaa	
ins-15	Fwd: ggggacaactttgtatagaaaagttgaaatctagaaactatatttttttgttgaa	810
	Rev: ggggactgcttttttgtacaaacttgtcattatctgaaaattaatttacatttg	
ins-16	Fwd: ggggacaactttgtatagaaaagttggcaataaaaattaaaaaattttgagtaa	2061
	Rev: ggggactgcttttttgtacaaacttgtcattgtaaaagtgattttgaaaattttga	
ins-17	Fwd: ggggacaactttgtatagaaaagttggccgcgtgccaaatcaccgtt	2061
	Rev: ggggactgcttttttgtacaaacttgtcatttggatcacagatactcgctt	
ins-18	Fwd: ggggacaactttgtatagaaaagttggatgctttttagaatgtcc	2061
	Rev: ggggactgcttttttgtacaaacttgtcattgtgttaaattaaaatgagctt	
ins-19	Fwd: ggggacaactttgtatagaaaagttgggtgatggttgaaggcagg	756
	Rev: ggggactgcttttttgtacaaacttgtcatcgggaactaggtttgtatttat	
ins-20	Fwd: ggggacaactttgtatagaaaagttggtttaaatcctctgaagatgtgattcgt	2061
	Rev: ggggactgcttttttgtacaaacttgtcatctccacatcattaaataacatc	
ins-21	Fwd: ggggacaactttgtatagaaaagttgaatgtccgtttagagtttta	2061
	Rev: ggggactgcttttttgtacaaacttgtcatggttcaactcaaaaaggaaaaat	
ins-22	Fwd: ggggacaactttgtatagaaaagttgttoctttaatgttcagctatgcgaagt	2061
	Rev: ggggactgcttttttgtacaaacttgtcatttttgttggttagttgt	
ins-23	Fwd: ggggacaactttgtatagaaaagttggaatggagcttctcaaattcaa	1716
	Rev: ggggactgcttttttgtacaaacttgtcattatcgaaattccagaaa	
ins-24	Fwd: ggggacaactttgtatagaaaagttgagcattccggaattttctggaattt	2061
	Rev: ggggactgcttttttgtacaaacttgtcatggtgcagagcatctggctgaa	
ins-25	Fwd: ggggacaactttgtatagaaaagttgaaacgatctctttctataacttttacattcc	758
	Rev: ggggactgcttttttgtacaaacttgtcatatttcaaatttttacaaccttctaca	
ins-26	Fwd: ggggacaactttgtatagaaaagttgttggtcattttaggaccaaaggag	2061
	Rev: ggggactgcttttttgtacaaacttgtcatttccttcgctgagaagt	
ins-27	Fwd: ggggacaactttgtatagaaaagttgaatttttcaaaatttcaaaaccccataac	2061
	Rev: ggggactgcttttttgtacaaacttgtcatggtagagaagtcgagagaactgaaataa	
ins-28	Fwd: ggggacaactttgtatagaaaagttgttctttagtcattttcctttgaaaactaagtc	2061
	Rev: ggggactgcttttttgtacaaacttgtcatattggagagtttagtcgaaaatc	
ins-29	Fwd: ggggacaactttgtatagaaaagttgctttaaaatggttaattttgtagt	2061
	Rev: ggggactgcttttttgtacaaacttgtcatttttttatttcacaatataatatac	
ins-30	Fwd: ggggacaactttgtatagaaaagttgaagagcacaaaataacgga	1288
	Rev: ggggactgcttttttgtacaaacttgtcattctcacaaaaaaagtgagttgg	
ins-31	Fwd: ggggacaactttgtatagaaaagttggtatttatacaacaa	648
	Rev: ggggactgcttttttgtacaaacttgtcatggtgatggttgaaggcaggt	
ins-32	Fwd: ggggacaactttgtatagaaaagttgtattttacactttcgccaca	2061
	Rev: ggggactgcttttttgtacaaacttgtcattttcagacaaagtagtt	
ins-33	Fwd: ggggacaactttgtatagaaaagttggagcaatcgcgctctattgg	1193
	Rev: ggggactgcttttttgtacaaacttgtcatttttgttcaaaaaatcag	
ins-34	Fwd: ggggacaactttgtatagaaaagttgatttttgtctgaaaaattgaaatagt	1834
	Rev: ggggactgcttttttgtacaaacttgtcatctttgggaaaatggat	
ins-35	Fwd: ggggacaactttgtatagaaaagttggctaggctaaatgacgccctt	2061
	Rev: ggggactgcttttttgtacaaacttgtcattgctggaaaattagac	
ins-36	Fwd: ggggacaactttgtatagaaaagttgtttttattgattttaacgataaattattga	1283
	Rev: ggggactgcttttttgtacaaacttgtcattctggaaaaaaaacaacaatttttct	
ins-37	Fwd: ggggacaactttgtatagaaaagttgttgcactgctgccgggctc	361
	Rev: ggggactgcttttttgtacaaacttgtcatggtgttcaatcgtcta	
ins-38	Fwd: ggggacaactttgtatagaaaagttggaatctcgaatctcattgaaaatccagt	1293
	Rev: ggggactgcttttttgtacaaacttgtcatattttccagttgaaatttgtaatttcag	
ins-39	Fwd: ggggacaactttgtatagaaaagttgaccgaattctaacca	2062
	Rev: ggggactgcttttttgtacaaacttgtcatggcggaagcgg	
GFP Fwd	ttctacttcttttactgaacg	
GFP Rev	ctccactgacagaaaatttg	
	RT-PCR Primers	
actin	FWD: ctcttgccccatcaaccatg	
	REV: cttgcttggagatccacatc	
ins-7	FWD: catgcgaatcgaatactgaa	
	REV: cactgttttcgaatgaagtc	
ins-8	FWD: cgacttttgtatttgaatcg	
	REV: cagcagagtaagaagagtcc	

(continued from previous page)

TABLE 2.5: Primer sequences for all primers used for genotyping or performing RT-PCR experiments (see Materials and Methods).

PART I, CHAPTER 3

DISCUSSION

In this study, we report widespread and dynamic spatiotemporal expression of *C. elegans* insulins during development and under different physiological and environmental conditions. Not all expression patterns may completely capture endogenous insulin expression for several reasons. First, the promoter fragments used may lack regulatory elements required for expression in some tissues or to repress expression in others. Second, expression was annotated to the resolution of individual cells in some but not all tissues. Annotating at the level of individual cells is challenging, especially in neurons where insulins are abundantly expressed. Thus, the overlap in expression for neuronal insulins may be lower than estimated here. Third, we did not observe GFP expression in the germline, most likely because of transgene silencing [131]. Finally, insulins are secreted peptides that may act cell-nonautonomously [83], [132]. Nonetheless, we provide both a first comprehensive dataset as well as a set of transgenic strains, both of which enable future studies of the functional dynamics of the entire *C. elegans* insulin gene family *in vivo*.

Several examples illustrate how the insulin expression patterns provide a resource for the derivation of functional hypotheses. First, the expression patterns of individual insulins can likely be used to predict specific functions. For instance, we found that *ins-3* is expressed in the distal tip cell, spermatheca and the spermatheca-uterine valve. Previously, it has been shown that perturbations

of *ins-3* result in defects in germline proliferation, and that this is due to function of *ins-3* in the soma [87]. Second, changes in expression of individual insulins can likely be used to infer specific functions as well. For example, it has been shown that *daf-28* is involved in dauer formation and we find that its expression is turned off in dauers ([86], this study). Third, the expression data can likely be used to derive hypotheses about complex functional redundancies. For instance, 14 insulins change in expression as the animals age; 8 of which increase and 6 of which decrease in expression. Future studies of which insulins are receptor agonists *versus* antagonists will be important to derive hypotheses regarding combinatorial insulin function in lifespan regulation.

Remarkably, pair-wise combinations of insulin loss/knockdown did not result in defects in dauer formation. This could be due to inefficient insulin knockdown in neuronal tissues required for dauer formation [63]. Alternatively, there may be more complex patterns of redundancies between more than two insulins. The lack of 1:1 insulin relationships is supported by the observation of two clusters in the expression network, rather than simple pair-wise co-expression patterns.

Two insulins, *ins-7* and *ins-8,* share high sequence similarity and expression overlap through development. We find that *ins-8* levels increase in the absence of *ins-7,* but did not detect compensatory changes in *ins-7* expression upon loss of *ins-8.* Knockdown of *ins-7* in an *ins-8* mutant or *vice versa* did not affect dauer formation. However, loss of *ins-7* slightly extends lifespan (Fig. 3.1) [71]. This suggests that, while *ins-8* increases upon loss of *ins-*

7, it cannot fully compensate for the loss of *ins-7* in modulating longevity, further illustrating the lack of 1:1 relationships between insulins. Additionally, while loss of *ins-7* extends lifespan, it does not recapitulate the dramatic lifespan extension caused by a loss-of-function in *daf-2*. Together, this data suggests that *ins-7* and *ins-8* may genetically interact with other insulins. Alternatively, it is conceivable that the overexpression of *ins-8* in the *ins-7(tm1907)* rather than the loss of *ins-7* may be responsible for the observed lifespan extension of *ins-7* mutants, which would suggest that *ins-8* is an antagonist whereas *ins-7* is an agonist. However, dauer formation was not observed upon loss of *ins-7* nor were *ins-8(tm4144)* mutants dauer defective (Fig. 2.1; Fig. 2.2). This illustrates that *ins-8* is not likely an antagonist.

In the wild, *C. elegans* is exposed to a variety of environmental conditions. Food and temperature serve as modulators of dauer formation [133]. By entering dauer, development ceases until a favorable environment becomes available. Intuitively, differential insulin activity could ensure that a whole organism response, such as dauer formation, only occurs under specific conditions and not in response to any type of stress. Remarkably, we found that insulins that share high expression overlap during development are distinct from those that share similarities under different conditions (Fig. 3.2). This may reflect a need for specificity in coordinating development *versus* responding to different stresses. The expansion of the insulin family and its genetic wiring may provide the animal with a complex and highly organized repertoire of responses that can be tailored according to developmental or environmental need. In biological systems,

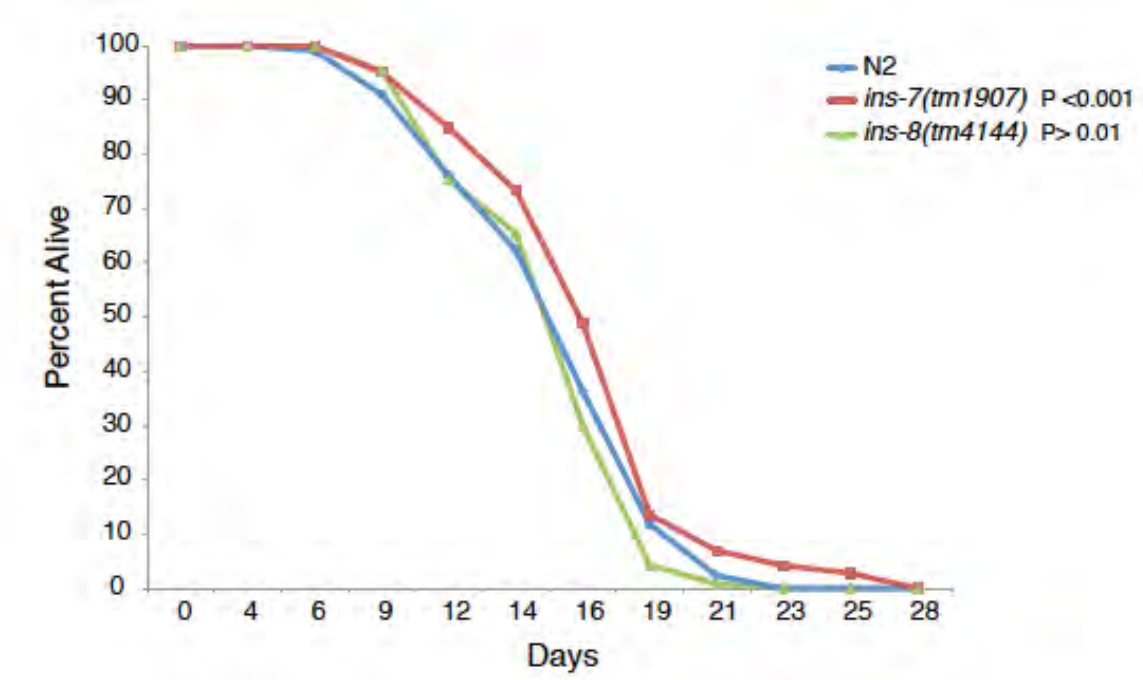

FIGURE 3.1: Lifespan analyses of insulin mutants. Lifespan phenotypes of *ins-8(tm4144)* (red) and *ins-7(tm1907)* (green) lifespan as compared to N2 (blue). Lifespans were performed in duplicate at 20°C. Mean and maximum lifespans are as follows: N2=16.5 ±1; 23 days; *ins-7(tm1907)*=18 ±2, 28 days; *ins-8(tm4144)*= 16 ±2, 23 days. Prism 5 was used to calculate and perform survival curve comparisons. Significance was determined using the log-rank (Mantel-Cox) test.

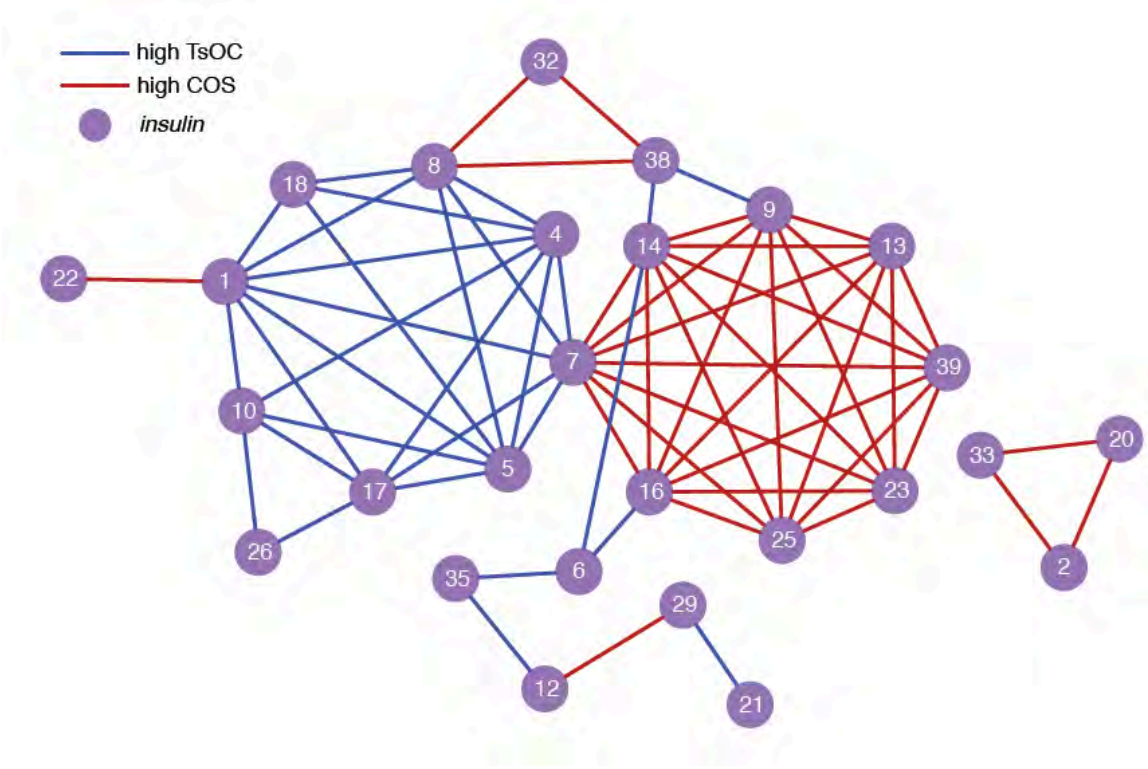

FIGURE 3.2: A co-expression network of the insulins (circles) that share the top 5% average TsOC through six larval/adult stages (blue edge) and the top 5% of conditional overlap (COS; red edge). Distinct clusters are observed whereby no insulins are both connected through high TsOC and high COS.

different components can be interchangeable under certain conditions, but perform distinct functions under other conditions. Such redundancy, or degeneracy, contributes to the robustness, complexity and evolvability of a system [134], [135]. We propose that the *C. elegans* insulin family has evolved to attain a type of “block design”, a term used in combinatorial mathematics. An evolved block design can lead to the formation of different functional alliances in different cells for different developmental *versus* environmental conditions (Fig. 3.3). Cooperative action between insulins may provide a robust framework for interpreting physiological and environmental cues and ensuring that the DAF-2 receptor initiates the appropriate response. For instance, *daf-28* and *ins-6* cooperate in modulating dauer formation. However, each insulin also functions specifically in dauer entry or exit, respectively [86].

C. elegans likely utilize 40 insulins to achieve both specificity and redundancy to maintain fitness in a complex environment. The total possible number of combinations in different sets, for instance with 3, 4 or even more, is immense, and potentially provides the animal with a large and flexible repertoire of possibilities to recognize and respond appropriately to many environmental stimuli. Future studies will illuminate the generality of this observation for insulins in other nematodes, as well as other gene families in *C. elegans* and other complex multicellular organisms such as humans.

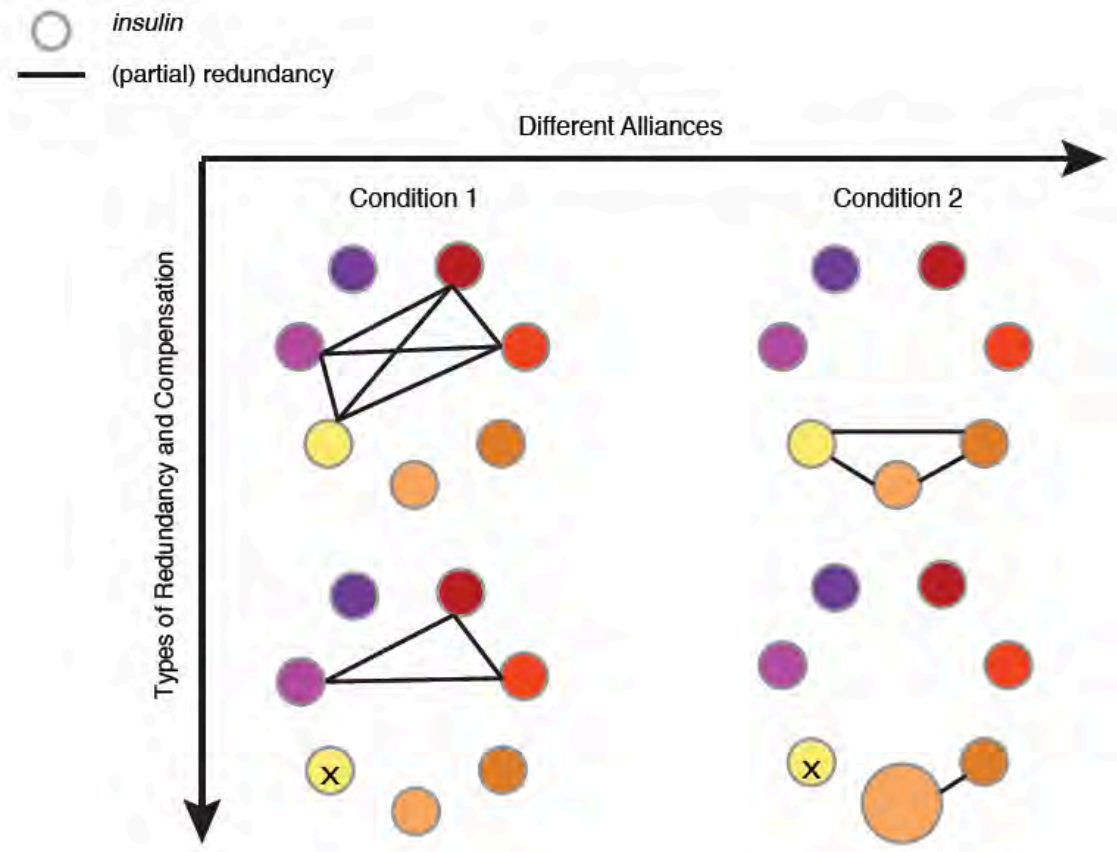

FIGURE 3.3: Model for complexity and robustness in gene families. A “block design” or “alliances” in insulins under a given condition. A colored node represents one insulin. An edge represents overlapping function. Different alliances allow for the appropriate response to different conditions (top row). Although different conditions likely require different insulins, some (yellow node) may always be shared between conditions. Loss of single insulin activity does not cause a phenotypic affect due to redundancy (bottom left) and/or compensation (bottom right) with other insulins.

Concluding remarks and future directions

Why do *C. elegans* have a large insulin gene family and how do they function? To answer “why” the expansion of this gene family occurred will take comparative evolutionary studies, including other *Caenorhabditis* species, to begin to elucidate. “How do the insulins function?” is a question that will require further dissection of the molecular mechanisms shared among this gene family and the insulin receptor. From our study and others, examining the insulin gene family by expression and mutation has revealed complex orchestration of physiology by the insulin ligands. The insulins appear to be functioning as a combinatorial network: a system of signals that orchestrate a systematic physiological response. We now need more sensitive and directed studies to further elucidate this gene family. In the following, based on the current literature and from our study, I will share my thoughts on how the insulins are functioning and what future directions would be most informative for gaining greater insight into this gene family.

Redefining insulin “function”

For many insulins, loss of function or overexpression has yielded no measureable phenotype. Perhaps unobserved phenotypes are in part because of the phenotypes themselves being analyzed: dauer and lifespan require coordinated and systematic changes in metabolism, gene expression, and tissue reorganization within the entire organism. As a result, there is an elaborate orchestration of molecular events that must occur in order for the animal to dauer

and/or increase lifespan. While some loss of single insulin genes can cause changes in dauer and lifespan, the majority do not. To gain granularity on the function of the insulins, more specific, context-dependent contributions of individual insulins should be measured.

Mutations in the DAF-2 receptor lead to dramatic changes in metabolism [136]. Dauer, the phenotypic readout for metabolic change, is the response to harsh environmental conditions (*i.e.* high temperature, low food and crowding) [133]. Dauer is a whole-organismal response whereby development ceases, the cuticle and oral orifices are sealed, and pharyngeal muscles do not pump. Dauer is a highly programmed, step-wise physiological process that takes up to 72 hours until complete [137]. Changes in metabolism that enable the animal to dauer thus occur in systematic steps. However, we do not know how or exactly which metabolic pathways are modulated to cause dauer and if changes to these pathways can be uncoupled. What is the influence of the insulins on metabolism? How many insulins modulate metabolism? Mutating one insulin that, for instance, alters the flux through a single metabolic pathway, may not be sufficient to induce a whole-organismal response like dauer. However, the combinatorial loss of insulins altering multiple metabolic pathways may be a synthetic interaction resulting in a measurable change in whole organismal physiology such as dauer. For instance, single loss-of-function mutations in *daf-28* or *ins-6* result in no dauer phenotypes at an ambient temperature and in the presence of food. Upon loss of both *daf-28* and *ins-6*, however, ~40% animals form dauers in the same conditions. Genetic studies using gain-of-function mutations, illustrate that *daf-28*

influences metabolism to promote dauer, even in optimal conditions. Interestingly, *ins-6(-)*, as well as a few others, have been reported to have increased fat content when compared to wild-type animals [138]. What metabolic changes do the loss of each insulin illicit? Does the change in fat content contribute to the dauer phenotype observed in the *daf-28; ins-6* double mutant? Further, are the metabolic phenotypes of these mutants similar to that observed for *daf-2(-)* animals, that also have increased fat content and a dauer constitutive phenotype? With the advent of metabolomic technologies, studying the influence of the insulins on metabolism will be more feasible and tractable.

To date, no single insulin mutation or overexpression recapitulates the *daf-2(-)* phenotype. With the recently developed use of clustered, regularly interspaced, short palindromic repeats (CRISPR)-associated endonuclease Cas9 to target genomic sequences, we now have the ability to precisely modify genomes using an efficient, low cost approach. With new genome editing technologies, the genetic manipulative possibilities are endless [139]–[141]. For example, gene deletions for each insulin, and in all possible combinations, can be generated and subsequently interrogated. One could also attempt to sequentially knock out all of the insulin genes to determine whether the *daf-2(-)* phenotype can ever be fully recapitulated.

Investigating insulin protein expression and function

Do all 40 insulins encode a functional protein? In mammals, proprotein convertases, PC1 and PC2, process precursors of the insulin peptide.

Computational predictions and mutational analyses identified four homologous enzymes in *C. elegans:* three PC1 homologs, AEX-5, BLI-4, and KPC-1, and one PC2 homolog, EGL-3 [142]–[144]. Two of these enzymes, EGL-3 and KPC-1, have been demonstrated to successfully process, at least in part, four insulin proteins, INS-3, INS-4, INS-6 and DAF-28 *in vivo*. Kao *et al* generated a full-length DAF-28::GFP protein and observed successful expression and secretion *in vivo* [84]. However, only one study has described the structure of an insulin, INS-6, and successfully illustrated that it binds and activates the human insulin receptor [82]. It is unknown if INS-6 can bind and activate the *C. elegans* receptor. These data support the fact that insulin genes can encode functional protein, and future studies will elucidate whether this is true for the remaining insulin family members.

In mammals, insulin, IGFs and relaxins are synthesized and secreted from the pancreas, liver, and ovaries, respectively. Although, IGFs can be synthesized in a number of peripheral tissues and enter into systemic circulation [145]. In *C. elegans*, insulin-like genes show widespread patterns of gene expression with most being expressed in neuronal tissue and the intestine. Neurons, along with the intestine, have been illustrated to be the major tissues in which the IIS pathway modulates dauer and lifespan, respectively. Proprotein convertases involved in insulin processing are also expressed in neurons, intestine and some muscle cells [146]. In what tissues are the insulins synthesized and/or secreted? Will these tissues overlap with gene expression patterns reported for the insulin family? Studying the spatiotemporal expression of insulin protein in addition to

gene expression will be instrumental to gaining further understanding of their function.

The extent to which insulins act cell autonomously or non-autonomously also remains unknown. However, there are at least two examples where an insulin is expressed under a specific condition in one tissue and affects physiology through interactions with a second, local tissue [147, 148]. In both models, environmental cues are first sensed by sensory neurons and these sensory neurons mediate insulin activity to other tissues. For example, INS-1 is released from the AIA when an odor is present. Under short odor exposure, *ins-1* inhibits downstream calcium transients in a different neuron, the AWC; however, after long odor exposure, *ins-1* may completely suppress calcium transients even after odor removal. On the other hand, INS-1 acts in AIA interneurons, which receive direct synaptic inputs from sensory neurons and also send synaptic outputs to ASER. These results suggest that INS-1 secreted from AIA interneurons provides feedback to ASER to generate plasticity of chemotaxis. This feedback loop acts to tune sensory responses to external stimuli [147].

A second study illustrated that the nervous system can also signal to the intestine. Under normal conditions, the nervous system secretes agonistic ligands, INS-4, INS-6 and DAF-28, to increase IIS signaling in the intestine thus sequestering intestinal DAF-16. Under unfavorable environmental conditions, antagonistic ligands, INS-1 and INS-18, and a decrease of agonistic ligands are secreted to decrease IIS signaling in the intestine thus activating DAF-16 to initiate dauer formation [148]. Neuropeptides can be considered hormones in that

they act as long range signaling molecules [58]. How far can the insulins travel in the worm? In *C. elegans*, insulins may be similarly released from cells and act some distance from their site of release. Understanding the signaling network of insulins from synthesis to site of action will further elucidate how this gene family modulates physiology.

Investigating the insulin receptor and downstream signaling

It has been proposed that DAF-2 is a bifunctional gene as *daf-2* alleles can be grouped into two phenotypic classes based on pleiotorphy [74]. Given its multiple downstream effectors and diverse biological functions, is it possible that alternate forms of the DAF-2 receptor exist? There are six predicted isoforms of *daf-2* [146]. In a recent study, two of these isoforms, *daf-2a* and *daf-2c*, were examined for their ability to rescue *daf-2* mutants. Interestingly, not only do these two isoforms illustrate different intracellular localizations, but also functional diversity: *daf-2c* only rescued avoidance behavior defects of *daf-2* mutants, whereas *daf-2a* was effective in rescuing lifespan, dauer formation and thermotolerance [149]. The mammalian insulin receptor has a modular structure whereby two isoforms of the receptor differ slightly in their affinity for insulin and IGF [150]. As mammalian insulin/IGF receptors can form hybrid dimers, perhaps the different isoforms of *daf-2* can dimerize forming many more receptor combinations in *C. elegans*. If this were true, this may reveal a DAF-2 signaling network and reveal how DAF-2 is able to coordinate many different signaling components.

Alternatively, some question whether other DAF-2-like receptors could be present. There is at least one report of a *daf-2*-independent insulin effect [151]. In mammals, G-protein coupled receptors (GPCRs) bind relaxins, members of the insulin superfamily. One computational study interrogated the *C. elegans* genome for insulin receptor-like domains using the extracellular domain sequence of insulin receptors and related RTKs from human to worm and found 56 putative matches [152]. Interestingly, many of the 56 genes clustered along the genome, a common product of recent duplication events. Are any of these functional DAF-2-like receptors? Can *C.* elegans insulins also bind GPCRs? Given the strong evidence of combinatorial features of the insulin signaling network, it would be worthwhile to genetically investigate this possibility.

Is DAF-2 expressed similarly on every cell in *C. elegans*? The redundant yet specific biological effects of the IIS pathway could also be attributed to differences in receptor distribution among tissues with different capacities for metabolic response to a given signal. It is known that, while the insulin receptor is expressed on every mammalian cell, the number of receptors per cell varies from 40 on erythrocytes to 300,000 on adipocytes and hepatocytes [153], [154]. As a result, some tissues including the liver, fat and muscle are more important for insulin signaling in mammals than others [155], [156]. In *C. elegans* dauer formation, genetic mosaic analyses illustrate a larger contribution of *daf-2* signaling originates in neuronal cell lineages [157]. Intestinal IIS pathway activity has also been implicated to be an important determinant of longevity [71], [158]. Comparing the number of receptors, and also what form of the receptor, occurs

on different cell types may be insightful in determining on which tissues insulin signaling is most important and how signaling may differ between tissues.

The IIS pathway has been illustrated to function within a network of signaling events composed of multiple inputs and branchpoints [159]. For instance, the TOR pathway similarly controls development, metabolism and lifespan in *C. elegans*. A conserved component of TOR signaling, *daf-15*/*raptor*, functions to mediate *daf-16*-regulated dauer and metabolic phenotypes. Further, DAF-16 can negatively regulate *daf-15/raptor* [160]. In addition, mutations in *daf-16* and *rsks-1,* a ribosomal protein S6 kinase involved in a branch of the TOR signaling pathway, synergistically prolong lifespan 5-fold. Tissue-specific epistasis analyses suggest intestinal DAF-16 is activated by interacting signals between *daf-2* signaling and *rsks-1* in the germline [161]. In addition to the TOR signaling pathway, the IIS pathway also interacts with the TGF-β signaling pathway that also regulates the dauer decision. The IIS pathway can be negatively regulated by the TGF-β pathway through a phosphatase, PDP-1, which also, interestingly, decreases expression of a subset of insulins [162]. At least one sequential signaling model has been proposed whereby environmental cues sensed by sensory neurons trigger TGF-β signaling which leads to DAF-16 activation by antagonistic insulin expression. DAF-16 and a downstream TGF-β transcription factor, DAF-12, and then together initiate dauer formation [148]. Further, hundreds of genes have been predicted to be regulated by DAF-16 and comprise functional classes including stress response, antimicrobials, steroid

synthesis, metabolism, lipid synthesis, protein and peptide degradation and signaling [70], [163].

The variety of functions of the IIS pathway, and interconnected pathways, illustrate the importance of multiple systems that keep the animal living. This also reveals the extensive crosstalk and network wiring of signaling components downstream of DAF-2. How is intracellular activity of DAF-2 different upon binding of different insulins? Can we use the insulins to uncouple the molecular mechanisms, and thus physiology, downstream of the receptor? Gaining greater understanding of how insulin ligands specifically affect IIS pathway signaling will likely shed light on how the IIS signaling network is orchestrated. Further, as the function of the ten mammalian insulin superfamily members is not entirely solved, understanding the overlap and specificity of IIS pathway signaling via insulin-like peptides in *C. elegans* may provide a foundation for understanding pathway crosstalk between growth factors in mammals.

Dissecting the insulin network

Our study suggests insulins cooperate to provide a robust framework for interpreting physiological and environmental cues and ensuring that the DAF-2 receptor initiates the appropriate response. *C. elegans* likely utilize 40 insulins to achieve both specificity and redundancy to maintain fitness in a complex environment. How would our proposed “block design” be physiologically attained? Previous data illustrates the IIS pathway activity is tissue-specific. For instance, restoring DAF-2 signaling in neurons alone brings the extended

lifespan of *daf-2* mutants back to that of wild-type. Restored DAF-2 pathway signaling in muscles rescues only dauer arrest, also proving that dauer and lifespan phenotypes can be uncoupled [164]. Further, intestinal DAF-16 is sufficient to increase lifespan of short-lived *daf-16(-)* animals by 50-60%; whereas, expression only in neurons moderately increases lifespan of *daf-16(-)* animals by 5-20% [158]. DAF-16 expression in the epidermis mediated cell-nonautonomous effects on germline proliferation [165]. Further, as discussed previously, cell non-autonomous activity has been illustrated whereby insulin secretion from one tissue exerts a physiological response in a nearby or distant tissue [147], [148]. The tissue-specific IIS pathway activity agrees with the tissue-specificity of insulin gene expression. Therefore, it is likely tissue-specificity of insulin binding likely plays a big role in how the IIS pathway coordinates physiology. Perhaps while insulins that bind DAF-2 receptors in the intestine modulate stress response and metabolism, insulins that bind receptors in the neurons may coordinate development and behavior. Different cell types express different genes. We know there are downstream signaling interactions between the IIS pathway and other pathways [40], [162]. It is conceivable that intracellular signaling mechanisms may differ significantly depending on the cell-type and other signals being received by a cell, and this may be sufficient to elicit specific physiological effect by a tissue in response to an environmental condition. Further studies testing tissue- or cell-specific rescue of insulins and measuring which downstream target tissues insulin-DAF-2 interactions occur will add significant depth to our working model.

Interestingly, IIS pathway tissue-specificity studies also revealed that DAF-16 activity in signaling cells upregulates DAF-16 in specific responding tissues [158]. Further examination of the proposed “FOXO-to-FOXO” signaling revealed that DAF-16 activity in the intestine activates DAF-16 in other tissues in part by down-regulating *ins-7* expression in the intestine [71]. In addition, many insulins are up-regulated in a *daf-2*(-) background suggesting that the IIS pathway can cause changes on insulin expression [70], [91]. Therefore, another network model has also been proposed: a biological neural network in which insulins regulate other insulins, referred to as the ILP-to-ILP network. Are insulins directing feedforward or feedback signals to other insulins? Feedforward and feedback signaling motifs among insulin-like genes are utilized by other species [71], [107], [132], [161]. Could ILP-to-ILP regulation elucidate how the proposed combinatorial effects occur? The idea of intercommunication between the insulins prompted a recent large-scale network analysis of insulin activity that examined global insulin gene expression changes by measuring mRNA levels of all 40 insulins in 35 insulin loss-of-function mutants. Of the possible 1190 interactions between the insulins, 101 interactions were observed, and regulation had both a positive and negative effect on insulin gene expression [91]. Network analyses investigating relationships between the number of regulators (in-degree) versus the number of targets (out-degree) revealed that the insulins appear to display hierarchical regulation, whereby some insulins have few inputs and many outputs, some have equal number input and output and others have many inputs with few outputs. Further functional examination of interactions

between deletion mutants illustrated both additive and synergistic and highlight functional relationships and differences among insulins in regulating dauer entry. Regulatory and genetic interactions were then combined to examine overall network architecture. Measuring node connectivity revealed parallel signaling pathways and significant compensation upon insulin loss [91]. The ILP-to-ILP regulatory and phenotypic circuit thus further illustrates network robustness, and agrees with our network model, at least in the context of regulating dauer, whereby the combinatorial efforts of insulins ensure the appropriate physiological response to the environment.

Context-dependent and cell/tissue-specific functional studies of insulin-like peptides in *C. elegans* remain unexplored. Given the complexity of the network with which insulins are interacting, it is likely these functional analyses will only provide some additional information towards why and how this large gene family contributes to animal physiology. Additionally, we know very little about the regulation of insulin expression. How is this gene family regulated? Further examination of what transcription factors regulate gene expression, as well as factors regulating protein secretion, will be very informative of exactly the cues for which the insulins respond and how the IIS pathway may regulate insulins themselves.

To fully appreciate the extent of gene diversification, a comprehensive, multiparameter network of this gene family is necessary. Current insulin networks are constructed from few parameters such as genetic interactions or, as in my study, gene spatiotemporal expression patterns. However, these models ignore

aspects of insulin functionality such as gene regulatory interactions, transcription factor spatiotemporal expression patterns, insulin-receptor interactions, or protein spatiotemporal expression. Therefore, inclusion of these parameters in future model networks will generate a more holistic understanding of insulin function. While these integrated networks have yet to be delineated for the majority of gene families, including the insulins, there are a few cases in which paralog divergence has been examined using this approach [97].

The *C. elegans* insulin gene family as a model for organismal complexity and robustness

Most genes in any genome are dispensable for viability. For instance, single gene deletions have revealed that in yeast only 1,100 of the 6,000 genes (18%) are essential [166]. Similarly, in worms 1,700 of 20,000 genes (8.5%) confer lethality when knocked down by RNAi [167]. Numerous functional screens have been performed using the yeast deletion collection and by RNAi in worms. Remarkably, combined these screens identified a ‘function’ for only a small proportion of genes, and that organisms are highly robust to genetic perturbations.

Robustness can be defined as a key property of evolutionary systems that allows a system to maintain function against internal and external perturbations [135]. Functional maintenance does not imply homeostasis, but rather a return to the original state or entrance into a new and different stable state. Robustness

has been explored using networks capturing cellular functions, metabolic networks and host-pathogen interactions, to name a few [168]–[170].

Biological systems are inherently complex and robust, but also exhibit fragility, especially over time. As mentioned previously, aging, in its simplicity, is the system-wide deterioration of an organism, and aging occurs among every living thing, even in the midst of robustness. The IIS pathway is one of the genetic contributors to aging and thus involved in maintaining organismal robustness over time. Revealing the functional contributions of the insulins in *C. elegans* will allow us to dissect the molecular mechanisms of the IIS pathway. Perhaps studying insulin function over time may give some insight into how these mechanisms are orchestrated, particularly in modulating metabolism, with age and in disease.

PART I BIBLIOGRAPHY

[1] C. López-otín, M. a Blasco, L. Partridge, and M. Serrano, "Europe PMC Funders Group The Hallmarks of Aging," vol. 153, no. 6, pp. 1194–1217, 2013.

[2] H. Gershon and D. Gershon, "Detection of inactive enzyme molecules in ageing organisms.," *Nature*, vol. 227, no. 5264, pp. 1214–1217, 1970.

[3] M. R. Klass, "Aging in the nematode Caenorhabditis elegans: Major biological and environmental factors influencing life span," *Mech. Ageing Dev.*, vol. 6, pp. 413–429, 1977.

[4] T. Stiernagle, "Maintenance of C. elegans.," *WormBook*, pp. 1–11, 2006.

[5] S. Brenner, "The genetics of Caenorhabditis elegans.," *Genetics*, vol. 77, no. 1, pp. 71–94, 1974.

[6] H. a Tissenbaum and L. Guarente, "Model organisms as a guide to mammalian aging.," *Dev. Cell*, vol. 2, no. 1, pp. 9–19, Jan. 2002.

[7] J. J. Collins, C. Huang, S. Hughes, and K. Kornfeld, "The measurement and analysis of age-related changes in Caenorhabditis elegans.," *WormBook*, pp. 1–21, 2008.

[8] C. Kenyon, J. Chang, E. Gensch, A. Rudner, and R. Tabtiang, "A C. elegans mutant that lives twice as long as wild type.," *Nature*, vol. 366, no. 6454, pp. 461–464, 1993.

[9] D. B. Friedman and T. E. Johnson, "A mutation in the age-1 gene in Caenorhabditis elegans lengthens life and reduces hermaphrodite fertility," *Genetics*, vol. 118, no. 1, pp. 75–86, 1988.

[10] C. Kenyon, "Ponce d'elegans: Genetic quest for the fountain of youth," *Cell*, vol. 84, no. 4. pp. 501–504, 1996.

[11] L. M. Kutscher and S. Shaham, "Forward and reverse mutagenesis in C. elegans," *WormBook*, pp. 1–26, 2014.

[12] N. A. Croll, J. M. Smith, and B. M. Zuckerman, "The aging process of the nematode Caenorhabditis elegans in bacterial and axenic culture.," *Exp. Aging Res.*, vol. 3, no. 3, pp. 175–189, 1977.

[13] T. Baba, T. Ara, M. Hasegawa, Y. Takai, Y. Okumura, M. Baba, K. A. Datsenko, M. Tomita, B. L. Wanner, and H. Mori, "Construction of Escherichia coli K-12 in-

frame, single-gene knockout mutants: the Keio collection.," *Mol. Syst. Biol.*, vol. 2, p. 2006.0008, 2006.

[14] J. F. Rual, J. Ceron, J. Koreth, T. Hao, A. S. Nicot, T. Hirozane-Kishikawa, J. Vandenhaute, S. H. Orkin, D. E. Hill, S. van den Heuvel, and M. Vidal, "Toward improving Caenorhabditis elegans phenome mapping with an ORFeome-based RNAi library," *Genome Res.*, vol. 14, no. 10 B, pp. 2162–2168, 2004.

[15] L. S. Yilmaz and A. J. M. Walhout, "Worms, bacteria, and micronutrients: an elegant model of our diet," *Trends Genet.*, vol. 30, no. 11, pp. 496–503, 2014.

[16] T. Boulin, J. F. Etchberger, and O. Hobert, "Reporter gene fusions.," *WormBook*, pp. 1–23, 2006.

[17] M. Chalfie, Y. Tu, G. Euskirchen, W. W. Ward, and D. C. Prasher, "Green fluorescent protein as a marker for gene expression," *Science (80-.).*, vol. 263, no. 5148, pp. 802–805, 1994.

[18] Y. Gavrieli, Y. Sherman, and S. A. Ben-Sasson, "Identification of programmed cell death in situ via specific labeling of nuclear DNA fragmentation," *J. Cell Biol.*, vol. 119, no. 3, pp. 493–501, 1992.

[19] J. E. Sulston, E. Schierenberg, J. G. White, and J. N. Thomson, "The embryonic cell lineage of the nematode Caenorhabditis elegans.," *Dev. Biol.*, vol. 100, no. 1, pp. 64–119, 1983.

[20] J. Collet, C. A. Spike, E. A. Lundquist, J. E. Shaw, and R. K. Herman, "Analysis of osm-6, a gene that affects sensory cilium structure and sensory neuron function in Caenorhabditis elegans," *Genetics*, vol. 148, no. 1, pp. 187–200, 1998.

[21] J. E. Sulston and H. R. Horvitz, "Post-embryonic cell lineages of the nematode, Caenorhabditis elegans," *Developmental Biology*, vol. 56, no. 1. pp. 110–156, 1977.

[22] K. Yen, T. T. Le, A. Bansal, S. D. Narasimhan, J.-X. Cheng, and H. a Tissenbaum, "A comparative study of fat storage quantitation in nematode Caenorhabditis elegans using label and label-free methods.," *PLoS One*, vol. 5, no. 9, Jan. 2010.

[23] A. A. Soukas, E. A. E. Kane, C. E. C. Carr, J. A. Melo, and G. Ruvkun, "Rictor/TORC2 regulates fat metabolism, feeding, growth, and life span in Caenorhabditis elegans," *Genes …*, vol. 23, no. 4, pp. 496–511, 2009.

[24] T. T. Le, H. M. Duren, M. N. Slipchenko, C.-D. Hu, and J.-X. Cheng, "Label-free quantitative analysis of lipid metabolism in living Caenorhabditis elegans.," *J. Lipid Res.*, vol. 51, no. 3, pp. 672–677, 2010.

[25] C. Wählby, L. Kamentsky, Z. H. Liu, T. Riklin-Raviv, A. L. Conery, E. J. O'Rourke, K. L. Sokolnicki, O. Visvikis, V. Ljosa, J. E. Irazoqui, P. Golland, G. Ruvkun, F. M. Ausubel, and A. E. Carpenter, "An image analysis toolbox for high-throughput C. elegans assays," *Nature Methods*, vol. 9, no. 7. pp. 714–716, 2012.

[26] A. R. Burns, T. C. Y. Kwok, A. Howard, E. Houston, K. Johanson, A. Chan, S. R. Cutler, P. McCourt, and P. J. Roy, "High-throughput screening of small molecules for bioactivity and target identification in Caenorhabditis elegans.," *Nat. Protoc.*, vol. 1, no. 4, pp. 1906–1914, 2006.

[27] S. J. Husson, W. S. Costa, C. Schmitt, and A. Gottschalk, "Keeping track of worm trackers *," *WormBook*, pp. 1–17, 2012.

[28] N. Stroustrup, B. E. Ulmschneider, Z. M. Nash, I. F. López-Moyado, J. Apfeld, and W. Fontana, "The Caenorhabditis elegans Lifespan Machine.," *Nat. Methods*, vol. 10, no. 7, pp. 665–670, 2013.

[29] X. Xu and S. K. Kim, "The early bird catches the worm: new technologies for the Caenorhabditis elegans toolkit," *Nature Reviews Genetics*, vol. 12, no. 11. pp. 793–801, 2011.

[30] E. Culetto and D. B. Sattelle, "A role for Caenorhabditis elegans in understanding the function and interactions of human disease genes.," *Hum. Mol. Genet.*, vol. 9, no. 6, pp. 869–877, 2000.

[31] C. elegans sequencing consortium, "Genome sequence of the nematode C. elegans: a platform for investigating biology. The C. elegans Sequencing Consortium [published erratum appears in Science 1999 Jan 1;283(5398):35]," *Science (80-.).*, vol. 282, pp. 2012–2018, 1998.

[32] D. Sinclair, K. Mills, and L. Guarente, "Aging in Saccharomyces cerevisiae.," *Annu. Rev. Microbiol.*, vol. 52, pp. 533–560, 1998.

[33] S. Goldstein, "Longevity, senescence and the genome," *Am. J. Hum. Genet.*, vol. 50, no. 2, pp. 451–452, 1992.

[34] L. A. Herndon, P. J. Schmeissner, J. M. Dudaronek, P. A. Brown, K. M. Listner, Y. Sakano, M. C. Paupard, D. H. Hall, and M. Driscoll, "Stochastic and genetic factors influence tissue-specific decline in ageing C. elegans.," *Nature*, vol. 419, no. 6909, pp. 808–814, 2002.

[35] D. A. Garsin, J. M. Villanueva, J. Begun, D. H. Kim, C. D. Sifri, S. B. Calderwood, G. Ruvkun, and F. M. Ausubel, "Long-lived C. elegans daf-2 mutants are resistant to bacterial pathogens.," *Science*, vol. 300, no. 5627, p. 1921, 2003.

[36] L. Fontana, L. Partridge, and V. D. Longo, “Extending healthy life span--from yeast to humans.,” *Science*, vol. 328, no. 5976, pp. 321–326, 2010.

[37] S. Broughton and L. Partridge, “Insulin/IGF-like signalling, the central nervous system and aging.,” *Biochem. J.*, vol. 418, no. 1, pp. 1–12, Feb. 2009.

[38] M. Barbieri, M. Bonafè, C. Franceschi, and G. Paolisso, “Insulin/IGF-I-signaling pathway: an evolutionarily conserved mechanism of longevity from yeast to humans.,” *Am. J. Physiol. Endocrinol. Metab.*, vol. 285, no. 5, pp. E1064–71, Nov. 2003.

[39] M. Tatar, A. Bartke, and A. Antebi, “The endocrine regulation of aging by insulin-like signals.,” *Science*, vol. 299, no. 5611, pp. 1346–51, Feb. 2003.

[40] C. M. Taniguchi, B. Emanuelli, and C. R. Kahn, “Critical nodes in signalling pathways: insights into insulin action.,” *Nat. Rev. Mol. Cell Biol.*, vol. 7, no. 2, pp. 85–96, 2006.

[41] A. Belfiore, F. Frasca, G. Pandini, L. Sciacca, and R. Vigneri, “Insulin receptor isoforms and insulin receptor/insulin-like growth factor receptor hybrids in physiology and disease,” *Endocrine Reviews*, vol. 30, no. 6. pp. 586–623, 2009.

[42] A. van der Horst and B. M. T. Burgering, “Stressing the role of FoxO proteins in lifespan and disease.,” *Nat. Rev. Mol. Cell Biol.*, vol. 8, no. 6, pp. 440–450, 2007.

[43] R. Fernandez, D. Tabarini, N. Azpiazu, M. Frasch, and J. Schlessinger, “The Drosophila insulin receptor homolog: a gene essential for embryonic development encodes two receptor isoforms with different signaling potential.,” *EMBO J.*, vol. 14, no. 14, pp. 3373–3384, 1995.

[44] H. a Tissenbaum and G. Ruvkun, “An insulin-like signaling pathway affects both longevity and reproduction in Caenorhabditis elegans.,” *Genetics*, vol. 148, no. 2, pp. 703–17, Feb. 1998.

[45] K. D. Kimura, “daf-2, an Insulin Receptor-Like Gene That Regulates Longevity and Diapause in Caenorhabditis elegans,” *Science (80-.).*, vol. 277, no. 5328, pp. 942–946, Aug. 1997.

[46] A. Skorokhod, V. Gamulin, D. Gundacker, V. Kavsan, I. M. Müller, and W. E. G. Müller, “Origin of insulin receptor-like tyrosine kinases in marine sponges,” *Biol. Bull.*, vol. 197, no. 2, pp. 198–206, 1999.

[47] P. De Meyts, I. J. Roth, D. M. Neville, and M. A. Lesniak, “Insulin interactions with its receptors,” vol. 55, no. 1, pp. 154–161, 1973.

[48] C. R. Kahn, P. Freychet, J. Roth, and D. M. Neville, “Quantitative aspects of the insulin-receptor interaction in liver plasma membranes.,” *J. Biol. Chem.*, vol. 249, no. 7, pp. 2249–2257, 1974.

[49] P. De Meyts, E. Van Obberghen, and J. Roth, “Mapping of the residues responsible for the negative cooperativity of the receptor-binding region of insulin.,” *Nature*, vol. 273, no. 5663, pp. 504–509, 1978.

[50] C. T. Christoffersen, K. E. Bornfeldt, C. M. Rotella, N. Gonzales, H. Vissing, R. M. Shymko, J. ten Hoeve, J. Groffen, N. Heisterkamp, and P. De Meyts, “Negative cooperativity in the insulin-like growth factor-I receptor and a chimeric IGF-I/insulin receptor.,” *Endocrinology*, vol. 135, no. 1, pp. 472–475, 1994.

[51] I. Claeys, G. Simonet, J. Poels, T. Van Loy, L. Vercammen, A. De Loof, and J. Vanden Broeck, “Insulin-related peptides and their conserved signal transduction pathway.,” *Peptides*, vol. 23, no. 4, pp. 807–16, Apr. 2002.

[52] W. Brogiolo, H. Stocker, T. Ikeya, F. Rintelen, R. Fernandez, and E. Hafen, “An evolutionarily conserved function of the drosophila insulin receptor and insulin-like peptides in growth control,” *Curr. Biol.*, vol. 11, no. 4, pp. 213–221, 2001.

[53] T. Ikeya, M. Galic, P. Belawat, K. Nairz, and E. Hafen, “Nutrient-dependent expression of insulin-like peptides from neuroendocrine cells in the CNS contributes to growth regulation in Drosophila,” *Curr. Biol.*, vol. 12, no. 15, pp. 1293–1300, 2002.

[54] J. Colombani, D. S. Andersen, and P. Leopold, “Secreted Peptide Dilp8 Coordinates Drosophila Tissue Growth with Developmental Timing,” *Science*, vol. 336, no. 6081. pp. 582–585, 2012.

[55] L. Duret, N. Guex, M. C. Peitsch, A. Bairoch, B. Lyon, F.-V. Cedex, and G. Biomedical, “New Insulin-Like Proteins with Atypical Disulfide Bond Pattern Characterized in Caenorhabditis elegans by Comparative Sequence Analysis and Homology ? Modeling New Insulin-Like Proteins with Atypical Disulfide Bond Pattern Characterized in Caenorhabditis,” *Genome Res.*, 1998.

[56] S. B. Pierce, M. Costa, R. Wisotzkey, S. Devadhar, S. a Homburger, a R. Buchman, K. C. Ferguson, J. Heller, D. M. Platt, a a Pasquinelli, L. X. Liu, S. K. Doberstein, and G. Ruvkun, “Regulation of DAF-2 receptor signaling by human insulin and ins-1, a member of the unusually large and diverse C. elegans insulin gene family.,” *Genes Dev.*, vol. 15, no. 6, pp. 672–86, Mar. 2001.

[57] W. Li, S. G. Kennedy, and G. Ruvkun, “daf-28 encodes a C. elegans insulin superfamily member that is regulated by environmental cues and acts in the DAF-2 signaling pathway.,” *Genes Dev.*, vol. 17, no. 7, pp. 844–58, Apr. 2003.

[58] C. Li and K. Kim, “Neuropeptides.,” *WormBook*, pp. 1–36, 2008.

[59] S. Jin Chan and D. F. Steiner, “Insulin Through the Ages: Phylogeny of a Growth Promoting and Metabolic Regulatory Hormone1,” *Am. Zool.*, vol. 40, no. 2, pp. 213–222, Apr. 2000.

[60] P. De Meyts, “Insulin and its receptor: structure, function and evolution,” *Bioessays*, vol. 26, no. 12, pp. 1351–1362, 2004.

[61] Z. Fu, E. R. Gilbert, and D. Li, “Regulation of Insulin Synthesis and Secretion and Pancreatic Beta-Cell Dysfunction in Diabetes.,” *Curr. Diabetes Rev.*, 2012.

[62] D. L. Riddle, M. M. Swanson, and P. S. Albert, “Interacting genes in nematode dauer larva formation.,” *Nature*, vol. 290, no. 5808, pp. 668–671, 1981.

[63] P. J. Hu, “Dauer.,” *WormBook*, pp. 1–19, 2007.

[64] M. R. Klass, “A method for the isolation of longevity mutants in the nematode Caenorhabditis elegans and initial results.,” *Mech. Ageing Dev.*, vol. 22, pp. 279–286, 1983.

[65] J. Z. Morris, H. A. Tissenbaum, and G. Ruvkun, “A phosphatidylinositol-3-OH kinase family member regulating longevity and diapause in Caenorhabditis elegans.,” *Nature*, vol. 382, no. 6591, pp. 536–539, 1996.

[66] S. Gottlieb and G. Ruvkun, “daf-2, daf-16 and daf-23: Genetically interacting genes controlling dauer formation in Caenorhabditis elegans,” *Genetics*, vol. 137, no. 1, pp. 107–120, 1994.

[67] J. B. Dorman, B. Albinder, T. Shroyer, and C. Kenyon, “The age-1 and daf-2 genes function in a common pathway to control the lifespan of Caenorhabditis elegans,” *Genetics*, vol. 141, no. 4, pp. 1399–1406, 1995.

[68] S. Ogg, S. Paradis, S. Gottlieb, G. I. Patterson, L. Lee, H. a Tissenbaum, and G. Ruvkun, “The Fork head transcription factor DAF-16 transduces insulin-like metabolic and longevity signals in C. elegans.,” *Nature*, vol. 389, no. 6654, pp. 994–9, Oct. 1997.

[69] J. Wang and S. K. Kim, “Global analysis of dauer gene expression in Caenorhabditis elegans.,” *Development*, vol. 130, no. 8, pp. 1621–1634, 2003.

[70] C. T. Murphy, S. a McCarroll, C. I. Bargmann, A. Fraser, R. S. Kamath, J. Ahringer, H. Li, and C. Kenyon, “Genes that act downstream of DAF-16 to influence the lifespan of Caenorhabditis elegans.,” *Nature*, vol. 424, no. 6946, pp. 277–83, Jul. 2003.

[71] C. T. Murphy, S.-J. Lee, and C. Kenyon, “Tissue entrainment by feedback regulation of insulin gene expression in the endoderm of Caenorhabditis elegans.,” *Proc. Natl. Acad. Sci. U. S. A.*, vol. 104, no. 48, pp. 19046–50, Nov. 2007.

[72] G. J. Lithgow, T. M. White, D. A. Hinerfeld, and T. E. Johnson, “Thermotolerance of a long-lived mutant of Caenorhabditis elegans.,” *J. Gerontol.*, vol. 49, no. 6, pp. B270–B276, 1994.

[73] Y. Honda and S. Honda, “The daf-2 gene network for longevity regulates oxidative stress resistance and Mn-superoxide dismutase gene expression in Caenorhabditis elegans.,” *FASEB J.*, vol. 13, no. 11, pp. 1385–1393, 1999.

[74] D. Gems, A. J. Sutton, M. L. Sundermeyer, P. S. Albert, K. V. King, M. L. Edgley, P. L. Larsen, and D. L. Riddle, “Two pleiotropic classes of daf-2 mutation affect larval arrest, adult behavior, reproduction and longevity in Caenorhabditis elegans,” *Genetics*, vol. 150, no. 1, pp. 129–155, 1998.

[75] S. Luo, G. a. Kleemann, J. M. Ashraf, W. M. Shaw, and C. T. Murphy, “TGF-β and Insulin Signaling Regulate Reproductive Aging via Oocyte and Germline Quality Maintenance,” *Cell*, vol. 143, no. 2, pp. 299–312, Oct. 2010.

[76] E. M. H. Tank, K. E. Rodgers, and C. Kenyon, “Spontaneous age-related neurite branching in Caenorhabditis elegans.,” *J. Neurosci.*, vol. 31, no. 25, pp. 9279–9288, 2011.

[77] M. L. Toth, I. Melentijevic, L. Shah, A. Bhatia, K. Lu, A. Talwar, H. Naji, C. Ibanez-Ventoso, P. Ghose, A. Jevince, J. Xue, L. A. Herndon, G. Bhanot, C. Rongo, D. H. Hall, and M. Driscoll, “Neurite Sprouting and Synapse Deterioration in the Aging Caenorhabditis elegans Nervous System,” *Journal of Neuroscience*, vol. 32, no. 26. pp. 8778–8790, 2012.

[78] C.-L. Pan, C.-Y. Peng, C.-H. Chen, and S. McIntire, “Genetic analysis of age-dependent defects of the Caenorhabditis elegans touch receptor neurons.,” *Proc. Natl. Acad. Sci. U. S. A.*, vol. 108, no. 22, pp. 9274–9279, 2011.

[79] M. Tomioka, T. Adachi, H. Suzuki, H. Kunitomo, W. R. Schafer, and Y. Iino, “The insulin/PI 3-kinase pathway regulates salt chemotaxis learning in Caenorhabditis elegans.,” *Neuron*, vol. 51, no. 5, pp. 613–25, Oct. 2006.

[80] J. M. Conlon, “Evolution of the insulin molecule: insights into structure-activity and phylogenetic relationships.,” Jul. 2001.

[81] Z.-Y. Guo, Z.-S. Qiao, and Y.-M. Feng, “The in vitro oxidative folding of the insulin superfamily.,” *Antioxid. Redox Signal.*, vol. 10, no. 1, pp. 127–39, Jan. 2008.

[82] Q. xin Hua, S. H. Nakagawa, J. Wilken, R. R. Ramos, W. Jia, J. Bass, and M. A. Weiss, "A divergent INS protein in Caenorhabditis elegans structurally resembles human insulin and activates the human insulin receptor," *Genes Dev.*, vol. 17, no. 7, pp. 826–831, 2003.

[83] O. Billing, G. Kao, and P. Naredi, "Mitochondrial Function Is Required for Secretion of DAF-28/Insulin in C. elegans," *PLoS One*, vol. 6, no. 1, p. e14507, Jan. 2011.

[84] G. Kao, C. Nordenson, M. Still, A. Rönnlund, S. Tuck, and P. Naredi, "ASNA-1 positively regulates insulin secretion in C. elegans and mammalian cells.," *Cell*, vol. 128, no. 3, pp. 577–87, Feb. 2007.

[85] Z. Chen, M. Hendricks, A. Cornils, W. Maier, J. Alcedo, and Y. Zhang, "Two Insulin-like Peptides Antagonistically Regulate Aversive Olfactory Learning in C. elegans," *Neuron*, vol. 77, no. 3, pp. 572–585, 2013.

[86] A. Cornils, M. Gloeck, Z. Chen, Y. Zhang, and J. Alcedo, "Specific insulin-like peptides encode sensory information to regulate distinct developmental processes.," *Development*, vol. 138, no. 6, pp. 1183–93, Mar. 2011.

[87] D. Michaelson, D. Z. Korta, Y. Capua, and E. J. A. Hubbard, "Insulin signaling promotes germline proliferation in C. elegans.," *Development*, vol. 137, no. 4, pp. 671–80, Feb. 2010.

[88] Y. Matsunaga, K. Gengyo-Ando, S. Mitani, T. Iwasaki, and T. Kawano, "Physiological function, expression pattern, and transcriptional regulation of a Caenorhabditis elegans insulin-like peptide, INS-18," *Biochem. Biophys. Res. Commun.*, vol. 423, no. 3, pp. 478–483, 2012.

[89] T. Kawano, R. Nagatomo, Y. Kimura, K. Gengyo-Ando, and S. Mitani, "Disruption of ins-11, a Caenorhabditis elegans Insulin-Like Gene, and Phenotypic Analyses of the Gene-Disrupted Animal," *Biosci. Biotechnol. Biochem.*, vol. 70, no. 12, pp. 3084–3087, 2006.

[90] T. Kawano, Y. Ito, M. Ishiguro, K. Takuwa, T. Nakajima, and Y. Kimura, "Molecular cloning and characterization of a new insulin/IGF-like peptide of the nematode Caenorhabditis elegans.," *Biochem. Biophys. Res. Commun.*, vol. 273, no. 2, pp. 431–6, Jul. 2000.

[91] D. Andrea, F. De Abreu, A. Caballero, P. Fardel, N. Stroustrup, Z. Chen, K. Lee, W. D. Keyes, Z. M. Nash, I. F. Lo, F. Vaggi, A. Cornils, M. Regenass, A. Neagu, I. Ostojic, and C. Liu, "An Insulin-to-Insulin Regulatory Network Orchestrates Phenotypic Specificity in Development and Physiology," vol. 10, no. 3, pp. 17–19, 2014.

[92] T. Kawli and M.-W. Tan, “Neuroendocrine signals modulate the innate immunity of Caenorhabditis elegans through insulin signaling.,” *Nat. Immunol.*, vol. 9, no. 12, pp. 1415–24, Dec. 2008.

[93] S. Ohno, “Evolution by Gene Duplication,” *(1970)*, 1970.

[94] A. Force, M. Lynch, F. B. Pickett, A. Amores, Y. L. Yan, and J. Postlethwait, “Preservation of duplicate genes by complementary, degenerative mutations,” *Genetics*, vol. 151, no. 4, pp. 1531–1545, 1999.

[95] A. Burga, M. O. Casanueva, and B. Lehner, “Predicting mutation outcome from early stochastic variation in genetic interaction partners,” *Nature*, vol. 480, no. 7376. pp. 250–253, 2011.

[96] L. T. Macneil and A. J. M. Walhout, “Gene regulatory networks and the role of robustness and stochasticity in the control of gene expression,” pp. 645–657, 2011.

[97] C. A. Grove, F. De Masi, M. I. Barrasa, D. E. Newburger, M. J. Alkema, M. L. Bulyk, and A. J. M. Walhout, “A Multiparameter Network Reveals Extensive Divergence between C. elegans bHLH Transcription Factors,” *Cell*, vol. 138, no. 2, pp. 314–327, 2009.

[98] P. C. Hollenhorst, A. A. Shah, C. Hopkins, and B. J. Graves, “Genome-wide analyses reveal properties of redundant and specific promoter occupancy within the ETS gene family,” *Genes Dev.*, vol. 21, no. 15, pp. 1882–1894, 2007.

[99] J. W. Golden and D. L. Riddle, “The Caenorhabditis elegans dauer larva: developmental effects of pheromone, food, and temperature.,” *Dev. Biol.*, vol. 102, no. 2, pp. 368–378, 1984.

[100] H. Jeong, S. P. Mason, A. L. Barabási, and Z. N. Oltvai, “Lethality and centrality in protein networks.,” *Nature*, vol. 411, no. 6833, pp. 41–42, 2001.

[101] R. Kafri, A. Bar-Even, and Y. Pilpel, “Transcription control reprogramming in genetic backup circuits.,” *Nat. Genet.*, vol. 37, no. 3, pp. 295–9, Mar. 2005.

[102] R. Kafri, O. Dahan, J. Levy, and Y. Pilpel, “Preferential protection of protein interaction network hubs in yeast: evolved functionality of genetic redundancy.,” *Proc. Natl. Acad. Sci. U. S. A.*, vol. 105, no. 4, pp. 1243–1248, 2008.

[103] A. DeLuna, K. Vetsigian, N. Shoresh, M. Hegreness, M. Colón-González, S. Chao, and R. Kishony, “Exposing the fitness contribution of duplicated genes.,” *Nat. Genet.*, vol. 40, no. 5, pp. 676–681, 2008.

[104] A. R. O. Cavalcanti, R. Ferreira, Z. Gu, and W.-H. Li, "Patterns of gene duplication in Saccharomyces cerevisiae and Caenorhabditis elegans.," *J. Mol. Evol.*, vol. 56, no. 1, pp. 28–37, 2003.

[105] E. Yigit, P. J. Batista, Y. Bei, K. M. Pang, C. C. G. Chen, N. H. Tolia, L. Joshua-Tor, S. Mitani, M. J. Simard, and C. C. Mello, "Analysis of the C. elegans Argonaute Family Reveals that Distinct Argonautes Act Sequentially during RNAi," *Cell*, vol. 127, no. 4, pp. 747–757, 2006.

[106] S. Broughton, N. Alic, C. Slack, T. Bass, T. Ikeya, G. Vinti, A. M. Tommasi, Y. Driege, E. Hafen, and L. Partridge, "Reduction of DILP2 in Drosophila triages a metabolic phenotype from lifespan revealing redundancy and compensation among DILPs," *PLoS One*, vol. 3, no. 11, 2008.

[107] S. Grönke, D.-F. Clarke, S. Broughton, T. D. Andrews, and L. Partridge, "Molecular evolution and functional characterization of Drosophila insulin-like peptides.," *PLoS Genet.*, vol. 6, no. 2, p. e1000857, Feb. 2010.

[108] J. S. Reece-Hoyes, J. Shingles, D. Dupuy, C. a Grove, A. J. M. Walhout, M. Vidal, and I. a Hope, "Insight into transcription factor gene duplication from Caenorhabditis elegans Promoterome-driven expression patterns.," *BMC Genomics*, vol. 8, p. 27, Jan. 2007.

[109] N. J. Martinez, M. C. Ow, J. S. Reece-hoyes, M. I. Barrasa, V. R. Ambros, and A. J. M. Walhout, "Genome-scale spatiotemporal analysis of Caenorhabditis elegans microRNA promoter activity," *Genome Res.*, pp. 2005–2015, 2008.

[110] V. Vermeirssen, M. I. Barrasa, C. a Hidalgo, J. A. B. Babon, R. Sequerra, L. Doucette-Stamm, A.-L. Barabási, and A. J. M. Walhout, "Transcription factor modularity in a gene-centered C. elegans core neuronal protein-DNA interaction network.," *Genome Res.*, vol. 17, no. 7, pp. 1061–71, Jul. 2007.

[111] H. E. Arda, S. Taubert, L. T. MacNeil, C. C. Conine, B. Tsuda, M. Van Gilst, R. Sequerra, L. Doucette-Stamm, K. R. Yamamoto, and A. J. M. Walhout, "Functional modularity of nuclear hormone receptors in a Caenorhabditis elegans metabolic gene regulatory network.," *Mol. Syst. Biol.*, vol. 6, p. 367, May 2010.

[112] C. Kenyon, "The first long-lived mutants: discovery of the insulin/IGF-1 pathway for ageing.," *Philos. Trans. R. Soc. Lond. B. Biol. Sci.*, vol. 366, no. 1561, pp. 9–16, Jan. 2011.

[113] V. Praitis, E. Casey, D. Collar, and J. Austin, "Creation of low-copy integrated transgenic lines in Caenorhabditis elegans," *Genetics*, vol. 157, no. 3, pp. 1217–1226, 2001.

[114] K. Thoemke, W. Yi, J. M. Ross, S. Kim, V. Reinke, and D. Zarkower, "Genome-wide analysis of sex-enriched gene expression during C. elegans larval development.," *Dev. Biol.*, vol. 284, no. 2, pp. 500–8, Aug. 2005.

[115] C. A. Wolkow, "Life span: Getting the signal from the nervous system," *Trends in Neurosciences*, vol. 25, no. 4. pp. 212–216, 2002.

[116] Y. G. Tong and T. R. Bürglin, "Conditions for dye-filling of sensory neurons in Caenorhabditis elegans," *J. Neurosci. Methods*, vol. 188, no. 1, pp. 58–61, 2010.

[117] P. Shannon, A. Markiel, O. Ozier, N. S. Baliga, J. T. Wang, D. Ramage, N. Amin, B. Schwikowski, and T. Ideker, "Cytoscape: A software Environment for integrated models of biomolecular interaction networks," *Genome Res.*, vol. 13, no. 11, pp. 2498–2504, 2003.

[118] A. Raj, S. A. Rifkin, E. Andersen, and A. van Oudenaarden, "Variability in gene expression underlies incomplete penetrance.," *Nature*, vol. 463, no. 7283, pp. 913–918, 2010.

[119] L. R. Baugh, N. Kurhanewicz, and P. W. Sternberg, "Sensitive and Precise Quantification of Insulin-Like mRNA Expression in Caenorhabditis elegans.," *PLoS One*, vol. 6, no. 3, p. e18086, Jan. 2011.

[120] F. Simmer, M. Tijsterman, S. Parrish, S. P. Koushika, M. L. Nonet, A. Fire, J. Ahringer, and R. H. A. Plasterk, "Loss of the putative RNA-directed RNA polymerase RRF-3 makes C. elegans hypersensitive to RNAi," *Curr. Biol.*, vol. 12, no. 15, pp. 1317–1319, 2002.

[121] D. Dupuy, Q.-R. Li, B. Deplancke, M. Boxem, T. Hao, P. Lamesch, R. Sequerra, S. Bosak, L. Doucette-Stamm, I. a Hope, D. E. Hill, A. J. M. Walhout, and M. Vidal, "A first version of the Caenorhabditis elegans Promoterome.," *Genome Res.*, vol. 14, no. 10B, pp. 2169–75, Oct. 2004.

[122] J. S. Reece-Hoyes, J. Shingles, D. Dupuy, C. A. Grove, A. J. M. Walhout, M. Vidal, and I. A. Hope, "Insight into transcription factor gene duplication from Caenorhabditis elegans Promoterome-driven expression patterns.," *BMC Genomics*, vol. 8, p. 27, 2007.

[123] A. G. Fraser, R. S. Kamath, P. Zipperlen, M. Martinez-Campos, M. Sohrmann, and J. Ahringer, "Functional genomic analysis of C. elegans chromosome I by systematic RNA interference.," *Nature*, vol. 408, no. 6810, pp. 325–330, 2000.

[124] N. J. Martinez, M. C. Ow, J. S. Reece-Hoyes, M. I. Barrasa, V. R. Ambros, and A. J. M. Walhout, "Genome-scale spatiotemporal analysis of Caenorhabditis elegans microRNA promoter activity.," *Genome Res.*, vol. 18, no. 12, pp. 2005–15, Dec. 2008.

[125] V. Vermeirssen, B. Deplancke, M. I. Barrasa, J. S. Reece-Hoyes, H. E. Arda, C. A. Grove, N. J. Martinez, R. Sequerra, L. Doucette-Stamm, M. R. Brent, and A. J. M. Walhout, "Matrix and Steiner-triple-system smart pooling assays for high-performance transcription regulatory network mapping.," *Nat. Methods*, vol. 4, no. 8, pp. 659–664, 2007.

[126] D. S. Goldberg and F. P. Roth, "Assessing experimentally derived interactions in a small world.," *Proc. Natl. Acad. Sci. U. S. A.*, vol. 100, no. 8, pp. 4372–6, Apr. 2003.

[127] W. N. Tawe, M. L. Eschbach, R. D. Walter, and K. Henkle-Dührsen, "Identification of stress-responsive genes in Caenorhabditis elegans using RT-PCR differential display," *Nucleic Acids Res.*, vol. 26, no. 7, pp. 1621–1627, 1998.

[128] S. J. Lee, C. T. Murphy, and C. Kenyon, "Glucose Shortens the Life Span of C. elegans by Downregulating DAF-16/FOXO Activity and Aquaporin Gene Expression," *Cell Metab.*, vol. 10, no. 5, pp. 379–391, 2009.

[129] M. F. P. Heschl and D. L. Baillie, "The hsp70 multigene family of Caenorhabditis elegans," *Comparative Biochemistry and Physiology - B Biochemistry and Molecular Biology*, vol. 96, no. 4. pp. 633–637, 1990.

[130] L. T. MacNeil, E. Watson, H. E. Arda, L. J. Zhu, and A. J. M. Walhout, "Diet-induced developmental acceleration independent of TOR and insulin in C. elegans," *Cell*, vol. 153, no. 1, pp. 240–252, 2013.

[131] W. G. Kelly, S. Xu, M. K. Montgomery, and A. Fire, "Distinct requirements for somatic and germline expression of a generally expressed Caenorhabditis elegans gene," *Genetics*, vol. 146, no. 1, pp. 227–238, 1997.

[132] H. Bai, P. Kang, and M. Tatar, "Drosophila insulin-like peptide-6 (dilp6) expression from fat body extends lifespan and represses secretion of Drosophila insulin-like peptide-2 from the brain," *Aging Cell*, vol. 11, no. 6, pp. 978–985, 2012.

[133] D. L. Riddle, T. Blumenthal, B. J. Meyer, and J. R. Priess, *C. elegans II*, vol. 33. 1997.

[134] G. M. Edelman and J. A. Gally, "Degeneracy and complexity in biological systems.," *Proc. Natl. Acad. Sci. U. S. A.*, vol. 98, no. 24, pp. 13763–13768, 2001.

[135] H. Kitano, "Biological Robustness," vol. 5, no. November, 2004.

[136] B. P. Braeckman, K. Houthoofd, and J. R. Vanfleteren, "Intermediary metabolism.," *WormBook*, pp. 1–24, 2009.

[137] P. Y. Jeong, M. S. Kwon, H. J. Joo, and Y. K. Paik, "Molecular time-course and the metabolic basis of entry into Dauer in Caenorhabditis elegans," *PLoS One*, vol. 4, no. 1, 2009.

[138] K. Ashrafi, F. Y. Chang, J. L. Watts, A. G. Fraser, R. S. Kamath, J. Ahringer, and G. Ruvkun, "Genome-wide RNAi analysis of Caenorhabditis elegans fat regulatory genes.," *Nature*, vol. 421, no. 6920, pp. 268–272, 2003.

[139] J. Ablain, E. M. Durand, Y. Zhou, L. I. Zon, J. Ablain, E. M. Durand, S. Yang, Y. Zhou, and L. I. Zon, "Resource A CRISPR / Cas9 Vector System for Tissue-Specific Gene Disruption in Zebrafish Resource A CRISPR / Cas9 Vector System for Tissue-Specific Gene Disruption in Zebrafish," *Dev. Cell*, vol. 32, no. 6, pp. 756–764, 2015.

[140] Z. Cheng, P. Yi, X. Wang, Y. Chai, G. Feng, Y. Yang, X. Liang, Z. Zhu, W. Li, and G. Ou, "Conditional targeted genome editing using somatically expressed TALENs in C. elegans.," *Nat. Biotechnol.*, vol. 31, no. 10, pp. 934–7, 2013.

[141] T. Gaj, C. A. Gersbach, and C. F. Barbas, "ZFN, TALEN, and CRISPR/Cas-based methods for genome engineering," *Trends in Biotechnology*, vol. 31, no. 7. pp. 397–405, 2013.

[142] C. Thacker, M. Srayko, and A. M. Rose, "Mutational analysis of bli-4/kpc-4 reveals critical residues required for proprotein convertase function in C. elegans," *Gene*, vol. 252, no. 1–2, pp. 15–25, 2000.

[143] J. Kass, T. C. Jacob, P. Kim, and J. M. Kaplan, "The EGL-3 proprotein convertase regulates mechanosensory responses of Caenorhabditis elegans.," *J. Neurosci.*, vol. 21, no. 23, pp. 9265–9272, 2001.

[144] D. Sieburth, J. M. Madison, and J. M. Kaplan, "PKC-1 regulates secretion of neuropeptides.," *Nat. Neurosci.*, vol. 10, no. 1, pp. 49–57, 2007.

[145] H. Werner, D. Weinstein, and I. Bentov, "Similarities and differences between insulin and IGF-I : Structures , receptors , and signalling pathways," vol. 114, no. January, pp. 17–22, 2008.

[146] T. W. Harris, J. Baran, T. Bieri, A. Cabunoc, J. Chan, W. J. Chen, P. Davis, J. Done, C. Grove, K. Howe, R. Kishore, R. Lee, Y. Li, H. M. Muller, C. Nakamura, P. Ozersky, M. Paulini, D. Raciti, G. Schindelman, M. A. Tuli, K. Van Auken, D. Wang, X. Wang, G. Williams, J. D. Wong, K. Yook, T. Schedl, J. Hodgkin, M. Berriman, P. Kersey, J. Spieth, L. Stein, and P. W. Sternberg, "WormBase 2014: New views of curated biology," *Nucleic Acids Res.*, vol. 42, no. D1, 2014.

[147] C. H. A. Lin, M. Tomioka, S. Pereira, L. Sellings, Y. Iino, and D. van der Kooy, "Insulin signaling plays a dual role in Caenorhabditis elegans memory

acquisition and memory retrieval.," *J. Neurosci.*, vol. 30, no. 23, pp. 8001–11, Jun. 2010.

[148] W. L. Hung, Y. Wang, J. Chitturi, and M. Zhen, "A Caenorhabditis elegans developmental decision requires insulin signaling-mediated neuron-intestine communication," pp. 1767–1779, 2014.

[149] H. Ohno, S. Kato, Y. Naito, H. Kunitomo, M. Tomioka, and Y. Iino, "Role of synaptic phosphatidylinositol 3-kinase in a behavioral learning response in C. elegans," *Science (80-.).*, vol. 345, no. 6194, pp. 313–317, 2014.

[150] D. A. McClain, "Different ligand affinities of the two human insulin receptor splice variants are reflected in parallel changes in sensitivity for insulin action.," *Mol. Endocrinol.*, vol. 5, no. 5, pp. 734–739, 1991.

[151] S. H. Chalasani, S. Kato, D. R. Albrecht, T. Nakagawa, L. F. Abbott, and C. I. Bargmann, "Neuropeptide feedback modifies odor-evoked dynamics in Caenorhabditis elegans olfactory neurons.," *Nat. Neurosci.*, vol. 13, no. 5, pp. 615–21, May 2010.

[152] M. Dlaki, "A new family of putative insulin receptor-like proteins in C. elegans," *Current Biology*, vol. 12, no. 5. 2002.

[153] M. J. A. Saad, F. Folli, J. A. Kahn, and C. R. Kahn, "Modulation of insulin receptor, insulin receptor substrate-1, and phosphatidylinositol 3-kinase in liver and muscle of dexamethasone-treated rats," *J. Clin. Invest.*, vol. 92, no. 4, pp. 2065–2072, 1993.

[154] M. G. Myers and M. F. White, "Insulin signal transduction and the IRS proteins.," *Annu. Rev. Pharmacol. Toxicol.*, vol. 36, pp. 615–658, 1996.

[155] M. Camps, A. Castelló, P. Muñoz, M. Monfar, X. Testar, M. Palacín, and A. Zorzano, "Effect of diabetes and fasting on GLUT-4 (muscle/fat) glucose-transporter expression in insulin-sensitive tissues. Heterogeneous response in heart, red and white muscle.," *Biochem. J.*, vol. 282 (Pt 3, pp. 765–772, 1992.

[156] A. Guilherme, J. V Virbasius, V. Puri, and M. P. Czech, "Adipocyte dysfunctions linking obesity to insulin resistance and type 2 diabetes.," *Nat. Rev. Mol. Cell Biol.*, vol. 9, no. 5, pp. 367–377, 2008.

[157] J. Apfeld and C. Kenyon, "Cell Nonautonomy of C . elegans daf-2 Function in the Regulation of Diapause and Life Span," *Cell*, vol. 95, pp. 199–210, 1998.

[158] N. Libina, J. R. Berman, and C. Kenyon, “Tissue-specific activities of C. elegans DAF-16 in the regulation of lifespan.,” *Cell*, vol. 115, no. 4, pp. 489–502, Nov. 2003.

[159] S. D. Narasimhan, A. Mukhopadhyay, and H. a Tissenbaum, “InAKTivation of insulin/IGF-1 signaling by dephosphorylation.,” *Cell Cycle*, vol. 8, no. 23, pp. 3878–84, Dec. 2009.

[160] K. Jia, D. Chen, and D. L. Riddle, “The TOR pathway interacts with the insulin signaling pathway to regulate C. elegans larval development, metabolism and life span.,” *Development*, vol. 131, no. 16, pp. 3897–3906, 2004.

[161] D. Chen, P. W. Li, B. A. Goldstein, W. Cai, E. L. Thomas, F. Chen, A. E. Hubbard, S. Melov, and P. Kapahi, “Article Germline Signaling Mediates the Synergistically Prolonged Longevity Produced by Double Mutations in daf-2 and rsks-1 in C . elegans,” *CellReports*, vol. 5, no. 6, pp. 1600–1610, 2013.

[162] S. D. Narasimhan, K. Yen, A. Bansal, E. S. Kwon, S. Padmanabhan, and H. A. Tissenbaum, “PDP-1 links the TGF-?? and IIS pathways to regulate longevity, development, and metabolism,” *PLoS Genet.*, vol. 7, no. 4, 2011.

[163] C. T. Murphy, “The search for DAF-16 / FOXO transcriptional targets : Approaches and discoveries,” vol. 41, pp. 910–921, 2006.

[164] C. A. Wolkow, K. D. Kimura, M. S. Lee, and G. Ruvkun, “Regulation of C. elegans life-span by insulinlike signaling in the nervous system.,” *Science*, vol. 290, no. 5489, pp. 147–150, 2000.

[165] W. Qi, X. Huang, E. Neumann-haefelin, E. Schulze, and R. Baumeister, “Cell-Nonautonomous Signaling of FOXO / DAF-16 to the Stem Cells of Caenorhabditis elegans,” vol. 8, no. 8, 2012.

[166] et al. Giaever, “Functional profiling of the Saccharomyces cerevisiae genome.,” *Nature*, vol. 418, no. 6896, pp. 387–91, 2002.

[167] R. S. Kamath and J. Ahringer, “Genome-wide RNAi screening in Caenorhabditis elegans,” *Methods*, vol. 30, no. 4, pp. 313–321, 2003.

[168] J. Stelling, S. Klamt, K. Bettenbrock, S. Schuster, and E. D. Gilles, “Metabolic network structure determines key aspects of functionality and regulation.,” *Nature*, vol. 420, no. 6912, pp. 190–193, 2002.

[169] J. Stelling, U. Sauer, Z. Szallasi, F. J. Doyle, and J. Doyle, “Robustness of cellular functions,” *Cell*, vol. 118, no. 6. pp. 675–685, 2004.

[170] H. Kitano, "Towards a theory of biological robustness.," *Molecular systems biology*, vol. 3. p. 137, 2007.

[171] S. J. Russell and C. R. Kahn, "Endocrine regulation of ageing.," *Nat. Rev. Mol. Cell Biol.*, vol. 8, no. 9, pp. 681–691, 2007.

PREFACE TO PART II

SUMMARY

Aging can be modulated, at least in part, by diet. In Part II, I discuss how diet, dietary mimetics and other chemical compounds affect *C. elegans* lifespan (Chapter 4). I present my preliminary research that exemplifies how interactions between different diets and a drug can influence animal physiology (Chapter 5). Finally, in the last chapter, I discuss the implications of my research and future directions for gaining a greater understanding of the interactions between diet, drugs and *C. elegans* physiology (Chapter 6).

Data regarding the contribution of B12 to *C. elegans* lifespan, discussed in Chapter 4, was generated in a previously published manuscript:

Watson, E; Macneil, LT; **Ritter, AD**; Yilmaz, LS; Rosebrock, AP; Caudy, AA; Walhout, AJM (2014). Interspecies systems biology uncovers metabolites affecting C. elegans gene expression and life history traits. *Cell*. 156(4), 759–770. doi: 10.1016/j.cell.2014.01.047

The data presented in Chapter 5 was generated with the help of Gabrielle Giese. Gabrielle Giese performed the *Comamonas* DA1877 mutant screen, sequencing of mutants and performed replicate experiments for brood size, bacterial growth and lifespan experiments. Marian Walhout and I conceived the project. I performed all data analysis and experiments, except for the mutant screen. The data presented in Part II are preliminary and unpublished findings.

PART II

Diet-specific drug effects on *C. elegans*

PART II, CHAPTER 4

INTRODUCTION

Diet significantly impacts metabolism and physiology. Diet may also contribute appreciably to longevity. For instance, dietary restriction (DR) has been illustrated to have beneficial effects on longevity and is perhaps one of the most studied dietary contributors of aging [1]. DR, defined as the reduction of nutrient intake without causing malnutrition, can lead to significant increases in lifespan across vertebrate and invertebrate species [2]. While the exact molecular mechanisms of DR are not fully elucidated, examining DR in *C. elegans* has demonstrated basic mechanisms and downstream effectors including the TOR pathway and transcription factors such as SKN-1 [3], [4].

The dramatic influence of DR on lifespan has inspired a broader notion that diet alone could modulate lifespan. Additionally, the highly conserved lifespan-extending effects of DR and mutations in genetic pathways, such as the IIS pathway, have lead to research for pharmaceutical mimetics and other dietary supplements that target these mechanisms and similarly extend life. In the next chapter, I will discuss how use of *C. elegans* has revealed new relationships between diet, drugs and lifespan. I will also review the effects of diet and drugs on *C. elegans* lifespan and how lifespan is likely modulated by combinatorial interactions between diet, drugs and the animal. I will then present my preliminary data that illustrates diet-specific drug effects on *C. elegans* and discuss future directions of this work.

Diet effects on *C. elegans* lifespan

The “food limit” hypothesis has recently been challenged by the idea that “food quality” or composition may be a driving factor in modulating lifespan. Different types of bacteria influence *C. elegans* lifespan [5]–[10]. Recent work from our lab has shown that *C. elegans* lifespan is shortened on a *Comamonas* DA1877 diet when compared to *E. coli* OP50. In addition, *Comamonas* DA1877 diet resulted in an accelerated developmental rate and reduced brood size. On a diet of killed *Comamonas* DA1877 or *Comamonas* DA1877 diluted with *E. coli* OP50, the *C. elegans* accelerated developmental rate persists supporting the interpretation that a dietary bacterial signal can modulate physiology [6]. Indeed, differences in life history traits of animals fed *Comamonas* DA1877 versus *E. coli* OP50 can be attributed to, at least in part, the content of vitamin B12 in bacteria. Vitamin B12, however, did not explain the differences in lifespan of animals fed these two bacteria [11]. Nonetheless, the shortened lifespan of *C. elegans* fed *Comamonas* DA1877 relative to *E. coli* OP50 is not observed upon diluting *Comamonas* DA1877 with *E. coli* OP50 consistent with the possibility that bacterial nutritional content, distinct from vitamin B12, causes the observed difference in lifespan [6].

Genetically modifying the bacterial diet has revealed specific metabolic compounds and processes that affect lifespan. For instance, mutating an *E. coli* gene (*aroD*) involved in the biosynthesis of aromatic compounds, like folate, leads to increased lifespan. Adding folate back to the media shortened lifespan, comparable to wild-type, suggesting microbial folate synthesis may contribute to

C. elegans longevity. This hypothesis was further supported as inhibition of folate synthesis by a drug, sulfamethoxazole, led to a dose-dependent increase in *C. elegans* lifespan [12]. The ease with which the *C. elegans* diet can be genetically modified will allow for further investigation of metabolites, metabolic genes and pathways that contribute to lifespan [13], [14].

The use of *C. elegans* mutants has provided a powerful tool for unveiling mechanisms that modulate lifespan in response to diet. For instance, while there is no appreciable lifespan difference between wild-type animals fed *E. coli* OP50 versus *E. coli* HT115, *C. elegans* with mutations in the TOR complex-2-specific factor *Rictor* are short lived when propagated on *E. coli* OP50 but long lived by 76% on *E. coli* HT115 compared to wild-type animals [15]. One study used *C. elegans* mutants to determine that animals may employ adaptive strategies to cope with differences in these two *E. coli* strains [16]. Animals harboring a mutation in *alh-6*, a metabolic enzyme involved in the breakdown of proline, exhibit a 40% reduction in lifespan when fed OP50 compared to wild-type animals. However, when fed a diet of *E. coli* HT115, *alh-6* mutants exhibited a lifespan similar to wild-type animals. Proline supplementation to an HT115 diet significantly reduced the lifespan of *alh-6* mutants but not wild-type animals. Proline supplementation to an OP50 diet had no effect on *alh-6* mutant lifespan. Additionally, accumulation of the ALH-6 substrate, P5C, a toxic intermediate of proline catabolism, leads to the premature aging phenotype of *alh-6* mutants on an HT115 diet supplemented with proline. Together these data indicate that in wild-type animals, proline catabolism is activated on an *E. coli* OP50 diet and

ALH-6 facilitates the breakdown of P5C promoting survival. Without ALH-6, P5C accumulates and accelerates organismal aging [16]. The use of *C. elegans* mutants in this study thus revealed the importance of amino acid metabolism mediating lifespan on different diets.

In addition to dietary differences in nutritional quality and production of bacterial metabolites, the pathogenicity and/or toxicity of bacteria can modulate lifespan. *C. elegans* propagated on heat killed or antibiotic-treated *E. coli* OP50 have an extended lifespan compared to animals on live *E. coli* OP50 and show no signs of dietary restriction [17], [18]. Further, altering agar media that supports bacterial growth may shorten lifespan due to the induction of increased virulence of *E. coli* OP50 [9]. These studies agree with the influence of bacterial pathogenicity and toxicity in modulating lifespan, perhaps as a result of bacterial accumulation in the intestine [17], [19]–[21]. However, an opposing model suggests killing or altering growth media may affect the nutritional quality of bacteria. *C. elegans* propagated on a soil bacterium, *Bacillus subtilis*, has an extended lifespan compared to *E. coli* OP50. While this observation has been attributed to *B. subtilis* being less pathogenic than *E. coli* OP50, a recent study suggests the production of nitric oxide by *B. subtilis* enhances stress resistance, which in turn may contribute to increased lifespan of *C. elegans* [9], [22].

Distinguishing dietary versus pathogenic effects on *C. elegans* lifespan is not trivial. For instance, *C. elegans* was reported to have an extended lifespan on *E. coli* deficient in coenzyme Q (GD1) when compared to wild-type *E. coli* [23]. However, supplementation of Q isoforms to the GD1 *E. coli* diet did not rescue

lifespan extension in *C. elegans*. Moreover, GD1 *E. coli* have respiratory defective metabolism, and respiratory deficient *E. coli* significantly increase lifespan of *C. elegans* when compared to the wild-type *E. coli*. Respiratory deficient *E. coli* were hypothesized to either lack products produced by respiratory competent *E. coli* strains, or produce fermentation products such as acetate, ethanol, *etc.* that modulate *C. elegans* metabolism [24]. Alternatively, respiratory defective GD1 *E. coli* were shown to colonize more slowly in the gut compared to *E. coli* OP50. Delayed gut colonization and decreased bacterial load were hypothesized to increase survival in *C. elegans* as bacterial proliferation in the gut contributes to mortality [17], [25]. This is further supported by *C. elegans* lifespan extension as a result of adding antibiotics that slow bacterial growth such as ampicillin, kanamycin, sulfamethoxasole or trimethoprim [12], [17], [26]. However, it is still unclear whether pathogenesis, a metabolic byproduct, or lack of a metabolite in the respiratory defective diet, or in response to antibiotic treatment, causes lifespan extension in *C. elegans.*

Interestingly, bacteria can also modulate *C. elegans* lifespan through sensory mechanisms. Ablating olfactory and gustatory neurons in *C. elegans* can extend lifespan without affecting feeding behavior illustrating that perhaps even the “taste and smell” of food cues can stimulate changes in longevity [27], [28]. A recent genetic study illustrated different sensory neurons act with a neuromedin U receptor, *nmur-1,* to modulate lifespan effects in response to differences in lipopolysaccharide (LPS) on the cell wall of *E. coli* OP50 and *E. coli* HT115 [7]. Therefore, sensing different bacterial compositions may also influence lifespan.

Interactions between bacteria and *C. elegans* mirror the relationships between the gut microbiome and mammals. The mutualistic relationship between the gut microbiome and humans is important for host metabolism as nutrients from diet or supplied by the microbiota can affect human health. However, due to the genetic heterogeneity of mammals and the microbiome, long life and diverse diet, the mechanisms defining interactions between diet, the microbiome and aging are difficult to characterize. While it is too soon to know whether *C. elegans* will be a suitable model organism, the experimental tractability of the animal and the bacterial diet, short lifespan, and diverse bacterial food sources will certainly be advantageous tools for using *C. elegans* to form foundational hypothesis that can be tested in mammalian systems [13], [29]. For instance, *C. elegans* has been utilized to investigate how probiotics may promote health and longevity. Probiotic bacteria are living microorganisms that can be ingested and are believed to be beneficial on human health and longevity. Bifidobacteria, a lactic acid bacteria commonly used as a probiotic, suppresses *C. elegans* age-associated sensitivities to bacterial infection and extends lifespan [30], [31]. Investigating further using *C. elegans* mutants, researchers found that bifidobacteria may extend lifespan via modulation of the p38 MAPK pathway and found that the cell wall plays a key role in extending lifespan [32]. Whether these mechanisms are similarly activated in higher eukaryotes remains to be explored.

Drug effects on *C. elegans* lifespan

As a result of the potential for diet-mediated longevity, heroic efforts have been made to discover dietary and pharmacological interventions to extend the lifespan of *C. elegans* [33], [34]. For instance, one chemical, resveratrol, was identified in a screen measuring the biochemical activity of SIRT1, a protein shown to affect lifespan. SIRT1 promotes DR-mediated lifespan extension and regulates metabolic processes such as fatty acid oxidation in response to low energy states. The ability to allosterically induce SIRT1 activity opened the possibility of pharmacological mimetics and lead to the discovery of resveratrol, a polyphenol found in red wine and a potent SIRT1 activator. Interestingly, resveratrol increases lifespan in *C. elegans*, up to 18%, in *Drosophila* and in the short-lived fish *Nothobranchius furzeri* [35]–[37].

The *Free Radical Theory of Aging* suggests that reactive oxygen species (ROS) produced as a byproduct of normal metabolism, particularly electron transport chain (ETC) function in mitochondria, can damage macromolecules such as nucleic acids, lipids and proteins by oxidation. Elevated ROS production over time results in aging and associated phenotypes [38]–[40]. Therefore, compounds that reduce ROS-mediated damage may delay aging and extend lifespan. Compounds such as antioxidants Vitamin E, superoxide dismutase and catalase mimetics, eukaryion-8 (EUK-8) and EUK-134, lipoic acid, propyl gallate, trolox and taxifolinhave been shown to extend lifespan although it is still unkown if the mechanisms of action are indeed through reduction of ROS-mediated damage [41]–[43].

One approach to understanding the mechanisms of aging is by screening compounds to identify chemicals that delay aging in *C. elegans*. This approach has been used to identify new compounds that have life-extending effects such as ethosuximide, an anticonvulsant used in treating seizures experienced in epileptic patients. Ethosuximide extends lifespan of wild-type animals by 17%. Analyzing structurally related chemicals, trimethadione and DAEBL, both of which also extend lifespan, revealed that lifespan extension is likely due to their anticonvulsant activity [44]. This was further supported by neurological phenotypes including fast body movement and pharyngeal pumping. While the direct mechanism of these drugs remains unknown, Evason *et al.* (2005) illustrated the drug-mediated lifespan extension was likely different from lifespan extending genetic pathways including the IIS pathway, mitochondrial function, caloric intake and neuronal activity. Similar compounds used in treatment of neurological disease have also been revealed to extend *C. elegans* lifespan including valproic acid, lithium and antidepressants mianserin, mirtazapine, methiothepin and cyproheptadine [45]–[47].

Drugs that are used to treat metabolic disease can also have lifespan extending effects. One DR-mimetic, metformin, increases lifespan independent of the IIS pathway and increases healthspan via activity of the cellular metabolic sensor, AMP-activated protein kinase (AMPK) [48]. Interestingly, metformin shortened lifespan of *C. elegans* cultured axenically (i.e. in the absence of *E. coli*) or on UV-killed *E. coli* OP50, suggesting the lifespan-extending effect of metformin requires live *E. coli* bacteria. Moreover, on *E. coli* HT115, metformin

shortened animal lifespan whereas metformin had no lifespan effect on animals cultured on *E. coli* HB101; both strains differ from the lifespan extension of metformin on *E. coli* OP50 [26]. Cabreiro *et al*. determined that metformin disrupts *E. coli* OP50 folate metabolism thereby reducing the amount of bioavailable folate and methionine and, as a result, indirectly slows aging in the animal by both initiating a dietary restricted state and activating AMPK. However, the toxicity of metformin directly affects worm lifespan as well, reducing lifespan at high doses. This study reveals that metformin, used to treat metabolic disease in humans, can act on both bacteria and the animal raising the question of whether metformin similarly affects the human gut microbiome.

Measuring *C. elegans* lifespan and the use of FUdR

Lifespan of *C. elegans* is defined by the time animals are alive from the L4 larval stage (time = 0) (Fig. 1.1) until the day they are scored as dead, which typically occurs 2-3 weeks post-L4 stage. Measuring the maximum lifespan (i.e. time when 100% of animals are dead) and mean lifespan (i.e. time when 50% of animals are dead) is essential for quantifying aging of *C. elegans*. To measure lifespan, animals are maintained on standard growth media with a lawn of a single bacterial strain, typically *E. coli* OP50 or *E. coli* HT115, as the food source. Animals are scored as live or dead based on movement. At earlier times, when animals are less than 7-10 days adult, movement can be clearly seen. However, animals will significantly slow with age and move very little towards the end of life. During this time, death is scored as lack of movement upon prodding and the

animal is subsequently removed from the plate. Lifespan assays can also be performed in liquid and visualized using microscopy; however, these assays are not common as many complications arise with progeny contamination and the need to frequently transfer worms to fresh media throughout the duration of the assay [49], [50].

During the lifespan assay, adult animals must be transferred onto new plates every day to prevent contamination with progeny. Alternatively, the drug 2'-deoxy-5'fluorouridine (FUdR) is a DNA synthesis inhibitor commonly used to "sterilize" *C. elegans* and maintain a sterile aging population [51]–[53]. The use of FUdR can significantly lessen the amount of manual labor required to conduct lifespan assays and has been shown to have no effect on lifespan of wild-type animals [54], [55]. However, FUdR has been illustrated to influence lifespan under some conditions. For instance, lifespan of *tub-1* and *gas-1* mutants is extended in the presence of FUdR, and FUdR inhibits lifespan-extending effects of *ash-2* RNAi on wild-type animals [56]–[58].

FUdR inhibits thymidylate synthase (TS), an enzyme that uses 5,10-methylenetetrahydrofolate (CH_2THF) as a methyl donor to catalyze the conversion of dUMP to dTMP (Fig. 4.1). Upon entering the cell, FUdR is phosphorylated by thymidine kinase to form fluorodeoxyuridine monophosphate (FdUMP). FdUMP binds to the nucleotide-binding site of TS and forms a stable ternary complex with TS and CH_2THF. As a result, access of dUMP to the nucleotide-binding site is blocked thereby inhibiting dTMP synthesis. The lack of dTMP leads to decreased levels of dTTP, and in turn, perturbs levels of other

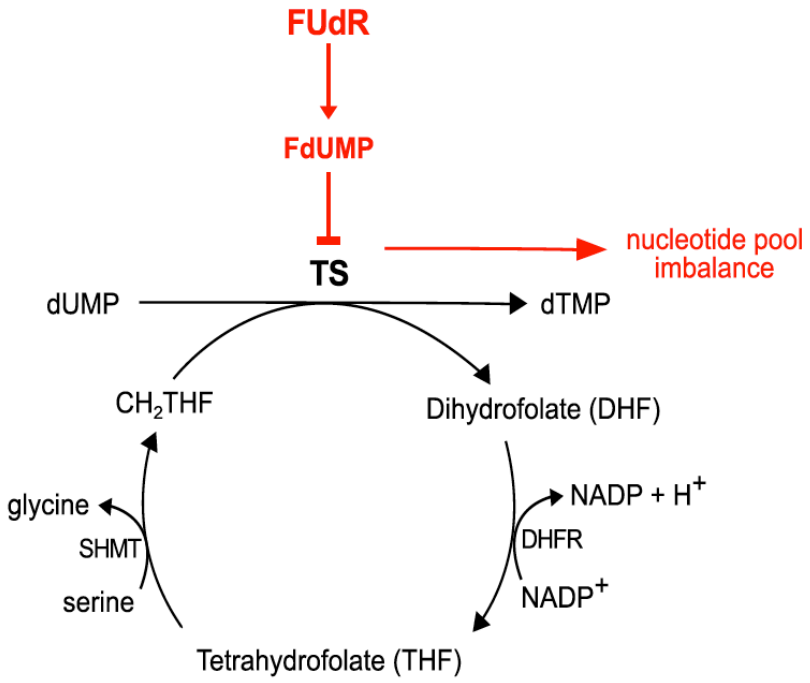

FIGURE 4.1: Mechanism of thymidylate synthase inhibition by FUdR. Thymidylate synthase (TS) catalyzes the conversion of deoxyuridine monophosphate (dUMP) to deoxythymidine monophosphate (dTMP), with 5,10-methylenetetrahydrofolate (CH_2THF) as the methyl donor. The conversion of dUMP to dTMP is a product of the folate cycle whereby dihydrofolate reductase (DHFR) reduces dihydrofolate (DHF) to tetrahydrofolate (THF). THF is then converted to CH_2THF via serine hydroxymethyltransferase (SHMT). The active metabolite of 5-fluorodeoxyuridine (FUdR), 5-fluorodeoxyuridine monophosphate (FdUMP) forms a stable ternary complex with TS and CH_2THF blocking access of dUMP. As a result, dTMP synthesis is inhibited leading to nucleotide pool imbalances of deoxyuridine triphosphate (dUTP) and deoxythymidine triphosphate (dTTP) and a rise of misincorporation of dUTP into DNA. NADP, nicotinamide adenine dinucleotide phosphate

deoxynucleotides (dATP, dGTP, dCTP). Additionally, TS inhibition via FdUMP causes dUMP to accumulate, inducing a downstream self-defeating base excision repair process. Accumulated dUMP can lead to increased levels of dUTP. dUTP can be mis-incorporated into DNA and subsequently removed by the base excision repair enzyme, uracil-DNA clycosylase (UDG). Yet during the synthesis phase of DNA repair, dUTP is reincorporated and continues cycling through dUTP removal and incorporation until DNA strand breaks and loss of DNA integrity leads to cell death. Loss of function in genes involved in DNA synthesis and base excision repair may lead to FUdR resistance. For instance, knockdown of UDG significantly increases resistance to FUdR [59]. Similarly, decreased expression of dUTPase, the enzyme that catalyzes the reaction of dUMP to dUTP, also increases resistance to FUdR [60]–[62].

Interestingly, FUdR has been shown to increase stress resistance and promote proteostasis in wild-type *C. elegans* [63]–[65]. Further, FUdR decreased age-dependent polyglutamine aggregation in a Huntington's disease model [65]. Although lifespan was unaffected, FUdR was also shown to affect the metabolic profile of wild-type and *daf-2* mutants [66]. The metabolic profile of *C. elegans* is extensively reorganized in the presence of *daf-2* mutation. A *daf-2* proteomic profile revealed upregulation of core intermediary metabolic pathways including glycolysis/gluconeogenesis, glycogenesis, pentose phosphate cycle, citric acid cycle, fatty acid B-oxidation, to name a few. The proteomic changes are very similar to that of dauers [67]. However, FUdR changes metabolite concentrations more dramatically in wild-type *C. elegans,* at least for some metabolites

measured, than the *daf-2* mutation. However, a few expected *daf-2*-dependent metabolic changes were unchanged after FUdR treatment, indicating that FUdR can interfere with metabolic changes that are a result of *daf-2* mutation [66]. All together, these studies illustrate that the effects of FUdR extend further than simply inhibiting reproduction. FUdR increases stress resistance, proteostasis and can significantly alter metabolism, all of which are phenotypes observed in long-lived animals and promote increased lifespan of *C. elegans.* FUdR may indirectly influence lifespan and therefore skew the results of a lifespan assay examining the effects of a gene or compound on lifespan.

PART II, CHAPTER 5

RESULTS

Diet-specific FUdR effects on *C. elegans* fertility and aging

The sterility-inducing effect of FUdR has been exploited for lifespan assays and has been shown to have no effect on longevity of wild-type (N2) animals [53]–[55]. However, these studies were conducted on the standard *E. coli* diet. Therefore, we tested whether FUdR would affect lifespan of wild-type worms on a different diet consisting of *Comamonas* DA1877. In agreement with previous reports, N2 lifespan on the *E. coli* OP50 diet was unaffected by the presence of FUdR. Surprisingly, FUdR dramatically increased the mean lifespan of N2 animals by an average of 10 days on the *Comamonas* DA1877 diet. Further, FUdR treatment extended mean lifespan of N2 animals by an average of 7 days on *Comamonas* DA1877 compared to *E. coli* OP50 (Fig. 5.1). These data illustrate FUdR affects *C. elegans* differently when fed two different diets: *E. coli* OP50 and *Comamonas* DA1877. I hypothesize that the lifespan extension of animals fed *Comamonas* DA1877 in the presence of FUdR is a result of FUdR altering *Comamonas* DA1877 metabolism, which in turn causes lifespan extension in *C. elegans.*

While performing lifespan assays, we observed that animals fed *Comamonas* DA1877 in the presence of FUdR laid many dead eggs, whereas animals on *E. coli* OP50 did not. This observation made us question whether animals fed *Comamonas* DA1877 may be more resistant to FUdR than animals fed *E. coli* OP50. Therefore, we qualitatively assessed at what concentration

A

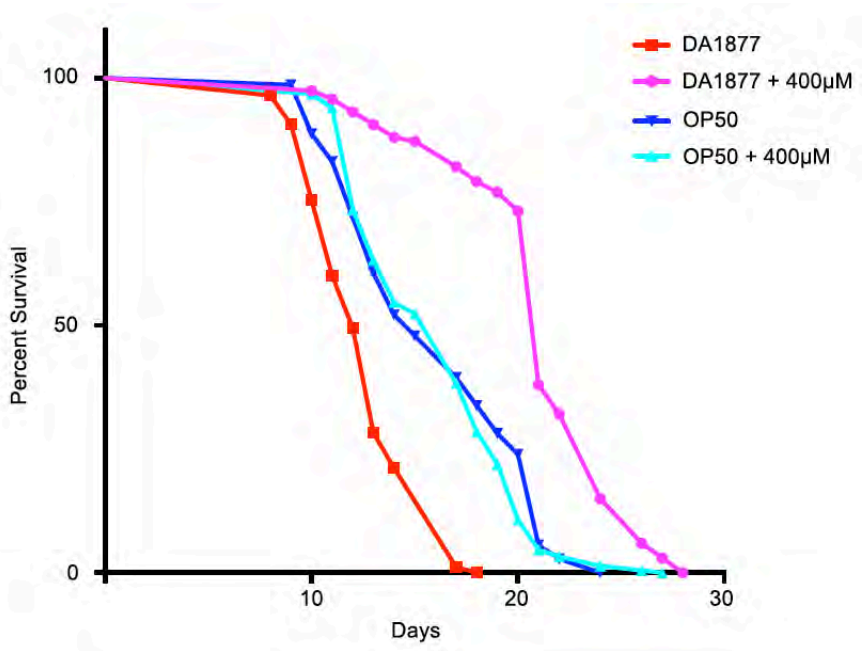

B

	Mean	SD ±
E. coli OP50 0μM	15.0	1.0
E. coli OP50 400μM	16.0	1.7
Comamonas DA1877 0μM	13.0	1.0
Comamonas DA1877 400μM	23.3	2.1

FIGURE 5.1: Diet-specific drug effects on *C. elegans* lifespan. *(A)* Representative lifespan of adult wild-type animals fed *Comamonas* DA1877 or *E. coli* OP50 in the presence of FUdR, as indicated. *(B)* Summary of three lifespan experiments. The mean represents the day at which 50% of the population is dead (i.e. mean lifespan) for a given condition, as indicated. The standard deviation (SD) is indicated for each condition (n ≈ 100 animals, per condition per experiment).

animals fed *Comamonas* DA1877 had viable progeny. We observed viable progeny of animals fed *Comamonas* DA1877 at a concentration of 10uM FUdR. Egg viability ceased, however, at 50uM FUdR. In contrast, animals fed *E. coli* OP50 had no viable progeny at 10uM FUdR.

Next, we quantitatively measured the brood size of animals fed either *E. coli* OP50 or *Comamonas* DA1877 bacteria in the presence or absence of 10 mM FUdR. In agreement with previous observations [6], in the absence of FUdR, we found that animals fed *Comamonas* DA1877 have a slightly reduced brood size compared to animals fed *E. coli* OP50. Also in agreement with the reported sterile-inducing effects of FUdR, animals on *E. coli* OP50 in the presence of FUdR did not have viable progeny [54]. Remarkably, however, animals fed *Comamonas* DA1877 had an average brood size of 253 and 246 in the absence and presence of FUdR, respectively. There is no statistical difference between the brood sizes of animals fed *Comamonas* DA1877 in the absence or presence of FUdR (Fig. 5.2A). As observed qualitatively, on a higher concentration of 50uM FUdR, *C. elegans* had no viable progeny when fed either bacterial diet. However, many dead eggs were present on the *Comamonas* DA1877 diet, while animals fed *E. coli* OP50 were sterile (Fig. 5.2B; data not shown). Taken together, these data illustrate that animals fed *E. coli* OP50 are more sensitive to FUdR than animals fed *Comamonas* DA1877.

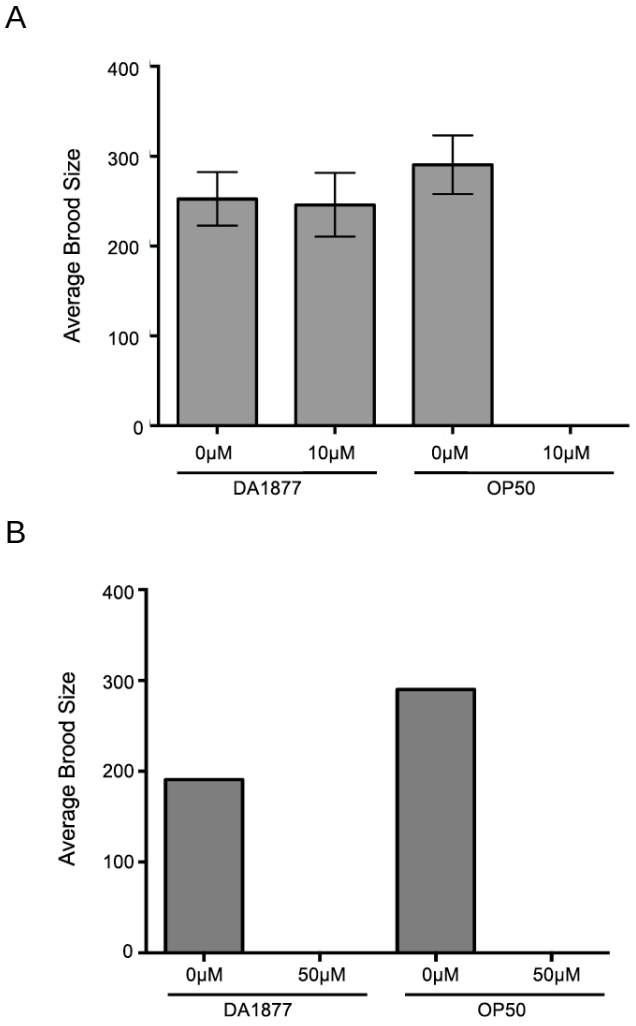

FIGURE 5.2: *C. elegans* fed *Comamonas* DA1877 require more FUdR to inhibit progeny production. Wild-type N2 animals were grown on two diets, *Comamonas* DA1877 and *E. coli* OP50, and in the presence of *(A)* 10μM and *(B)* 50μM FUdR, as indicated on the x-axis. Bars represent the average total number of progeny per animal (n = 30 animals). The SD is indicated in *(A)* for all animals combined.

Comamonas DA1877 are resistant to FUdR

To determine if the bacterial diet itself was affected by FUdR treatment, we tested whether bacterial grow was affected by FUdR. Growth of *E. coli* OP50 bacteria was sensitive to FUdR treatment in a dose-dependent manner; whereas, *Comamonas* DA1877 grew at a normal rate regardless of FUdR concentration (Fig. 5.3). Upon closer investigation of bacterial cell morphology, we observed *E. coli* OP50 bacterial cells had divided to form dramatically long bacteria after treatment with FUdR. Whereas *Comamonas* DA1877 bacteria also formed longer cells in the presence of FUdR, it was not to the extent of *E. coli* OP50 bacteria (Fig. 5.4). Taken together, these data illustrate that *E. coli* OP50 are more sensitive to FUdR than *Comamonas* DA1877.

Comamonas DA1877 mutants are sensitive to FUdR

Our lab previously generated a *Comamonas* DA1877 mutant collection via transposon mutagenesis consisting of 5,760 mutants [11]. To determine why *Comamonas* DA1877 was resistant to FUdR, we screened this collection for mutant bacteria that, in the presence of FUdR, showed decreased growth and therefore sensitivity to the drug similar to *E. coli* OP50. We found 14 mutants that conferred no or little growth in the presence of FUdR. After retesting, three mutants did not repeat the FUdR-sensitive phenotype and three exhibited slow growth in the absence of FUdR and were subsequently discarded as hits. The remaining eight mutants were sequenced to verify and map transposon insertions and identify the disrupted genes (Fig. 5.5). Of the eight mutants, two

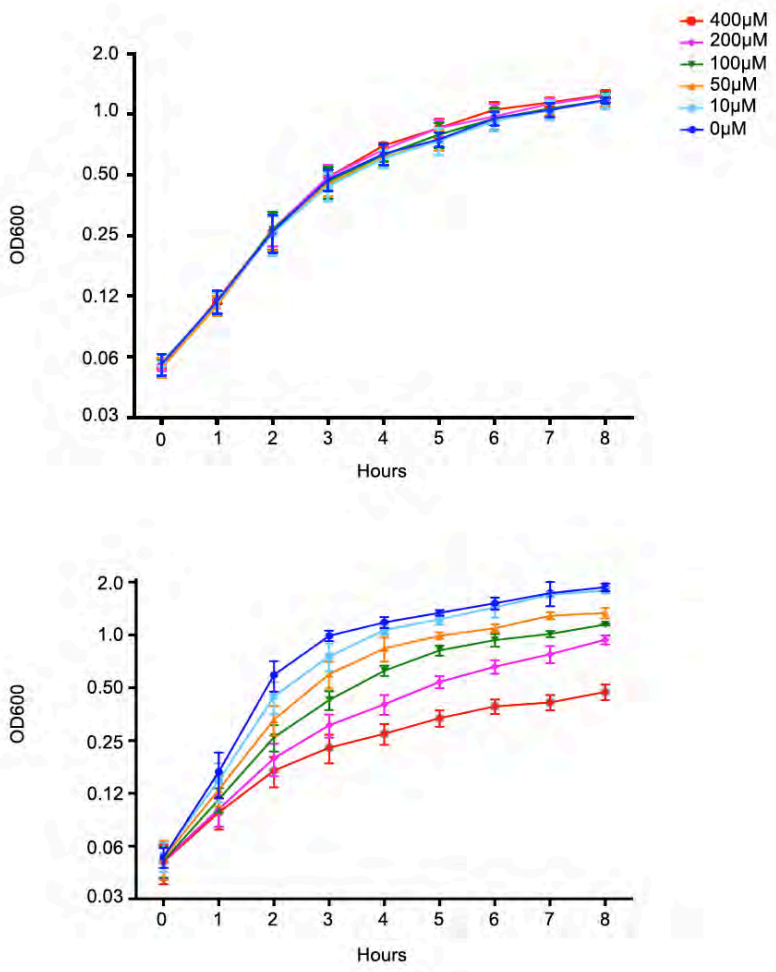

FIGURE 5.3: *Comamonas* DA1877 are resistant to FUdR. Bacterial growth of *Comamonas* DA1877 (above) and *E. coli* OP50 (below) in the presence of FUDR, as indicated. Each line represents the average growth (y-axis, log 2 scale; n = three replicates) over time (x-axis) of replicate experiments, with the SD indicated for each time point.

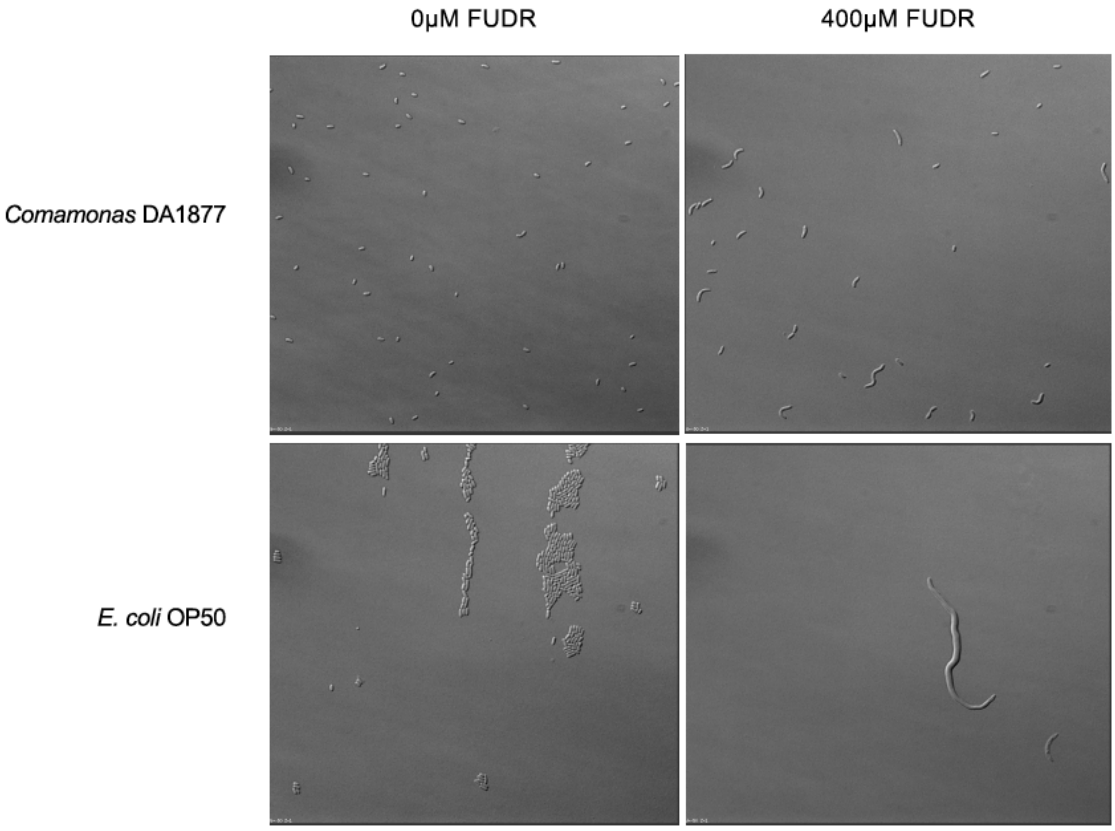

FIGURE 5.4: Drug effects on bacterial morphology. Microscopic images of *Comamonas* DA1877 and *E. coli* OP50 bacterial cells in the presence of FUdR, as indicated.

mutants contained insertions in the same gene, an ATP-dependent DNA helicase, although at different locations in the gene. Four of the eight mutants contained disruptions in genes involved in DNA replication and repair, one in glycerolipid metabolism, one zinc metalloprotease, one C4-type zinc-finger protein, and one is a gene of unknown identification or function. Therefore in total, seven unique genes were identified that, when disrupted, conferred *Comamonas* DA1877 sensitive to FUdR (Fig. 5.5; Table 5.1). Given the number of genes involved in DNA replication and repair that influenced FUdR sensitivity, I hypothesize that DNA repair and replication are important mechanisms that influence bacterial sensitivity to FUdR.

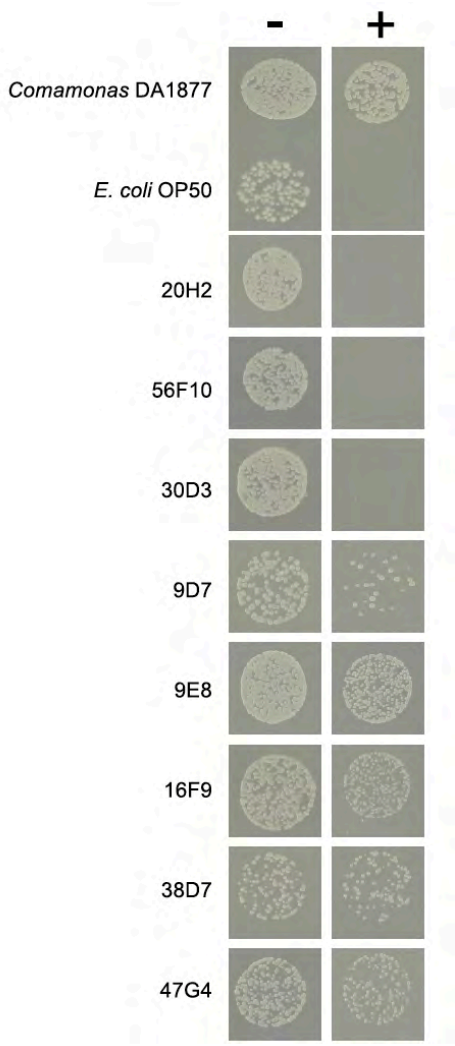

FIGURE 5.5: *Comamonas* DA1877 mutants are sensitive to FUdR. Representative pictures from an experimental spot retest assay. *Comamonas* DA1877, *E.coli* OP50 controls and *Comamonas* mutant bacteria hits (as listed; 1:10,000 dilution) are grown in the absence (-) or presence (+) of 800µM FUdR.

DA1877 mutant	gene/function	subsystem
20H2	hypothetical protein	uknown
56F10	Zinc metalloprotease (EC 3.4.24.-)	none
30D3	Chromosomal replication initiator protein DnaA	Cell Division Subsystem including YidCD, DNA-replication, DNA replication cluster 1
9D7	C4-type zinc-finger protein DksA/TraR family	none
9E.8	1-acyl-sn-glycerol-3-phosphate acyltransferase (EC 2.3.1.51)	Glycerolipid and Glycerophospholipid Metabolism in Bacteria, Ribosome post-transcriptional modification and chromosomal segregation cluster
16F9	ATP-dependent DNA helicase	DNA repair, bacterial UvrD and related helicases
38D7	Exodeoxyribonuclease V beta chain (EC 3.1.11.5)	DNA-replication, DNA repair, bacterial RecBCD pathway
47G4	ATP-dependent DNA helicase	DNA repair, bacterial UvrD and related helicases

Table 5.1: *Comamonas* DA1877 mutants sensitive to FUdR compared to wild type *Comamonas* DA1877. Eight mutants showed normal growth on standard LB solid media but little to no growth when grown on LB and FUdR. The predicted gene and or function for each mutant are listed (gene/function) as well as putative biological processes for which each gene participates (subsystem).

PART II MATERIALS AND METHODS

C. elegans maintenance

The N2 (Bristol) strain was used as the wild-type strain, and was maintained at 20°C using standard *C. elegans* techniques [68]. All bacteria used to seed Nematode Growth Media (NGM) plates were grown from a single colony on solid Luria Broth (LB) media plates (10g tryptone, 5g yeast extract, 10g NaCl, 15g agar in 1L MilliQ water; pH 7.0) at 37°C, shaking overnight. Plates were seeded 2-3 days before use.

Phenotypic Assays

For all diet-specific assays, animals were grown on the appropriate diet for at least one generation prior to the assay.

Brood sizes were determined by placing individual L4 animals onto plates containing different diets and/or drug, as indicated. Animals were transferred daily to new plates, respectively, and number of offspring on the plates was counted.

For lifespan assays, L4 animals were transferred onto NGM pates (approx. 25 animals per plate; four plates per condition) seeded with the diet and/or FUDR, as indicated. Animals were transferred to new NGM plates seeded with the appropriate bacteria daily until progeny production seized [49]. Every day thereafter, animals were checked for movement and pharyngeal pumping. If pumping or movement was not observed, animals were lightly prodded with

platinum wire. If after prodding no response was detected, they were considered dead, scored and removed. Animals that died from vulval bursting were censored.

Bacterial Growth in Liquid Media

Single colony inoculated cultures were grown in LB media (see above) overnight at 37°C, shaking. The following day, bacteria were transferred to fresh LB media with a starting OD no greater than 0.07. Each culture was grown at 37°C, shaking, with supplemented drug or nutrient as indicated. Culture volume was approximately 10% of the flask volume. Samples from each culture were measured at times indicated for each experiment. The optical density of the overnight culture was determined using an Eppendorf BioPhotometer Plus at 600nm wavelength. As necessary, samples were diluted to ensure a measured OD did not exceed 0.600 for optimized accuracy, linearity and reproducibility. Images of bacteria were taken using a DeltaVision Deconvolution Florescence Microscope.

***Comamonas* DA1877 mutant screen**

The *Comamonas* DA1877 mutant library was generated previously as described in [11]. The library was spotted onto Singer Plusplates containing LB and gentamicin (final concentration=10µg/mL) in a 1536-colony format using the RoToR HAD robot (Singer Instruments). 1536-colony format plates from 96-well glycerol stocks were generated using methods modified from [69]. In summary, the RoToR HAD robot uses disposable plastic pads with 96, 384 or 1536 pins to

precisely transfer bacteria onto solid agar plates. To build the 1536-colony “quad array,” 96-colony plates of the *Comamonas* DA1877 mutant library are first generated by spotting from 96-well plates of glycerol stocks onto solid agar plates. 96-colony solid plates were stored in plastic bags and incubated at 37°C overnight. A single transfer from four separate 96-colony plates is then used to build a 384-colony plate in which each *Comamonas* DA1877 mutant is present once. These plates were then incubated at 37°C for approximately eight hours. Finally, four transfers from the same 384-colony plate are used to create the 1536-colony plate in which each *Comamonas* DA1877 is present in quadruplicate. *Comamonas* DA1877 mutant strains are grown on both LB and LB-gentamicin at 25°C overnight. Each 1536-colony plate was then replicated onto two plates: LB-gentamicin and LB-gentamicin-FUdR. 800μM FUdR was used as growth of *E. coli* OP50 at this concentration was strongly inhibited, whereas *Comamonas* DA1877 growth was not, and therefore easing visual screening for changes in bacterial growth. Replica plates were stored in bags and grown up to two days at 20°C. A hit was considered positive if at least two of the four colonies showed little to no growth on LB-gentamicin-FUdR but not LB-gentamicin plates.

Positive hits were retested by spotting bacteria onto LB-gentamicin and LB-gentamicin with 400μM and 800μM FUdR. Briefly, each mutant strain was grown in liquid LB media with gentamicin at 37°C overnight to saturation. Each culture was then diluted with LB media so that OD600=1. 10-fold serial dilutions were then prepared and 10μL from each dilution (from 10^{-3} to 10^{-6}) was spotted

onto LB-gentamicin and LB-gentamicin-FUdR solid plates. Plates were allowed to dry and then stored at 37°C overnight. The retest was considered positive if diluted mutant bacteria grew normally on LB-gentamicin, but little to no growth was observed on LB-gentamicin-FUdR.

PART II, CHAPTER 6

DISCUSSION

In this study, we report that FUdR can have differential effects on *C. elegans* reproduction and lifespan in a bacteria-dependent manner. FUdR can also cause dramatic lifespan extension to wild-type *C. elegans* on a *Comamonas* DA1877 diet. The use of FUdR in measuring *C. elegans* lifespan was historically exploited for its ability to inhibit progeny production and thus maintain a sterile adult population. The amount of FUdR used for lifespan assays ranges dramatically in the literature, from 1uM to 400uM. However, our data, in agreement with previously published studies, illustrate that FUdR should be used with caution when measuring *C. elegans* lifespan and, in particular, when examining lifespan on bacterial diets other than *E. coli* OP50. For experiments where FUdR must be utilized, previous reports suggest a low dose concentration of 1uM will cause sterility yet have minimal influence on lifespan [56], [70]. However, these studies analyzed FUdR concentration effects on animals with a diet of *E. coli* OP50. We demonstrate that any concentration less than 10uM will have no sterility-inducing effect on animals fed *Comamonas* DA1877. Taken together, the genotype of the animal and bacterial diet should be considered in determining the effective dose of FUdR. Additionally, as there may be interactions between FUdR, bacteria and the animal, effects of the bacterial diet on *C. elegans* physiology should be validated in the absence of FUdR. Environmental conditions, including temperature, also influence the lifespan of *C.*

elegans. FUdR may interact with other environmental, dietary or genetic factors and should be tested when used for assays, as any observed effects of these factors on *C. elegans* physiology may be dependent on FUdR.

FUdR differentially affects bacterial growth of *E. coli* OP50 and *Comamonas* DA1877

The function of FUdR inhibiting the TS enzyme is conserved across many species. As a result, the mechanism of FUdR has been exploited to prevent reproduction in *C. elegans.* However, due to the conservation of its target, FUdR likely affects bacterial TS enzyme and subsequently bacterial DNA synthesis. Therefore, one should not assume that FUdR is only affecting *C. elegans* TS enzyme when utilized for assays. We show that FUdR inhibits *E. coli* OP50 growth and dramatically changes cell morphology, whereas, surprisingly, *Comamonas* DA1877 growth appears largely unaffected.

Why does FUdR affect *E. coli* OP50 but not *Comamonas* DA1877 growth? One hypothetical explanation for *Comamonas* DA1877 resistance to FUdR is that FUdR never actually reaches the bacterial TS enzyme. FUdR could fail to enter the cell, be efficiently effluxed from the cell, and/or degraded by enzymes made by *Comamonas* DA1877. Although, bacterial elongation and the lifespan extension of *C. elegans* on *Comamonas* DA1877 in the presence of FUdR suggests FUdR is affecting the bacteria. Nonetheless, our data is not definitive. *Comamonas* DA1877 may also be resistant to FUdR due to TS mutation, such that there is reduced affinity for the ligand, FdUMP. Reduced affinity for FdUMP

has been suggested to explain, at least in part, FUdR resistance in some cell lines [71], [72].

To try and address this question, we screened the *Comamonas* DA1877 mutant library for bacteria that conferred sensitivity to FUdR. From this experiment, we found mutants with disruptions in genes involved in DNA synthesis and repair, bacterial metabolism and a few with unknown function. Whether these genes contribute to *Comamonas* DA1877 resistance to FUdR remains unexplored. However, thymineless death, a term used to describe the depletion of TTP pools following TS inhibition, is exacerbated in *E. coli* lacking proteins involved in DNA repair mechanisms, including UvrD helicase and RecBCD, genes identified in our screen [73], [74]. UvrD helicase is involved in nucleotide excision repair, mismatch repair, and dismantles RecA on single strand DNA thus inhibiting homologous recombination [75]. RecBCD is a double-strand exonuclease and catalyst of double-strand-break repair by homologous recombination [73]. Additionally, RecA recombinase, a central protein in homologous recombination, also activates bacterial DNA-damage, or SOS, response by indirectly upregulating SOS-response genes. Elongated, filamentous bacterial cells are a characteristic phenotype associated with the SOS response [76], [77]. This morphological change is also observed in our bacterial cultures incubated with FUdR, indicating that FUdR is likely initiating the SOS response (Fig. 5.4). With this knowledge, perhaps *Comamonas* DA1877 DNA repair pathways are more efficient at repairing DNA allowing these bacteria to be more tolerant of FUdR-induced damage. Mutating these genes may not

render *Comamonas* DA1877 sensitive to FUdR specifically, but rather cause the bacteria to be sensitized to any drug that can disrupt DNA.

The genotype of the *E. coli* OP50 strain should be considered when exploring why this strain is sensitive to FUdR compared to *Comamonas* DA1877. *E. coli* OP50 is a mutant strain of *E. coli* that, although mechanistically unknown, renders the OP50 strain a uracil auxotroph. The standard NGM medium used to propagate *C. elegans* has limited uracil and therefore prevents overgrowth of the bacterial lawn, which could obscure worm movement [68]. For this reason, *E. coli* OP50 was used as the food source during the establishment of *C. elegans* as a model organism and subsequently remained the laboratory standard. However, uracil auxotrophy occurs through inactivating enzymes involved in *de novo* pyrimidine synthesis, such as orotidylate decarboxylase (OMP decarboxylase) and carbamoyl phosphate synthetase II (CPS II), or by inhibiting nucleotide transporters involved in pyrimidine salvage pathways. Uridine nucleotides are precursors for *de novo* synthesis of thymine nucleotides. Whether the uracil auxotrophic phenotype of *E. coli* OP50 enhances its sensitivity to FUdR has not been explored. Additionally, it is unknown what other mutations exist in the *E. coli* OP50 genome and whether those may also contribute to its sensitivity to FUdR. It would be of interest, then, to test wild-type *E. coli* and compare its FUdR sensitivity to that of *E. coli* OP50.

As FUdR alters bacterial growth and physiology and is a known inhibitor of thymidylate synthase, an enzyme involved in folate metabolism, it is highly likely that FUdR will modulate metabolic processes of *E. coli* OP50 and *Comamonas*

DA1877. FUdR has been illustrated to cause changes in the metabolic profile of wild-type and mutant *daf-2 C. elegans*. We illustrate that mutations in at least one metabolic enzyme, 1-acyl-sn-glycerol-3-phosphate acylteransferase, render *Comamonas* DA1877 sensitive to FUdR (Table 5.1). The next step will be to determine whether reproduction or lifespan of *C. elegans* is altered when propagated on the identified *Comamonas* DA1877 mutant bacteria, either in the absence or presence of FUdR.

FUdR effects on *C. elegans* are diet-dependent

Our data shows FUdR affects *C. elegans* reproduction and lifespan in a diet-dependent manner. However, we do not know if the phenotypic response is mediated through the bacteria, from direct interactions between FUdR and the animal, or both. One hypothesis is that *Comamonas* DA1877 renders FUdR ineffective either by metabolizing it or by making or expressing an unknown component, albeit metabolite, enzyme, etc., that effectively “neutralizes” the drug. This would be consistent with our data demonstrating *Comamonas* DA1877 resistance to FUdR and continued *C. elegans* reproduction in the presence of FUdR when fed *Comamonas* DA1877. To determine this, one should first examine the effects of FUdR and killed bacteria on *C. elegans* reproduction and lifespan. Measuring *C. elegans* phenotypes in the presence of killed bacteria and FUdR will address whether resistance of *Comamonas* DA1877 fed animals to FUdR is mediated through bacterial inactivation of the compound. For instance, if metabolically active *Comamonas* DA1877 bacteria “neutralize” FUdR, one might

expect animals to have increased sensitivity to FUdR in the presence of killed *Comamonas* DA1877. In addition, it may be of importance to know how much FUdR is reaching the animal through the NGM media in the presence or absence of live bacteria. A report recently illustrated that less FUdR is absorbed by *C. elegans* in the presence of live *E. coli* OP50 bacteria. In addition, the concentration of FUdR in NGM medium with live *E. coli* OP50 present decreased faster than with dead bacteria. These data illustrate bacteria can metabolize the drug and lower absorption by *C. elegans* [78]. Interestingly, this was observed for *E. coli* OP50, raising the question as to whether this will be similarly observed for *Comamonas* DA1877 or whether *Comamonas* DA1877 will have greater efficiency in degrading FUdR, as animals can reproduce in the presence of higher amounts of FUdR on live *Comamonas* DA1877 bacteria (Fig. 5.2).

Further, it is unknown whether the bacterial-specific FUdR effects on *C. elegans* reproduction are the same as on lifespan. For instance, the mechanism that allows *C. elegans* to reproduce on *Comamonas* DA1877 in the presence of FUdR may be different from the lifespan extending effects of FUdR. Perhaps modulation of these two phenotypes requires different mechanisms. The data presented here serve as a foundation from which further hypotheses can be derived. While not definitively proven, it is highly likely that bacteria modify the *C. elegans* response to FUdR, through what mechanism remains unexplored.

Future directions

The chemotherapeutic 5-FU is an antimetabolite that is broken down to FdUMP and inhibits TS similarly to FUdR. In addition, 5-FU can be converted to FUTP and FdUTP, which disrupt RNA synthesis [79]. 5-FU is one of the most effective drugs used to treat colorectal cancer and its use has been associated with changes in the intestinal microbiota [80]–[83]. Human patients treated with 5-FU and other fluoropyrimidines illustrate severe diarrhea, likely due to the killing of commensal bacteria in the gut [81]. The significant side effects of chemotherapeutic agents on the intestinal microbiota have increased interest in discovering interventions to reduce intestinal-induced toxicities. For instance, camptothecin, a human topoisomerase I inhibitor used in the treatment of colorectal cancer, causes severe diarrhea. However, inhibiting the B-glucuronidase enzyme in bacterial cells, including *E. coli*, alleviates drug toxicity [84]. Other interventions such as probiotic treatment have also been prescribed to alleviate severe diarrhea in patients under treatment for colon cancer [85].

We have illustrated that *C. elegans* reproduction and lifespan can serve as proxies to investigate bacterial-specific FUdR effects. Is the bacterial-specific effect limited to FUdR? Can other DNA synthesis inhibitors or chemotherapeutics modulate *C. elegans* physiology in a bacteria-specific manner? The interactions between the host and microbe comprise complex networks; however, with genetic tools, such as RNAi and bacterial mutant collections, one can manipulate both the host and the microbe to begin dissecting these interactions. *C. elegans* can be propagated on a variety of bacterial diets [6], [8], [86]. In addition, *C.*

elegans have already been utilized for drug discovery and screening of small-molecule compounds to treat disease [87]. The high conservation of molecular pathways involved in cancer means that *C. elegans* data could be predictive for drug-target interactions in mammals [88]. The advantages of *C. elegans* as a model to examine the interaction between bacteria, chemotherapeutic agents, and their targets may be beneficial for gaining insight into counterparts in mammals.

PART II BIBLIOGRAPHY

[1] H. W. Park, “Longevity, aging, and caloric restriction: Clive Maine McCay and the construction of a multidisciplinary research program.,” *Hist. Stud. Nat. Sci.*, vol. 40, no. 1, pp. 79–124, 2010.

[2] S. D. Katewa and P. Kapahi, “Dietary restriction and aging, 2009,” *Aging Cell*, vol. 9, no. 2, pp. 105–112, 2010.

[3] M. D. W. Piper, L. Partridge, D. Raubenheimer, and S. J. Simpson, “Dietary restriction and aging: A unifying perspective,” *Cell Metabolism*, vol. 14, no. 2. pp. 154–160, 2011.

[4] C. J. Kenyon, “The genetics of ageing.,” *Nature*, vol. 464, no. 7288, pp. 504–12, Mar. 2010.

[5] J. D. Coolon, K. L. Jones, T. C. Todd, B. C. Carr, and M. A. Herman, “Caenorhabditis elegans genomic response to soil bacteria predicts environment-specific genetic effects on life history traits,” *PLoS Genet.*, vol. 5, no. 6, 2009.

[6] L. T. MacNeil, E. Watson, H. E. Arda, L. J. Zhu, and A. J. M. Walhout, “Diet-induced developmental acceleration independent of TOR and insulin in C. elegans,” *Cell*, vol. 153, no. 1, pp. 240–252, 2013.

[7] W. Maier, B. Adilov, M. Regenass, and J. Alcedo, “A neuromedin u receptor acts with the sensory system to modulate food type-dependent effects on C. elegans lifespan,” *PLoS Biol.*, vol. 8, no. 5, 2010.

[8] L. Avery and B. B. Shtonda, “Food transport in the C.elegans pharynx,” *J. Exp. Biol.*, vol. 206, pp. 2441–2457, 2003.

[9] D. A. Garsin, J. M. Villanueva, J. Begun, D. H. Kim, C. D. Sifri, S. B. Calderwood, G. Ruvkun, and F. M. Ausubel, “Long-lived C. elegans daf-2 mutants are resistant to bacterial pathogens.,” *Science*, vol. 300, no. 5627, p. 1921, 2003.

[10] G. Grompone, P. Martorell, S. Llopis, N. González, S. Genovés, A. P. Mulet, T. Fernández-Calero, I. Tiscornia, M. Bollati-Fogolín, I. Chambaud, B. Foligné, A. Montserrat, and D. Ramón, “Anti-Inflammatory Lactobacillus rhamnosus CNCM I-3690 Strain Protects against Oxidative Stress and Increases Lifespan in Caenorhabditis elegans,” *PLoS One*, vol. 7, no. 12, 2012.

[11] E. Watson, L. T. Macneil, A. D. Ritter, L. S. Yilmaz, A. P. Rosebrock, A. a. Caudy, and A. J. M. Walhout, “Interspecies systems biology uncovers metabolites affecting C. elegans gene expression and life history traits,” *Cell*, vol. 156, no. 4, pp. 759–770, 2014.

[12] B. Virk, G. Correia, D. P. Dixon, I. Feyst, J. Jia, N. Oberleitner, Z. Briggs, E. Hodge, R. Edwards, J. Ward, D. Gems, and D. Weinkove, “Excessive folate synthesis limits lifespan in the C. elegans : E. coli aging model.,” *BMC Biol.*, vol. 10, no. 1, p. 67, 2012.

[13] T. Baba, T. Ara, M. Hasegawa, Y. Takai, Y. Okumura, M. Baba, K. A. Datsenko, M. Tomita, B. L. Wanner, and H. Mori, “Construction of Escherichia coli K-12 in-frame, single-gene knockout mutants: the Keio collection.,” *Mol. Syst. Biol.*, vol. 2, p. 2006.0008, 2006.

[14] L. S. Yilmaz and A. J. M. Walhout, “Worms, bacteria, and micronutrients: an elegant model of our diet,” *Trends Genet.*, vol. 30, no. 11, pp. 496–503, 2014.

[15] A. A. Soukas, E. A. E. Kane, C. E. C. Carr, J. A. Melo, and G. Ruvkun, “Rictor/TORC2 regulates fat metabolism, feeding, growth, and life span in Caenorhabditis elegans,” *Genes …*, vol. 23, no. 4, pp. 496–511, 2009.

[16] S. Pang and S. P. Curran, “Adaptive capacity to bacterial diet modulates aging in C. elegans,” *Cell Metab.*, vol. 19, no. 2, pp. 221–231, 2014.

[17] D. Garigan, A. L. Hsu, A. G. Fraser, R. S. Kamath, J. Abringet, and C. Kenyon, “Genetic analysis of tissue aging in Caenorhabditis elegans: A role for heat-shock factor and bacterial proliferation,” *Genetics*, vol. 161, no. 3, pp. 1101–1112, 2002.

[18] D. Gems and D. L. Riddle, “Genetic, behavioral and environmental determinants of male longevity in Caenorhabditis elegans,” *Genetics*, vol. 154, no. 4, pp. 1597–1610, 2000.

[19] M. W. Tan, S. Mahajan-Miklos, and F. M. Ausubel, “Killing of Caenorhabditis elegans by Pseudomonas aeruginosa used to model mammalian bacterial pathogenesis.,” *Proc. Natl. Acad. Sci. U. S. A.*, vol. 96, no. 2, pp. 715–720, 1999.

[20] L. A. Herndon, P. J. Schmeissner, J. M. Dudaronek, P. A. Brown, K. M. Listner, Y. Sakano, M. C. Paupard, D. H. Hall, and M. Driscoll, “Stochastic and genetic factors influence tissue-specific decline in ageing C. elegans.,” *Nature*, vol. 419, no. 6909, pp. 808–814, 2002.

[21] J. E. Irazoqui, J. M. Urbach, and F. M. Ausubel, “Evolution of host innate defence: insights from Caenorhabditis elegans and primitive invertebrates.,” *Nat. Rev. Immunol.*, vol. 10, no. 1, pp. 47–58, 2010.

[22] I. Gusarov, L. Gautier, O. Smolentseva, I. Shamovsky, S. Eremina, A. Mironov, and E. Nudler, “Bacterial nitric oxide extends the lifespan of C. elegans,” *Cell*, vol. 152, no. 4, pp. 818–830, 2013.

[23] P. L. Larsen and C. F. Clarke, “Extension of life-span in Caenorhabditis elegans by a diet lacking coenzyme Q.,” *Science*, vol. 295, no. 5552, pp. 120–123, 2002.

[24] R. Saiki, A. L. Lunceford, T. Bixler, P. Dang, W. Lee, S. Furukawa, P. L. Larsen, and C. F. Clarke, “Altered bacterial metabolism, not coenzyme Q content, is responsible for the lifespan extension in Caenorhabditis elegans fed an Escherichia coli diet lacking coenzyme Q,” *Aging Cell*, vol. 7, no. 3, pp. 291–304, 2008.

[25] F. Gomez, G. C. Monsalve, V. Tse, R. Saiki, E. Weng, L. Lee, C. Srinivasan, A. R. Frand, and C. F. Clarke, “Delayed accumulation of intestinal coliform bacteria enhances life span and stress resistance in Caenorhabditis elegans fed respiratory deficient E. coli.,” *BMC Microbiol.*, vol. 12, no. 1, p. 300, 2012.

[26] F. Cabreiro, C. Au, K. Y. Leung, N. Vergara-Irigaray, H. M. Cochemé, T. Noori, D. Weinkove, E. Schuster, N. D. E. Greene, and D. Gems, “Metformin retards aging in C. elegans by altering microbial folate and methionine metabolism,” *Cell*, vol. 153, no. 1, pp. 228–239, 2013.

[27] J. Apfeld and C. Kenyon, “Cell Nonautonomy of C . elegans daf-2 Function in the Regulation of Diapause and Life Span,” *Cell*, vol. 95, pp. 199–210, 1998.

[28] J. Alcedo and C. Kenyon, “Regulation of C. elegans Longevity by Specific Gustatory and Olfactory Neurons,” *Neuron*, vol. 41, no. 1, pp. 45–55, 2004.

[29] S. Montalvo-Katz, H. Huang, M. D. Appel, M. Berg, and M. Shapira, “Association with soil bacteria enhances p38-dependent infection resistance in caenorhabditis elegans,” *Infect. Immun.*, vol. 81, no. 2, pp. 514–520, 2013.

[30] T. Ikeda, C. Yasui, K. Hoshino, K. Arikawa, and Y. Nishikawa, “Influence of lactic acid bacteria on longevity of Caenorhabditis elegans and host defense against Salmonella enterica serovar Enteritidis,” *Appl. Environ. Microbiol.*, vol. 73, no. 20, pp. 6404–6409, 2007.

[31] T. Komura, C. Yasui, H. Miyamoto, and Y. Nishikawa, “Caenorhabditis elegans as an alternative model host for legionella pneumophila, and protective effects of bifidobacterium infantis,” *Appl. Environ. Microbiol.*, vol. 76, no. 12, pp. 4105–4108, 2010.

[32] T. Komura, T. Ikeda, C. Yasui, S. Saeki, and Y. Nishikawa, “Mechanism underlying prolongevity induced by bifidobacteria in Caenorhabditis elegans,” *Biogerontology*, vol. 14, no. 1, pp. 73–87, 2013.

[33] J. J. Collins, K. Evason, and K. Kornfeld, “Pharmacology of delayed aging and extended lifespan of Caenorhabditis elegans,” *Exp. Gerontol.*, vol. 41, no. 10, pp. 1032–1039, 2006.

[34] L. Fontana and L. Partridge, “Promoting Health and Longevity through Diet: From Model Organisms to Humans,” *Cell*, vol. 161, no. 1, pp. 106–118, 2015.

[35] K. T. Howitz, K. J. Bitterman, H. Y. Cohen, D. W. Lamming, S. Lavu, J. G. Wood, R. E. Zipkin, P. Chung, A. Kisielewski, L.-L. Zhang, B. Scherer, and D. A. Sinclair, “Small molecule activators of sirtuins extend Saccharomyces cerevisiae lifespan.,” *Nature*, vol. 425, no. 6954, pp. 191–196, 2003.

[36] M. Viswanathan, S. K. Kim, A. Berdichevsky, and L. Guarente, “A role for SIR-2.1 regulation of ER stress response genes in determining C. elegans life span,” *Dev. Cell*, vol. 9, no. 5, pp. 605–615, 2005.

[37] D. R. Valenzano, E. Terzibasi, T. Genade, A. Cattaneo, L. Domenici, and A. Cellerino, “Resveratrol prolongs lifespan and retards the onset of age-related markers in a short-lived vertebrate,” *Curr. Biol.*, vol. 16, no. 3, pp. 296–300, 2006.

[38] D. Harman, “Aging: a theory based on free radical and radiation chemistry.,” *J. Gerontol.*, vol. 11, pp. 298–300, 1956.

[39] R. M. Anson and R. G. Hansford, “Mitochondrial influence on aging rate in Caenorhabditis elegans,” *Aging Cell*, vol. 3, no. 1. pp. 29–34, 2004.

[40] S. D. Narasimhan, K. Yen, and H. A. Tissenbaum, “Converging Pathways in Lifespan Regulation,” *Current Biology*, vol. 19, no. 15. 2009.

[41] S. Melov, J. Ravenscroft, S. Malik, M. S. Gill, D. W. Walker, P. E. Clayton, D. C. Wallace, B. Malfroy, S. R. Doctrow, and G. J. Lithgow, “Extension of life-span with superoxide dismutase/catalase mimetics.,” *Science*, vol. 289, no. 5484, pp. 1567–1569, 2000.

[42] L. A. Harrington and C. B. Harley, “Effect of vitamin E on lifespan and reproduction in Caenorhabditis elegans.,” *Mech. Ageing Dev.*, vol. 43, no. 1, pp. 71–78, 1988.

[43] M. G. Benedetti, A. L. Foster, M. C. Vantipalli, M. P. White, J. N. Sampayo, M. S. Gill, A. Olsen, and G. J. Lithgow, “Compounds that confer thermal stress resistance and extended lifespan,” *Exp. Gerontol.*, vol. 43, no. 10, pp. 882–891, 2008.

[44] K. Evason, C. Huang, I. Yamben, D. F. Covey, and K. Kornfeld, “Anticonvulsant medications extend worm life-span.,” *Science*, vol. 307, no. 5707, pp. 258–262, 2005.

[45] K. Evason, J. J. Collins, C. Huang, S. Hughes, and K. Kornfeld, “Valproic acid extends Caenorhabditis elegans lifespan,” *Aging Cell*, vol. 7, no. 3, pp. 305–317, 2008.

[46] G. McColl, D. W. Killilea, A. E. Hubbard, M. C. Vantipalli, S. Melov, and G. J. Lithgow, “Pharmacogenetic analysis of lithium-induced delayed aging in Caenorhabditis elegans,” *J. Biol. Chem.*, vol. 283, no. 1, pp. 350–357, 2008.

[47] M. Petrascheck, X. Ye, and L. B. Buck, “An antidepressant that extends lifespan in adult Caenorhabditis elegans.,” *Nature*, vol. 450, no. 7169, pp. 553–556, 2007.

[48] B. Onken and M. Driscoll, “Metformin induces a dietary restriction-like state and the oxidative stress response to extend C. elegans healthspan via AMPK, LKB1, and SKN-1,” *PLoS One*, vol. 5, no. 1, 2010.

[49] G. L. Sutphin and M. Kaeberlein, “Measuring Caenorhabditis elegans life span on solid media.,” *Journal of visualized experiments : JoVE*, no. 27. 2009.

[50] J. J. Collins, C. Huang, S. Hughes, and K. Kornfeld, “The measurement and analysis of age-related changes in Caenorhabditis elegans.,” *WormBook*, pp. 1–21, 2008.

[51] H. Gershon and D. Gershon, “Detection of inactive enzyme molecules in ageing organisms.,” *Nature*, vol. 227, no. 5264, pp. 1214–1217, 1970.

[52] R. . Hosono and R. . Hosono, “Sterilization and growth inhibition of C. elegans by 5-fluorodeoxyuridine.,” *Exp. Gerontol.*, vol. 13, pp. 369–374, 1978.

[53] D. H. Mitchell, J. W. Stiles, J. Santelli, and D. R. Sanadi, “Synchronous growth and aging of Caenorhabditis elegans in the presence of fluorodeoxyuridine.,” *J. Gerontol.*, vol. 34, no. 1, pp. 28–36, 1979.

[54] S. Gandhi, J. Santelli, D. H. Mitchell, J. W. Stiles, and D. R. Sanadi, “A simple method for maintaining large, aging populations of Caenorhabditis elegans.,” *Mech. Ageing Dev.*, vol. 12, no. 2, pp. 137–150, 1980.

[55] R. Hosono, Y. Mitsui, Y. Sato, S. Aizawa, and J. Miwa, “Life span of the wild and mutant nematode Caenorhabditis elegans. Effects of sex, sterilization, and temperature.,” *Exp. Gerontol.*, vol. 17, no. 2, pp. 163–172, 1982.

[56] L. Aitlhadj and S. R. Stürzenbaum, “The use of FUdR can cause prolonged longevity in mutant nematodes,” *Mech. Ageing Dev.*, vol. 131, no. 5, pp. 364–365, 2010.

[57] J. M. van Raamsdonk and S. Hekimi, “FUdR causes a twofold increase in the lifespan of the mitochondrial mutant gas-1,” *Mech. Ageing Dev.*, vol. 132, no. 10, pp. 519–521, 2011.

[58] E. L. Greer, T. J. Maures, A. G. Hauswirth, E. M. Green, D. S. Leeman, G. S. Maro, S. Han, M. R. Banko, O. Gozani, and A. Brunet, “Members of the H3K4 trimethylation complex regulate lifespan in a germline-dependent manner in C. elegans.,” *Nature*, vol. 466, no. 7304, pp. 383–7, Jul. 2010.

[59] J. A. Fischer, S. Muller-Weeks, and S. J. Caradonna, “Fluorodeoxyuridine modulates cellular expression of the DNA base excision repair enzyme uracil-DNA glycosylase,” *Cancer Res.*, vol. 66, no. 17, pp. 8829–8837, 2006.

[60] C. E. Canman, T. S. Lawrence, D. S. Shewach, H. Y. Tang, and J. Maybaum, “Resistance to fluorodeoxyuridine-induced DNA damage and cytotoxicity correlates with an elevation of deoxyuridine triphosphatase activity and failure to accumulate deoxyuridine triphosphate,” *Cancer Res.*, vol. 53, no. 21, pp. 5219–5224, 1993.

[61] C. E. Canman, H. Y. Tang, D. P. Normolle, T. S. Lawrence, and J. Maybaum, “Variations in patterns of DNA damage induced in human colorectal tumor cells by 5-fluorodeoxyuridine: implications for mechanisms of resistance and cytotoxicity,” *Proc Natl Acad Sci U S A*, vol. 89, no. 21, pp. 10474–10478, 1992.

[62] S. E. Koehler and R. D. Ladner, “Small interfering RNA-mediated suppression of dUTPase sensitizes cancer cell lines to thymidylate synthase inhibition.,” *Mol. Pharmacol.*, vol. 66, no. 3, pp. 620–626, 2004.

[63] S. Angeli, I. Klang, R. Sivapatham, K. Mark, D. Zucker, D. Bhaumik, G. J. Lithgow, and J. K. Andersen, “A DNA synthesis inhibitor is protective against proteotoxic stressors via modulation of fertility pathways in Caenorhabditis elegans,” *Aging (Albany. NY).*, vol. 5, no. 10, pp. 759–769, 2013.

[64] N. Feldman, L. Kosolapov, and A. Ben-Zvi, “Fluorodeoxyuridine improves Caenorhabditis elegans proteostasis independent of reproduction onset.,” *PLoS One*, vol. 9, no. 1, p. e85964, 2014.

[65] J. Brunquell, P. Bowers, and S. D. Westerheide, “Fluorodeoxyuridine enhances the heat shock response and decreases polyglutamine aggregation in an HSF-1-dependent manner in Caenorhabditis elegans,” *Mech. Ageing Dev.*, vol. 141–142, pp. 1–4, 2014.

[66] S. K. Davies, A. M. Leroi, and J. G. Bundy, “Fluorodeoxyuridine affects the identification of metabolic responses to daf-2 status in Caenorhabditis elegans,” *Mech. Ageing Dev.*, vol. 133, no. 1, pp. 46–49, 2012.

[67] G. Depuydt, F. Xie, V. A. Petyuk, A. Smolders, H. M. Brewer, D. G. Camp, R. D. Smith, and B. P. Braeckman, “LC-MS proteomics analysis of the insulin/IGF-1-deficient caenorhabditis elegans daf-2(e1370) mutant reveals extensive restructuring of intermediary metabolism,” *J. Proteome Res.*, vol. 13, no. 4, pp. 1938–1956, 2014.

[68] S. Brenner, “The genetics of Caenorhabditis elegans.,” *Genetics*, vol. 77, no. 1, pp. 71–94, 1974.

[69] J. S. Reece-Hoyes, A. Diallo, B. Lajoie, A. Kent, S. Shrestha, S. Kadreppa, C. Pesyna, J. Dekker, C. L. Myers, and A. J. M. Walhout, “Enhanced yeast one-hybrid assays for high-throughput gene-centered regulatory network mapping,” *Nature Methods*, vol. 8, no. 12. pp. 1059–1064, 2011.

[70] N. Stroustrup, B. E. Ulmschneider, Z. M. Nash, I. F. López-Moyado, J. Apfeld, and W. Fontana, “The Caenorhabditis elegans Lifespan Machine.,” *Nat. Methods*, vol. 10, no. 7, pp. 665–670, 2013.

[71] M. E. Kitchens, A. M. Forsthoefel, K. W. Barbour, H. T. Spencer, and F. G. Berger, “Mechanisms of acquired resistance to thymidylate synthase inhibitors: the role of enzyme stability.,” *Mol. Pharmacol.*, vol. 56, no. 5, pp. 1063–1070, 1999.

[72] C. P. Spears, B. G. Gustavsson, M. Berne, R. Frosing, L. Bernstein, and A. A. Hayes, “Mechanisms of innate resistance to thymidylate synthase inhibition after 5-fluorouracil,” *Cancer Res.*, vol. 48, no. 20, pp. 5894–5900, 1988.

[73] H. Nakayama, K. Nakayama, R. Nakayama, and Y. Nakayama, “Recombination-deficient mutations and thymineless death in Escherichia coli K12: reciprocal effects of recBC and recF and indifference of recA mutations.,” *Can. J. Microbiol.*, vol. 28, no. 4, pp. 425–430, 1982.

[74] E. C. Siegel, “Ultraviolet-Sensitive Mutator Strain of Escherichia coli K-12,” *J. Bacteriol.*, vol. 113, no. 1, pp. 145–160, 1973.

[75] X. Veaute, S. Delmas, M. Selva, J. Jeusset, E. Le Cam, I. Matic, F. Fabre, and M.-A. Petit, “UvrD helicase, unlike Rep helicase, dismantles RecA nucleoprotein filaments in Escherichia coli.,” *EMBO J.*, vol. 24, no. 1, pp. 180–189, 2005.

[76] P. A. Morganroth and P. C. Hanawalt, “Role of DNA replication and repair in thymineless death in Escherichia coli,” *J. Bacteriol.*, vol. 188, no. 14, pp. 5286–5288, 2006.

[77] N. C. Fonville, D. Bates, P. J. Hastings, P. C. Hanawalt, and S. M. Rosenberg, “Role of RecA and the SOS response in thymineless death in Escherichia coli,” *PLoS Genet.*, vol. 6, no. 3, 2010.

[78] S. Q. Zheng, A. J. Ding, G. P. Li, G. S. Wu, and H. R. Luo, “Drug Absorption Efficiency in Caenorhbditis elegans Delivered by Different Methods,” *PLoS One*, vol. 8, no. 2, 2013.

[79] D. B. Longley, D. P. Harkin, and P. G. Johnston, “5-fluorouracil: mechanisms of action and clinical strategies.,” *Nat. Rev. Cancer*, vol. 3, no. 5, pp. 330–338, 2003.

[80] R. Holma, R. Korpela, U. Sairanen, M. Blom, M. Rautio, T. Poussa, M. Saxelin, and P. Osterlund, “Colonic Methane Production Modifies Gastrointestinal Toxicity Associated With Adjuvant 5-Fluorouracil Chemotherapy for Colorectal Cancer,” *Journal of Clinical Gastroenterology*. p. 1, 2012.

[81] M. J. van Vliet, H. J. M. Harmsen, E. S. J. M. de Bont, and W. J. E. Tissing, “The role of intestinal microbiota in the development and severity of chemotherapy-induced mucositis,” *PLoS Pathogens*, vol. 6, no. 5. pp. 1–7, 2010.

[82] I. Von Bültzingslöwen, I. Adlerberth, A. E. Wold, G. Dahlén, and M. Jontell, “Oral and intestinal microflora in 5-fluorouracil treated rats, translocation to cervical and mesenteric lymph nodes and effects of probiotic bacteria.,” *Oral Microbiol. Immunol.*, vol. 18, no. 5, pp. 278–284, 2003.

[83] X. B. Lin, L. A. Dieleman, A. Ketabi, I. Bibova, M. B. Sawyer, H. Xue, C. J. Field, V. E. Baracos, and M. G. Gänzle, “Irinotecan (CPT-11) chemotherapy alters intestinal microbiota in tumour bearing rats,” *PLoS One*, vol. 7, no. 7, 2012.

[84] B. D. Wallace, H. Wang, K. T. Lane, J. E. Scott, J. Orans, J. S. Koo, M. Venkatesh, C. Jobin, L.-A. Yeh, S. Mani, and M. R. Redinbo, “Alleviating cancer drug toxicity by inhibiting a bacterial enzyme.,” *Science*, vol. 330, no. 6005, pp. 831–835, 2010.

[85] Y. Zhu, T. Michelle Luo, C. Jobin, and H. A. Young, “Gut microbiota and probiotics in colon tumorigenesis,” *Cancer Letters*, vol. 309, no. 2. pp. 119–127, 2011.

[86] E. A. E. Abada, H. Sung, M. Dwivedi, B. J. Park, S. K. Lee, and J. Ahnn, “C. elegans behavior of preference choice on bacterial food,” *Mol. Cells*, vol. 28, no. 3, pp. 209–213, 2009.

[87] T. C. Y. Kwok, N. Ricker, R. Fraser, A. W. Chan, A. Burns, E. F. Stanley, P. McCourt, S. R. Cutler, and P. J. Roy, “A small-molecule screen in C. elegans yields a new calcium channel antagonist.,” *Nature*, vol. 441, no. 7089, pp. 91–95, 2006.

[88] N. V Kirienko, K. Mani, and D. S. Fay, “Cancer models in Caenorhabditis elegans.,” *Dev. Dyn.*, vol. 239, no. 5, pp. 1413–1448, 2010.